GROWTH RATE DEPENDENT CARBON CATABOLITE REPRESSION (CCR) IS DETERMINED BY MOLECULAR CROWDING (MC) IN *E. COLI* CELLS

by

Yi Zhou

M.E, National University of Singapore, 2003

B. E. Zhejiang University, 1999

Submitted to the Graduate Faculty of

Medicine in partial fulfillment

of the requirements for the degree of

Doctor of Philosophy in Cellular and Molecular Pathology

University of Pittsburgh

2011

UNIVERSITY OF PITTSBURGH

SCHOOL OF MEDICINE

This dissertation was presented

by

Yi Zhou

It was defended on

[December 09, 2011]

and approved by

Dr .Yoram Vodovotz, PhD, Department of Surgery

Dr. Judith Klein-Seetharaman, PhD, Department of Structural Biology

Dr. Naftali Kaminski, MD, Department of Medicine

Dr. Ziv Bar-Joseph, PhD, Machine Learning Department

Carnegie Mellon University

Committee Chair: Dr. Reza Zarnegar, PhD, Department of Pathology

Dissertation Advisor: Dr. Zoltan N. Oltvai, MD, Department of Pathology

GROWTH RATE DEPENDENT CARBON CATABOLITE REPRESSION (CCR) IS DETERMINED BY MOLECULAR CROWDING (MC) IN E. COLI CELLS

Yi Zhou, M.E.

University of Pittsburgh, 2011

Comprehensive analyses of metabolic networks by integrating genome information with various omic data can lead to the development of a system-level understanding of cell metabolism not only from a regulatory perspective, but also from the perspective of evolutionary optimization. Indeed, the principles and boundary conditions uncovered by system biology analyses may contribute to the accurate prediction of metabolic activities in fast growing cells, such as *Escherichia coli* (*E. coli*) cells and cancer cells.

With a resilient metabolic network evolved to adapt to a complex and partly unpredictable environment, *E. coli* cells have developed many molecular mechanisms to ensure fast cell growth at any permissive growth conditions. Of these, carbon catabolite repression (CCR), in which one substrate is preferentially utilized in the presence of others, is one of the most important mechanisms that determine the utilization strategies of carbon substrates by *E. coli* cells. The mechanism of CCR has been examined by investigating the individual molecules involved in its pathways. However, the physiological significance of sequential substrate consumption is still not fully understood.

To study the fundamental principles on which the evolutionary selection of CCR is based, a mathematical modeling approach called flux balance analysis (FBA) with a molecular crowding (MC) constraint (FBAwMC) was developed and tested by our collaborator, Prof. Alexei Vazquez. This model correctly predicted the sequential substrate consumption behavior of *E. coli* cells grown in a mixed substrate medium without including any prior knowledge of CCR. Therefore, the result of the FBAwMC modeling suggests that CCR may be part of a larger set of solutions of systems optimization under molecular crowding (MC) constraint that *E. coli* cells employ to ensure their optimal growth.

In order to explore the potential relationship between MC and CCR, in this thesis work we reexamined the sequential substrate uptake behavior under different growth rates in *E coli*. Cell growth kinetics and substrate consumption in single substrate culture displayed distinct features compared to mixed substrate culture. The microarray data comparisons between the single- and mixed substrate culture were performed and evident repressive effects on transporter genes supports the notion that CCR was activated both in mixed- and single substrate culture. Moreover, the accelerated cell growth in mixed culture indicates there is a correlation between CCR activation and cell growth rate in mixed substrate culture. Therefore, we aimed to study the relationship between CCR and cell growth rate. We find that CCR is a regulatory mechanism that is only activated in *E. coli* cells in a fast growth phase, suggesting that it is one of the molecular mechanisms that protects physiological processes from excessive MC in rapidly growing cells. We also find that cell volume regulation is actively involved in facilitating CCR to implement the MC regulated adaptation. To examine the growth advantage gained in mixed substrate, the metabolic genes in central metabolism network were compared at different growth rates. Microarray result also confirms that high proliferation rate is correlated with metabolic pathway selection, such as that of the glycolysis pathway.

To provide further support to this notion, we also performed studies that aimed to interrupt the CCR and/or alter MC. We found that CCR is a necessary mechanism for *E. coli* cells to grow in multiple substrates. MC alteration was also seen upon CCR disruption, and cell growth was only resumed after MC homeostasis was restored. We aimed to overcome the repressive effects caused by CCR and study cell physiology upon CCR disruption in mixed substrate culture. Cell growth inhibition upon inducers addition, which activates the transporter genes originally repressed by CCR, supports that CCR is a necessary mechanism for *E. coli* cells

to grow in multiple substrates. Moreover, substrate consumption kinetics was slowed down and MC alteration was observed upon CCR disruption.

To further study the relationship between MC and cell growth, we altered cell MC through transient protein expression and genome deletion as well as morphology disruption. Cells with different MC levels displayed growth phenotypes in cell growth and substrate consumption. It shows that both CCR activation and optimal MC are critical for fast cell growth.

Although it is difficult to isolate MC effects on cell metabolism from the influences exerted by other factors, such as volume regulation, cumulatively our results suggests that MC is a critical constraint of cell metabolism, and that CCR is one of the mechanisms responsible for the optimization of cell metabolism under this boundary condition. More generally, our results indicate that the physiological significance of evolved regulatory mechanism should be interpreted by considering the optimization processes and the boundary conditions the given biological process is under.

TABLE OF CONTENTS

ACKNOWLEDGEMENT

To me, my Ph.D. thesis work is a journey of making something work from something that didn't work. I wouldn’t have been able to complete it without the support of many people.

First, I would like to express my deep appreciation and gratitude to my Ph.D. mentor Dr. Zoltan N. Oltvai. Dr. Oltvai is surprisingly tolerant and patient. More than that, his guidance and insights are invaluable and will continue to be an inspiration to encourage me to contribute to this exciting world of science. Dr. Oltvai, thank you for your support throughout this tough but wonderful journey!

Next, I thank sincerely Dr. Yoram Vodovotz, Dr. Judith Klein-Seetharaman, Dr. Naftali Kaminski, Dr. Ziv Bar-Joseph and Dr. Reza Zarnegar for their service on my dissertation committee. Their suggestions, comments and continuous support have been a critical part in achieving my goals.

I would like to thank all the previous and present members of the Oltvai Lab, Jiangxia Liu, Basak Isin, Krin Kay, and Qasim Beg, without whom my work could not have been accomplished. I particularly appreciate Jiangxia Liu and her family for all the enjoyable scientific and non-scientific discussions as well as great time together.

Finally, and importantly, I extend my thanks to all members of my family, especially my grandparents, Dingbo Wen and Deqiu Xue, my mother Siying Wen, my father Zhilie Zhou and my lovely son Hongyi Wang. Finally, I thank my husband, Jianjun Wang, who worked hard to help my research by contributing scientific suggestions and taking care of my boy in the weekends alone. I could have not succeeded without their unconditional love and support. Thank you all!

1.0 INTRODUCTION

During the billions of years of evolution, cells have evolved in a complex and mostly unpredictable environment that ultimately resulted in the natural selection of highly potent metabolic capabilities for most resilient and adaptive free-living organisms. Among these, in bacteria and many unicellular eukaryotes several molecular regulatory mechanisms have evolved that work synergistically to achieve maximum cell growth once the proper nutrients are available. In the past, a large number of experimental and theoretical studies have been performed that aimed to understand these mechanisms. Of these, a set of systems biology approaches have studied the cell's metabolic network by integrating genomic-, transcriptomic-, proteomic- and metabolomic data to generate biological insights based on system optimization from an evolutionary perspective. However, even though the modeling can predict cell metabolic phenomena, such as the sequence of nutrients uptake by bacteria, the relationship between the modeling conditions and the cell's intrinsic characteristics remains often ignored.

This thesis focuses on gaining insight into the potential relationship between a known molecular mechanism (carbon catabolite repression (CCR) in *Escherichia coli* metabolism) and a known innate physicochemical constraint of the cell (molecular crowding (MC)). An improved understanding of this relationship will not only contribute to the better understanding of cell metabolism, but would also facilitate the development of increased production capabilities in the fermentation industry, and may provide insight into new therapeutic approaches for the treatment of cancer, autoimmunity, and infectious diseases.

1.1 CARBON CATABOLITE REPRESSION

1.1.1 Carbon catabolite repression (CCR) and diauxie growth

Most bacteria can utilize multiple substrates from the environment. A set of enzymes are required for the transport and metabolism of each individual substrate. Under certain conditions, certain substrates, such as glucose, are taken up preferentially from the environment, and this uptake activates a set of genes that facilitate the catabolism of the preferred substrate while it represses simultaneously the consumption of other substrates. This phenomenon was first described in the early 1940s by Jacques Monod. Briefly, in *Escherichia coli* cells that were cultured in growth media containing two different carbon sources, glucose, sucrose, or fructose was always consumed first, followed by the consumption of a second carbohydrate, such as lactose, maltose, mannitol, or arabinose. Moreover, after the first substrate was almost completely used up, cells stopped growing for a period of time and then growth resumed after consumption of the second substrate was activated. Monod called this phenomenon diauxie growth (Monod 1942). During the following years, this growth pattern was also observed in *Bacillus subtilis* and other organisms. Eventually, this phenomenon, in which the utilization of less favored substrates are prevented in the presence of the preferred substrates, started to be known as *carbon catabolite repression* (CCR) (Contesse 1969).

1.1.2 The phosphotransferase system (PTS) and its function in CCR

The mechanism of CCR has been mostly studied in *E. coli* and *B. subtilis.* Its effects are commonly referred to as “glucose induced repressive effects” (Gorke and Stulke 2008). This

repression is mediated through both transcriptional repression and protein-protein interaction inhibition on the substrate transporter genes (Bruckner and Titgemeyer 2002; Deutscher, Francke et al. 2006; Deutscher 2008). Specifically, the CCR effects are exerted mainly through the phosphoenolpyruvate (PEP) and carbohydrate phosphotransferase systems (PTS), which catalyzes the uptake and phosphorylation of the substrates in bacteria (Postma, Lengeler et al. 1993; Deutscher, Francke et al. 2006; Cases, Velazquez et al. 2007).

The basic composition of the PTS is similar among different bacterial species (Postma, Lengeler et al. 1993). The PTS contains a hydrophilic, cytoplasmic components enzyme I (EI) and the histidine protein (HPr), and a hydrophobic membrane domain containing protein enzyme II (EII). The carbonhydrate specificity is determined by EII. *E. coli* has four EII superfamilies, classified by their distinct evolutionary origins (Saier MH 2005): (i) the glucose-fructose-lactose superfamily, containing the glucose superfamily, the fructose-mannitol family, and the lactose family; (ii) the ascorbate-galactitol superfamily containing the ascorbate family and the galactitol family; (iii) the mannose family; and (iv) the dihydroxyacetone family. *E. coli* contains at least 15 different EII complexes that are composed of a hydrophobic domain, EIIB, EIIC, and a hydrophilic domain, EIIA. The EII complexes recognize substrates and transport them into the cytoplasm. This process is followed by phosphorylation of HPr. The EII system couples substrate transport and simultaneous phosphorylation of the substrate through two coupled reactions, as below (terms defined in Figure 1):

$$\text{PEP+HPr} \xleftrightarrow{\text{EI}} \text{pyruvate+phosphor-HPr(P-} \quad (1)$$

$$\text{P-HPr+carbohydrate} \xleftrightarrow{\text{EII}} \text{HPr+carbonhydrate-P} \quad (2)$$

As shown in Figure 1, the substrate is recognized and engaged by the substrate specific enzyme II (EII) transporter complex. The EII complex is composed of the cytoplasmic soluble EIIA and two membrane permeases, EIIB and EIIC. The substrate is transported into the cytoplasm by EIIC and then phosphorylated by EIIB. The cytoplasmic EIIA transfers a phosphoryl group

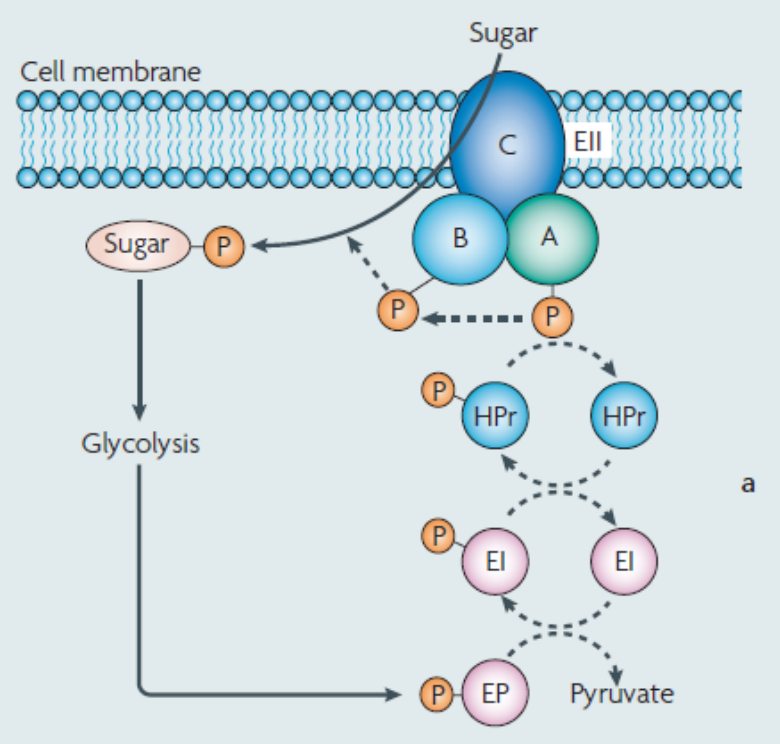

Figure 1.1 The phosphoenolpyruvate-carbonhydrate phosphotransferase system (PTS).

PTS is composed of three distinct components: enzyme I (EI), histidine protein (HPr) and enzyme II (EII). The phosphorylation chain reaction is initiated by autophosphorylation of EI with phosphoenolpyruvate (PEP). Finally, the phosphoryl group is transferred to the carbohydrate through EIIB, while the substrate is taken up by the transporter EIIC in the cell membrane The figure is adopted from (Gorke and Stulke 2008)

from HPr, which is originally derived from the autophosphorylation of EI to EIIB (Postma, Lengeler et al. 1993; Robillard and Broos 1999). EI and HPr are shared among different PTS substrates. Both EI and HPr relay a phosphoryl group from PEP to the EII complexes (as shown in equation 1 and 2). Therefore, the EII complexes are present in the cytoplasm both in non-

phosphorylated and phosphorylated forms. The inactivation of EII complexes is dependent on the substrate consumption state (Bettenbrock, Sauter et al. 2007).

1.1.3 The cytoplamic components EI (enzyme I) and HPr (histine Protein)

Compared to the substrate specificity of EII, EI and HPr are generic to different PTSs. EI (63kD) is encoded by the *ptsI* gene and is highly conserved in various bacteria (Hu and Saier Jr 2002). EI is autophosphorylated in the presence of Mg^{2+} at the N-3 position of the imidazole ring of a histidine (His-189) in *E. coli* (Weigel, Kukuruzinska et al. 1982). The N-terminus of EI (EI-N) accepts the phosphoryl group from phosphor-HPr but not PEP (Herzberg, Chen et al. 1996; Chen, Zhang et al. 2002). The C-terminus of EI (EI-C) contains the PEP binding site and is necessary for its dimerization (Patel, Vyas et al. 2006).

To prevent sugar phosphate accumulation, the phosphotransfer potential of PEP is under stringent regulation (Weigel, Kukuruzinska et al. 1982). One of the regulatory mechanisms is dependent on the status of the monomer/dimer transition of EI. It is found that only the dimer accepts the phosphoryl group on PEP (Patel, Vyas et al. 2006). This dimerization of EI governs substrate uptake and phosphoryl transfer to a certain degree, because when dimerization is inhibited substrate uptake declined even with unlimited quantities of PEP being available (Liu and Roseman 1983).

The reaction constant, K_a of EI dimerization has also been studied. The range of K_a varied ~1000 times by adjusting various parameters, including temperature, the presence of the ligands Mg^{2+} and PEP, pH, and ionic strength (Patel, 2006 ;Patel, 2006). However, the potential ligands, such as sugar phosphates were found to have no significant effects on K_a. Moreover, subsequent

mutation analysis studies have shown that the major determinants of the dimerization process were the ligands but not the phosphorylation of EI (Patel, Vyas et al. 2006).

As shown in Figure 1, all of the phosphotransfer reactions of the PTS (except the last the phosphorylation of the sugar acceptor) are readily reversible. Therefore, considering the wide dynamic range of its dimerization potential, the phosphorylation initiator is expected to influence the cascade significantly considering the wide dynamic range of its dimerization potential (K_a with ~1000 times variation) (Patel, Vyas et al. 2006; Patel, Vyas et al. 2006).

The EI's partner, HPr, is encoded by the ptsH gene and its active site resides at His-15 in most enteric bacteria (Weigel, Powers et al. 1982; Powers DA 1984; Deutscher, Kessler et al. 1985). HPr interacts with EI (Garrett, Seok et al. 1999) and $EIIA^{Glc}$ (the enzyme II of glucose PTS) (Wang, Louis et al. 2000) without inducing any significant conformational change in the PTS binding partners. Also, the EIIA:HPr complex forms without major conformation change. The central part of the binding surface consists mainly of hydrophobic residues (Herzberg 1992). The binding of the phosphoryl group in $EIIA^{Glc}$ is stabilized by His-75 (Liao DI 1991) and by Arg-17 in HPr (Herzberg, Reddy et al. 1992). $EIIA^{Glc}$ interacts with $EIIB^{Glc}$ and HPr with an almost identical binding surface (Deutscher, Francke et al. 2006). No point mutation in $EIIA^{Glc}$ could be identified that fully abolishes the phosphoryl transfer among the PTS partners, indicating that the interactions between $EIIA^{Glc}$ and HPr or $EIIA^{Glc}$ and $EIIB^{Glc}$ include multiple interactions (Sondej, Seok et al. 2000; Cai, Williams et al. 2003).

1.1.4 $EIIA^{Glc}$ is the central regulatory unit of CCR

In enteric bacteria, the global regulation of carbon metabolism involves transcription factors such as Crp (cyclic AMP receptor protein) (Malan, Kolb et al. 1984; Okamoto and

Freundlich 1986; Yao, Hirose et al. 2011) and Mlc (Kimata, Inada et al. 1998; Lee, Boos et al. 2000; Seitz, Lee et al. 2003), etc. They regulate the process of nutrient uptake by controlling the activation or repression of substrate related operons. The glucose specific EII, $EIIA^{Glc}$ regulates carbon catabolism through exerting effects on the transcription factors, such as Crp (cAMP receptor protein). Moreover, mutational analyses revealed that mutations in the crr gene (that encodes $EIIA^{Glc}$) restored *E. coli* cell growth on non-PTS carbon sources (Saier, 1972 ;Saier, 1976). These data indicate that $EIIA^{Glc}$ regulate the transport and/or metabolism of both PTS and some non-PTS carbon sources to exert CCR effects.

1.1.4.1 $EIIA^{Glc}$ exerts CCR effects through cAMP dependent transcription regulation

Intracellular cAMP (Cyclic adenosine monophosphate) binds to and activates Crp. Subsequently, activated Crp can activate the promoters of more than 100 downstream genes related to carbon metabolism (Malan, Kolb et al. 1984; Tagami and Aiba 1998; Busby and Ebright 1999). Crp-cAMP complex can adopt different conformations to activate different genes and operons with different binding affinities (Takahashi, Blazy et al. 1989; Harman 2001; Dai, Lin et al. 2004; Tworzydło, Polit et al. 2005; Fic, Bonarek et al. 2009). Consequently, by regulating the intracellular cAMP level, carbon catabolism can be regulated. Moreover, the active form, cAMP-CRP, also regulates the regulatory RNAs, such as CyaR and Spot42, to exert carbon repression and control substrate consumption (Møller, Franch et al. 2002; Papenfort, Pfeiffer et al. 2008), indicating that cAMP-CRP also indirectly regulates gene expression and carbon catabolism.

cAMP is synthesized by adenylate cyclase, which is encoded by the gene, cya. Expression of *cyaA* is regulated by Crp/cAMP in *E. coli* by a negative auto-feedback mechanism (Aiba 1985; Jovanovich 1985; Kawamukai, Kishimoto et al. 1985). The phosphorylation level of

$EIIA^{Glc}$ was found to play an important role in CCR by controlling intracellular cAMP synthesis (Kimata, Takahashi et al. 1997; Hogema 1998; Bettenbrock, Sauter et al. 2007). Both the non-phosphorylated and phosphorylated forms of $EIIA^{Glc}$ bind to adenylate cyclase. However, only the phosphorylated form of $EIIA^{Glc}$ ($P\sim EIIA^{Glc}$) stimulates cAMP synthesis by adenylate cyclase (Park, Lee et al. 2006). It was also found that the catalytic activity of adenylate cyclase resides in its N-terminaldomain, while its C-terminal domain is responsible for its interaction with $EIIA^{Glc}$ (Reddy, Hoskins et al. 1995; Park, Lee et al. 2006). A C-terminal truncated version of adenylate cyclase produces 10 times more cAMP in a *crr* strain than that in the wild-type strain, indicating that the C-terminal domain acts as an inhibitory switch (Crasnier, Dumay et al. 1994). Yet, the increase is only four fold when transcriptional regulation of the cya gene by CRP/cAMP is prevented by replacing the cya promoter with a constitutive *bla* promoter (Inada, Takahashi et al. 1996). This indicates that cAMP production is controlled mainly at a post-translational level instead of a transcriptional level.

In the presence of extracellular glucose or other PTS substrates, the ratio of the phosphoryl donor, PEP, to pyruvate is low and $EIIA^{Glc}$ is mostly in a dephosphorylated state. PTS transfers the phosphoryl group to glucose efficiently to support glucose metabolism. As a result, the phosphoryl group on $EIIA^{Glc}$ is quickly removed (Hogema BM, 1998 and Bettenbrock K 2007). A recent study also found that the levels of $P\sim EIIA^{Glc}$ and secreted cAMP were correlated. A low cAMP level was associated with a low $P\sim EIIA^{Glc}$ concentration (Bettenbrock, Sauter et al. 2007). *crp* mRNA degradation was also found to be accelerated in glucose cultured *E. coli* cells (365-Ishizuka, 1993). By decreasing intracellular cAMP, $EIIA^{Glc}$ prevents the catabolism of other substrates by lowering the level of cAMP activated Crp.

In summary, by manipulating the intracellular cAMP level or availability of activated Crp, the consumption of glucose is facilitated by preventing the activity of genes related to the consumption of other substrates.

1.1.4.2 CCR effects exerted by $EIIA^{Glc}$ through inhibition of substrate transporters

Besides regulating the intracellular cAMP level, $EIIA^{Glc}$ also exerts its inhibitory effects through protein-protein interactions. In its non-phosphorylated form, $EIIA^{Glc}$ binds to constituents of transporters of non-preferred substrates to inhibit their transport, including the lactose permease, LacY (Nelson 1983; Hogema, Arents et al. 1999), the glycerol kinase, GlpK (Hurley, Faber et al. 1993), and the maltose transporter, malK (Böhm, Diez et al. 2002; Chen, Lu et al. 2003).

The specific inhibitory effects on each substrates' transport varies. For example, at least four molecules of $EIIA^{Glc}$ are needed to completely inhibit the glycerol kinase activity on one GlpK tetramer (van der Vlag J 1995). This indicates that a sufficient amount of $EIIA^{Glc}$ is required to repress glycerol catabolism, and the repression will be alleviated if the $EIIA^{Glc}$ concentration decreases significantly. Another (repressed) target of $EIIA^{Glc}$, LacY is an H^+ symporter and drives the uptake of lactose, melibiose and other galactosides (Kaback 1997; Kaback, Sahin-Tóth et al. 2001). Different substrates cause different binding stoichiometries between LacY and $EIIA^{Glc}$. In the presence of the preferred substrates, such as lactose, LacY causes maximum binding of $EIIA^{Glc}$ (Sondej, Weinglass et al. 2002; Sondej, Vázquez-Ibar et al. 2003). Therefore, a sufficient amount of substrate is needed to counter the repressive effects of $EIIA^{Glc}$.

$EIIA^{Glc}$ also inhibits ATP-binding subunit proteins of the ATP-binding cassette (ABC) transporters, such as MalK. The maltose transporter MalK associates with the two permease

subunits, MalF and MalG. The binding of maltose to MalFGK stimulates ATP hydrolysis to transport maltose into the cell (Chen, Sharma et al. 2001; Böhm, Diez et al. 2002). The ATPase domain resides in the N-terminal of MalK, while its regulatory domain is in its C-terminal that is commonly bound by $EIIA^{Glc}$ to prevent maltose import (Forst, Schulein et al. 1993; Schneider 2001). These mechanisms enable $EIIA^{Glc}$ to repress the substrates' metabolism when the substrates are present and compete with glucose (Saier MH and Desai JD 1983) in mixed substrate growth media. Therefore, the intracellular concentration of $EIIA^{Glc}$ in its non-phosphorylated form is a key factor that contributes to CCR effects on the secondary non-PTS substrate utilization.

1.1.5 CCR effects are mediated by the cAMP independent regulators, Mlc and carbon intermediates

Mlc is a global transcription regulator in *E. coli*. It is a repressor that binds to five operons/genes in *E. coli* including *ptsHI* (Kim, Nam et al. 1999; Plumbridge 1999), *ptsG* (Kimata, Inada et al. 1998; Plumbridge 1999), *malT*, the transcription activator of maltose operon (Decker, Plumbridge et al. 1998), and itself, *mlc* (Decker, Plumbridge et al. 1998). Mlc is sequestered to the membrane when the glucose transporter, $EIIBC^{Glc}$ is in a non-phosphorylated state (Lee, Boos et al. 2000; Nam, Cho et al. 2001). Mlc only binds to the non-phosphorylated form of $EIIBC^{Glc}$ but Mlc anchoring to the membrane is necessary to eliminate Mlc-mediated repression (Seitz, Lee et al. 2003; Tanaka, Itoh et al. 2004). This regulatory mechanism facilitates the derepression of the consumption of other substrates when the glucose concentration in the media is very low.

Mlc also exerts CCR effects on the non-PTS sugars, such as maltose. It inhibits the transcription of the maltose regulon specific transcription factor, malT, and prevents the activation of downstream transporter genes, such as maltose transporter, malEKG (Decker, Plumbridge et al. 1998). Other non-PTS sugars (e.g., arabinose, rhamnose, and xylose) and the substrate intermediates (i.e., glycerol-3-P and glycerol) also have repressive effects on malT and malK (Eppler and Boos 1999; Eppler, Postma et al. 2002). Even Gluconate-6-P and glycerol-3-P affect CCR by elevating the intracellular cAMP concentration, which is independent of $P\sim EIIA^{Glc}$ and Crp concentration (Hogema, Arents et al. 1997; Eppler and Boos 1999). Therefore, CCR effects are a combined effect of all the regulatory machineries involved in the regulation of carbon substrate metabolism.

1.1.6 Relief of CCR restriction by genetic manipulations

In industrial applications, *E. coli* cells are used in fermentations to produce bio-fuel (e.g., ethanol) or recombinant proteins. The understanding of CCR in *E. coli* cells could therefore provide a guideline for genetic modification to achieve a higher production yield of the desired products. For example, the low-cost substrate lignocellulose are commonly used in fermentation by *E. coli* to be converted to ethanol or other byproducts. Yet the hydrolysis of lignocelluloses produces a mixture of substrates, including glucose, arabinose and xylose. Under CCR regulation, wild type cells tend to consume glucose first then the other two substrates. This results in a slow substrate consumption and low ethanol production yield. Moreover, the accumulation of acetic acid in the culture media also slows down cell growth.

To counter the CCR constraint and to make the cells consume substrates simultaneously, a *ptsI* mutant was produced by fosfomycin selection to consume the substrates and produce

ethanol more efficiently (Cordaro, Melton et al. 1976; Lindsay, Bothast et al. 1995). A *ptsG* gene knock-out strain was found to consume the three substrates simultaneously at higher speed and produce more ethanol and metabolize all acetic acid in the media (Hernandez-Montalvo, Valle et al. 2001; Nichols, Dien et al. 2001). Overexpressing the *mlc* gene from a plasmid also reduced acetate accumulation and glucose uptake rate (Hosono, Kakuda et al. 1995; Plumbridge 2002). By adding the glucose analog, α-MG, into the 20g/l glucose culture medium, the *E. coli* mutant, ptsG$^-$ cells increased recombinant protein production by 50% and had a decreased acetate secretion (Chou, Bennett et al. 1994). In summary, by interfering with a PTS factor, CCR can be relieved to a certain degree to benefit substrate consumption. However, cell growth is compromised accordingly.

1.2 INTRODUCTION TO MOLECULAR CROWDING

Molecular crowding (MC) (also termed as volume exclusion (R.John 2001)) refers to the fact that macromolecules, such as proteins, which occupy ~30% of the total cell volume, reduce the volume of cytosol available for other molecules. As a result, the effective concentration of proteins in the cytosol increases. The environment inside the cell provides the basic constraint for all the biochemical reactions through controlling the concentrations, thermodynamics, and kinetics of the intracellular molecules. In such a crowded environment (Figure 1.2 A), the intracellular molecules can easily exert non-specific influence of steric repulsions on specific reactions and processes (Rivas, Ferrone et al. 2004).

1.2.1 Influences of MC on cellular biochemical processes: diffusion, reaction rate, protein-protein association and protein folding

The high MC environment in the cell has profound effects on many aspects of cellular information processing, such as the thermodynamic activities of the reactions or processes being involved. Among them, the diffusion coefficient is susceptible to the concentration of the intracellular molecules or, in another word, to the level of MC. Fluorescent molecules have been used to study how small molecules diffuse intracellularly in eukaryotic cells and in *E. coli* cells. It was found that the diffusion of molecules, such as GFP, was three- to four- fold slower in eukaryotic cells and 11-fold slower in *E. coli* cells compared to its diffusion in water (Swaminathan, Hoang et al. 1997; Elowitz, Surette et al. 1999). These findings indicate that the crowded intracellular environment can significantly affect the kinetics of diffusion dependent reactions and signaling pathways. As a result, the overall cell physiology will also be affected.

Volume exclusion by the macromolecules also influences reaction rates through affecting their effective concentrations. The effective concentration of a macromolecule is limited by MC more significantly than that of a small molecule because the accessible space is determined by the size of the molecule (Minton 2001), as illustrated in Figure 1.2 B and C. This notion was experimentally confirmed using hemoglobin; It was observed that the activity coefficient displayed non-linearity with the actual concentration of hemoglobin (Ross PD 1977). It implies that the effective concentration is altered by the thermodynamic influence of the intracellular environment. Quantitative analysis with cell extracts showed that there is a positive correlation between the weight of a molecule and its activity coefficient in *E. coli* cells (Zimmerman 1993). This further provides support to the notion that MC effects are mainly exerted by macromolecules (Zimmerman and Trach 1991; Zimmerman 1993). With MC increasing, the

diffusion-limited reactions are slowed down, while the transition state-limited reactions are accelerated due to the increased protein association (Zimmerman and Minton 1993). Consequently, the effects of MC on biochemical reactions are complicated by the fact that it increases thermodynamics activities while slowing down the diffusion rate. The net results are determined by the actual nature of each reaction (Zimmerman and Minton 1993; Allen P 1997).

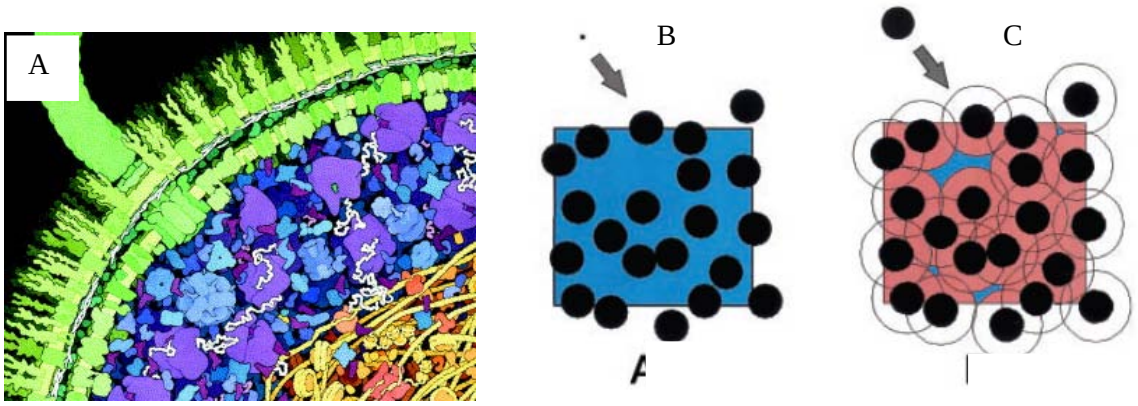

Figure 1.2 Crowded intracellular environment of *E. coli* and the diagram of excluded volume (in black and pink) and available volume (in blue).
A. Representation of the approximate numbers, shapes and density of packing of macromolecules inside a cell of *E. coli*. Small molecules are not shown. This figure is adopted from(Ellis, 2001). The effective available volume to infinitesimal micromolecule molecule (B) and a macromolecule which has comparable size to the background molecule (C) is different. The available volume decreases dramatically when macromolecule size increases as shown in C. This two figures are adopted from (Minton 2001).

As stated above, increasing MC (i. e., cytoplasmic macromolecular density) enhances protein-protein association. It was found that the self-association of a protein, fibrinogen, was increased by the addition of a secondary crowding molecules, bovine serum albumin (BSA) (Rivas, Fernandez et al. 1999). Moreover, the self-association of the bacterial cell division protein, FtsZ, was found to form linear oligomers of indefinite length when FtsZ concentration was raised to 1g/L and the concentration of the crowding agent (cyanmethemoglobin or BSA) was ~150g/L. The correct spatial distribution of FtsZ polymerization regulates cell cycle in *E.*

coli cells (Lan, Daniels et al. 2009). Thus, it can be expected that MC can affect cell cycle by altering the self-association of the cell cycle molecules, including FtsZ, in *E. coli* cells.

Finally, MC also has a critical influence on protein folding by chaperon proteins. Usually, there are two types of chaperons: “steric” chaperones that provide structural information for the correct assembly of their target proteins, and “non-steric” chaperones that are responsible for preventing the aggregation of polypeptide chains (R.John 1990; Ellis 1998; Sauer, Knight et al. 2000). MC was found to affect the functional efficiency of chaperones in *vitro*. For example, the molecular chaperone in *E. coli* cells, the GroEL tetramer, recovered from a urea-induced denatured form when the crowding agent, Ficoll 70 at 300g/L, was added to the buffer (Galán, Sot et al. 2001). Additionally, another chaperone, GroES, which exerts its effect together with GroEL, was observed to retain unfolded polypeptides in the fluid phase when crowding agents were maintained at 200g/L. These results demonstrate that MC overcomes aggregation caused by incorrectly folded peptides through promoting the association between the peptides and their chaperon proteins (Ellis 1997; Ellis 2001) .

1.2.2 MC effects on PTS in *E. coli* cells

The crowded intracellular environment forces all the molecular mechanisms of a cell to evolve so that the innate MC constraint is not violated. Among all the signaling complexes, PTS in *E. coli* cells has been studied to understand how MC affects signal transduction and metabolite channeling of PTS (Kholodenko, Rohwer et al. 1998; Rohwer, Postma et al. 1998).

As introduced in section 1.1, PTS is a special enzyme complex that is responsible for carbon substrate transport and metabolism. In fast growing *E. coli* cells, ~30% of the cytosol is occupied by proteins (Figure 1.2A). PTS was studied *in vitro* to understand how PTS satisfies the

needs of fast cell growth in such a crowded intracellular environment. In a study of Rohwer et al., cell-free extracts were mixed with different crowding agents, including PEG6000 and PEG 3500, and the glucose specific PTS flux was measured (Kholodenko, 1998). The flux measurements of PTS demonstrate that PTS pathway responds to enzyme concentration of PTS more sensitively than a linear pathway (Rohwer, Postma et al. 1998). The structure of the enzyme complex PTS (shown in Figure.1.1) also facilitates high signaling sensitivity. The *in vitro* crowding experiment also shows that the PTS components decreased the flux-response when the enzyme concentration was high. Yet, the crowding agent, PEG, enhanced PTS complex formation and increased activity coefficient (Rohwer, Postma et al. 1998). Of note, PEG 3500 inhibited PTS activity at various enzyme concentrations while PEG 6000 increased PTS activity when enzyme concentration was low. This result implies that crowding agents with different sizes have different effects on PTS activity (Rohwer, Postma et al. 1998; Sun 2007). Taken together, the *in vitro* experimental results show that MC is able to exert effects on cell metabolism and growth through affecting the PTS flux in *E. coli* cells.

1.2.3 MC effects on nucleus structure and DNA related enzymes

MC has been shown to greatly extend the range of concentrations in which the enzymes or proteins are functional through the effects described above for PTS. Similarly, cell replication or DNA-protein interactions are also affected by MC. DNA nucleases have been characterized to test how MC alters their functions. It was shown that the volume exclusion effects of PEG enhanced the high salt solution inhibition on *E. coli* DNA ligase (K Hayashi ; K Hayashi 1985). A recent study also demonstrated that PEG substantially enhanced the hydrolysis of DNA by DNase I and S1 nuclease by increasing the enzyme's maximum reaction rate, V_{max}. However,

exonuclease activity was decreased by 20% (w/v) PEG. It indicates that MC has different effects on the catalytic activities of nucleases (Sasaki, Miyoshi et al. 2007). Other DNA enzymes and proteins were found to be affected by MC, as well. The RecA protein, which protects *E. coli* single strand DNA from being degraded during DNA repair, was found to increase its functional tolerance to high concentration of salts (NaCl and Mg^{2+}) in a high MC environment (Lavery and Kowalczykowski 1992; Courcelle and Hanawalt 2001). More linear products were generated from DNA ligases and T4 RNA ligases under MC influence. This could be due to the increased DNA-enzyme binding and/or enzyme activity (Zimmerman 1993; Zimmerman and Minton 1993). These results imply that in fast growing *E. coli* cells without a separated DNA replication territory, MC could promote cell growth by defining optimal reaction rates for all the involved replication processes.

In mammalian cells, MC has more specific effects, given that the nucleus is naturally separated from the cytoplasmic macromolecules (DE 2000; Johansson 2000). The compaction of chromatin was observed when higher crowding was induced by osmotic shock in HeLa and MCF7 cells. Although this is different from the crowding agent induced MC effects, morphological changes of the nucleus were seen, including the detachment of the lamina and the condensation of chromatin (Richter, Nessling et al. 2007). The condensed chromatin also prohibit gene transcription because silencing included by epigenetic chromatin modifications are prevented from being depressed when the DNA is too compact to be accessed by epigenetic modifying factors (Robert G 2005). The microstructures of nuclei, such as nucleoli and the promyelocytic leukemia protein (also called PML bodies) can also be stabilized by adding PEG or dextran (Ronald 2004). Moreover, the compacted nuclear environment may benefit from the enhanced interactions between the chromatin and the nuclear matrix in a crowded environment

(Pederson 2000; Richter, Nessling et al. 2008). Therefore, maintaining an optimal crowding is beneficial for replication related reactions and nucleus structure stabilization while satisfying the cell's normal physiological needs.

1.2.4 MC adjustment through osmosensing and volume regulation

MC is relevant to osmosensing and cell volume alteration, as MC changes significantly as the level of intracellular hydration varies due to osmotic stress (Baldwin, 1984 #151; Baldwin, 1995 #149). Osmotic stress changes the structures, aggregation, and function of individual macromolecules in the cytoplasm or on the cell membrane (Minton 2006). Cells have developed intrinsic mechanisms to adapt to MC change through volume regulation. Cell volume regulation maintains the concentration of cellular constituents because even minor changes in cell volume may cause dramatic functional alterations due to enzyme concentration change (Fulton 1982; Brown 1991; Minton, Colclasure et al. 1992; Lang, Busch et al. 1998). For example, mammalian cells can affect MC through ion channel regulation, such as $Na^+/K^+/Cl^-$ channels, to control cell volume (Okada 2004; Pasantes-Morales, Lezama et al. 2006). The volume change is highly correlated with cell growth in mammalian cells (Rouzaire-Dubois and Dubois 1998; Rouzaire-Dubois, O'Regan et al. 2005). It was found that cell growth in neuroblastoma cells was fully inhibited when cell volume was increased by 25% with the K^+ blocker, TEA. Moreover, the "bell" shape relationship between cell proliferation and cell volume indicates the presence of an optimal cell volume range for fast cell growth (Dubois and Rouzaire-Dubois 2004).

Cell volume alteration also influences metabolic pathways, such as part of glycolysis and glycogen synthesis, which are stimulated by cell swelling (Al-Habori, Peak et al. 1992; Peak, Al-Habori et al. 1992). The inhibition of protein proteolysis and synthesis was observed with cell

volume expansion, which could be recapitulated by insulin addition (Haussinger, Hallbrucker et al. 1991; Stoll, Gerok et al. 1992). This indicates that cell volume is related to hormone control to regulate proteolysis processes.

In a recent study, cell density and volume were measured throughout the yeast cell cycle. It was found that the cell density increased in the G1 phase with cell volume expansion. Yet, cell density decreased by the end of the G1 phase and in the S phase. Cell volume was observed to continuously expand till the S phase. This study also found that the change in yeast cell density at G1/S stage requires energy (in the form of ATP), TOR function and actin cytoskeleton function (Bryan, Goranov et al. 2010). Therefore, this work strongly suggests the interconnections of cell growth, cell cycle, MC, as well as cell volume dynamics.

Similarly, *E. coli* cells also have complete osmoregulatory machineries, including genes, ProP, BetP and OpuA (Wood 2006). Cells restore cellular hydration and volume by synthesizing or transporting solutes under genetic and biochemical control (Wood 1999). It is observed that cell growth and cell volume decrease when osmolarity increases in the media. This process is involved with the increase of thermodynamic activities of cytoplasmic K^+ (Cayley, 1991). However, the activation of these osmosensors are associated with the inactivation of other membrane enzymes or transporters, such as LacY, the lactose permease of *E. coli* (Houssin, Eynard et al. 1991; Culham, Henderson et al. 2003). Thus, osmotic stress clearly influences cell growth, and substrate uptake can only resume after optimal intracellular MC has been restored (Roth, Porter et al. 1985). At the same time, cell volume or cell size regulators may act as a metabolic sensor to dynamically couple cell size to metabolic rate. For example, in *B. subtilis* one of the cell size regulators is a metabolic sensor, the glucosyltransferase, UgtP, which localizes to the cell division site in a nutrient-dependent manner (Weart, Lee et al. 2007).

Moreover, the size of *E. coli* cells defective in gene pgm is only about 70% of the wild type cell size when cultured in LB (Lu and Kleckner 1994). The pgm is the pgcA homolog that encodes phosphoglucomutase, which is involved in the breakdown of glycogen and the metabolism of galactose and maltose. These results indicate that in bacteria, cell cycle, cell metabolism and cell size are closely related. However, in the studies above, it was not determined how a change in MC contributes to volume alteration.

1.2.5 Metabolic network analysis with flux-balance analysis (FBA) modeling

To understand how the innate physiochemical constraints, such as MC, regulate cell physiology and metabolism, different mathematical modeling approaches have been developed to understand biological evolution from a systems perspective. Among them, flux balance analysis (FBA) is widely used to study cell metabolism at the level of the whole metabolic network.

FBA is based on appropriate constraints to derive the steady-state metabolic capabilities of the system to maximize a certain biological aim without the need of accurate kinetic data for the metabolites or enzymes (Raman and Chandra 2009). However, the accuracy of the prediction also depends on the correct definitions of physiochemical constraints of the cell, such as the stoichiometric balance of mass and energy. FBA predicts the steady state of cells while satisfying certain innate constraints (Kauffman, Prakash et al. 2003).

Figure 1.3 briefly illustrates the work flow of FBA modeling (Schilling and Palsson 1998). As shown in Figure 1.3a and b, the first step of FBA is to define the system boundary, within which that the flux of internal metabolic reactions should always balance. Next, a matrix of mass balance equations is derived, which describes an equilibrium between in flux and out flux for each metabolite in the system (Fig 1.3c) to generate "**S**", the stoichiometric matrix (Fig. 1.3 d). The flux matrix, "**V**", is combined with "S" to

define the optimal solution space (Fig 1.3 e) within which the constraints, such as stated in Fig 1.3 f, are satisfied. Finally, for a given objective, such as maximal biomass production rate, the best solution of "**V**" will be found in the solution space (Fig 1.3g), while satisfying the constraints described as the boundary conditions of the equations stated in "**V**". Therefore, the final solution of "**V**" represents the cells' internal steady flux distribution when the metabolism network has been optimized to satisfy the constraints and achieve its physiological aim, such as fastest growth or maximum substrate uptake rate.

FBA modeling predicts cell behaviors more accurately when combined with additional constraints or biological knowledge (Segrè, Vitkup et al. 2002; Gianchandani, Chavali et al. 2010). Prediction accuracy can be greatly improved by incorporating new constraints or alternative modeling approaches. For example, predictions can be improved by: 1) using the mean cell composition for objection function considering that the mean composition of the cell varies with the growth rate (Pramanik and Keasling 1997); 2) incorporating genetic regulatory information using Boolean logic operators (Covert, Schilling et al. 2001; Mahadevan, Edwards et al. 2002; Min Lee, Gianchandani et al. 2008); 3) including thermodynamics to quantify the irreversibility of the reactions, such as energy balance (Beard, Liang et al. 2002); 4) introducing dynamic analysis to study the transient metabolism shift (Mahadevan, 2002 #1459) and 5) integrating spatial constraints (Beg, Vazquez et al. 2007; Vazquez, Beg et al. 2008). Although the modification of FBA provides more accurate prediction, the limitations cannot be ruled out, such as lack of comprehensive understanding of the metabolism network or precise mathematical definition of constraints. Therefore, the advantages of each specific FBA modeling are dependent on how accurately it extracts prior knowledge for the specific biological system for which the prediction will be given. The differences between the modeling and experimental results is usually the criteria for evaluating the efficacy of a given modeling/simulation. In the next section, the studies of metabolism in fast growing cells conducted by FBA simulation by including the important physicochemical constraint of molecular crowding (MC) will be discussed (Beg, Vazquez et al. 2007; Vazquez, Beg et al. 2008; Vazquez, De Menezes et al. 2008).

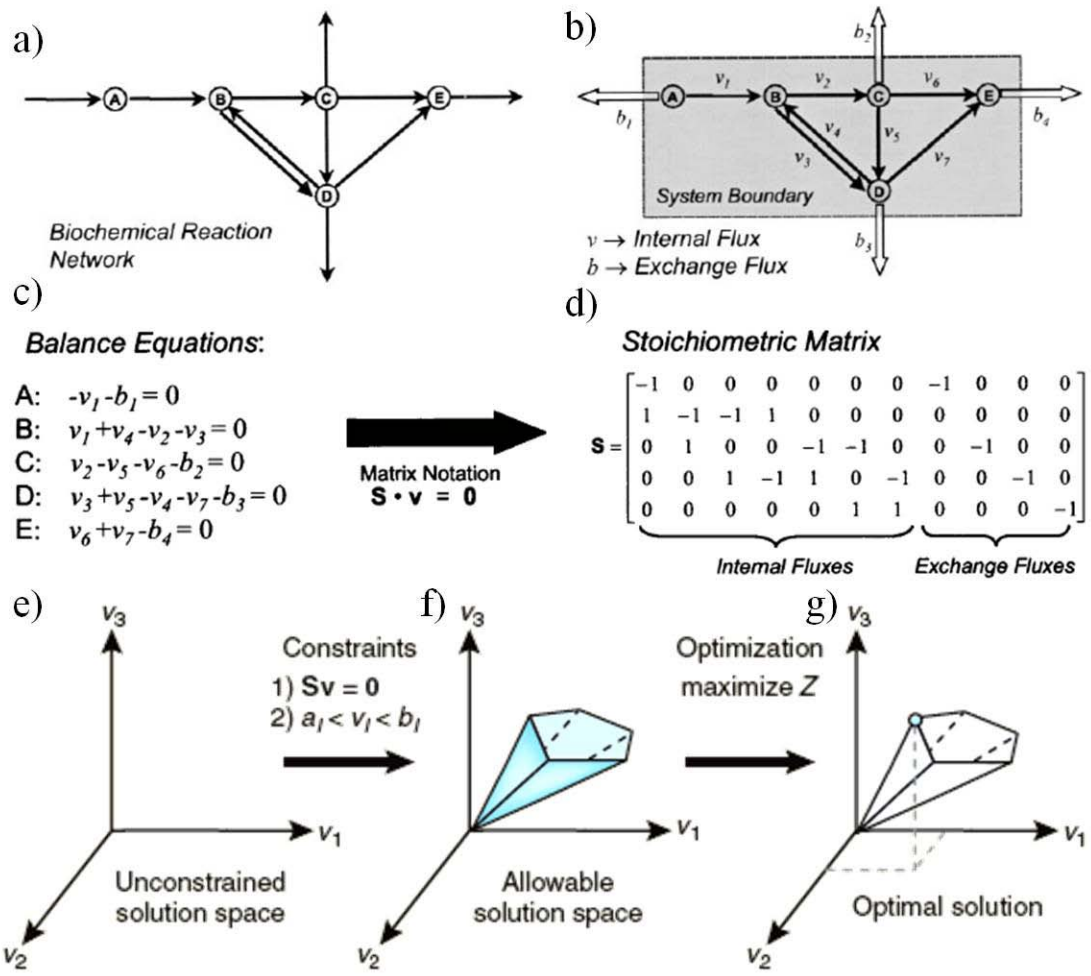

Figure 1.3 Flux balance analysis

a) A given metabolic network; b) the system boundary that includes all the internal metabolic reactions but not exchange processes across the system is defined; c) An equilibrium of in flux and out flux is derived for each metabolite in the system; d) The set of coupled ordinary differential equations are then represented to a matrix format, where "**S**" is the stoichiometric metrix and "**V**" is the flux matrix; e) Without any constraint, the solution for the metabolic fluxes is underdetermined; f) With additional constraints, e.g., the maximum uptake rate of a specified substrate, all the solutions that satisfy the constraints form an allowable solution space; g) Given an optimization objective, such as the maximal biomass production rate, FBA can identify the optimal solution of flux distribution within the allowable solution space (adopted from (Schilling and Palsson 1998)).

1.2.6 Cell growth and metabolism analysis with FBAwMC

As an important physical constraint for reactions in the intracellular environment, MC also regulates cell growth through different mechanisms, as introduced previously. MC's influence on *E. coli* cells has been studied experimentally and with mathematical modeling (Zimmerman and Trach 1991; Makinoshima, Nishimura et al. 2002; Beg, Vazquez et al. 2007; Molenaar, Van Berlo et al. 2009). In the following, relevant results of FBAwMC modeling will be introduced.

The behavior of *E. coli* cells in mixed substrates culture has been modeled to understand the strategy that cells have developed to gain maximum cell growth with limited nutrient supplies (Kovárová-Kovar and Egli 1998). The maximum growth rate was proposed to be determined by the growth restricting component in the substrate mixture (Kovárová-Kovar, 1998), or by the linear contribution of single-carbon consumption rates (Lendenmann, 1998), or by the nutrient quality and the ratio between RNA and protein (Scott, 2010). Yet, in all these studies, a prior knowledge of substrate consumption kinetics was needed. In contrast, FBA modeling with MC constraint (FBAwMC) gives accurate prediction of cell behavior in a mixed substrate culture media without any prior information about substrate consumption (Beg, Vazquez et al. 2007). In this work, the FBA model has included the following constraints:

1) The stationary reaction rates (fluxes) consuming and producing a metabolite should balance:

$$\sum_{i=1}^{N} S_{mi} f_i = 0 \qquad (1)$$

Where f_i denotes the flux of reaction *i*.

2) The totality of enzyme molecules should only occupy a limited space (MC constraint), which is less than the total cell volume:

$$\sum_{i=1}^{N} v_i n_i \leq V \qquad (2)$$

Where, v_i stands for the enzyme i's molar volume, and n_i represents the number of moles of the *i*th enzyme. Therefore, the total enzymes' volume shouldn't exceed the total cell volume, *V*.

FBAwMC correctly predicted not only the maximum cell growth of wild type and mutant *E. coli* strains in different growth media, but also the sequential substrate uptake behavior in mixed substrate culture that was composed of five different carbon substrates, including glucose. The sequential substrate consumption has been attributed to CCR effects, for which FBAwMC includes no relevant regulatory information. Therefore, it indicates that the molecular mechanism present in CCR has evolved in the context of the MC constraint. This is also implied by the fact that without an MC constraint FBA predicts simultaneous substrate uptake kinetics from mixed substrate containing growth media.

FBAwMC modeling also predicts a metabolic switch in *E. coli* cells when cells enter to a fast growing phase from a slow growth phase (Vazquez, Beg et al. 2008). In agreement with the model's predictions, metabolic flux measurements indicated a shift from the TCA cycle to the glycolysis pathway when the growth rate was higher than 0.3/hr. The measured enzyme activity with varied growth rates also supported the metabolism pathway switch. Therefore, the FBAwMC model sheds light on the linkage between glycolysis pathway utilization with growth rates under MC constraint. It indicates that cells tend to shift to the glycolysis pathway to satisfy faster growth needs due to enzyme concentration economics considering the spaces the enzymes need to occupy intracellularly.

Metabolic pathway selection under MC constraint is further supported by the results obtained from the modeling of mammalian cell metabolism (Vazquez, Liu et al. 2010). In this work, a simplified glucose metabolism pathway was used to calculate how cells organize the two pathways' utilization to maximize the ATP production rate under MC constraint (equation 2). It was discovered that cells shift to glycolysis pathway after the mitochondria number has reached the maximum volume fraction it could occupy. In turn, glycolysis pathway in the cytoplasm was activated, as the volume fraction of its enzymes needed to generate an ATP is significantly less than that of mitochondria. As a result, the ATP generation rate/ per enzyme is maximized by using glycolysis pathway. Therefore, FBAwMC modeling not only generated the prediction consistent with the experimental data about the metabolism switch, but it also demonstrated that the Warburg effects may be caused by the trade-off between the ATP generation capability and MC constraint.

In another study conducted in *S. cerevisiae*, the FBAwMC model correctly predicted the experimentally measured enzyme activities and metabolites concentrations of its glycolysis pathway. This strongly suggests that cells optimize its resources, including enzyme and metabolite volume fraction to be able to increase its metabolic rate of glycolysis pathway under MC constraint (Vazquez, de Menezes et al. 2008). Further experimental results also support cell density change along different cell phases in the *S. cerevisiae* cell cycle (Bryan, Goranov et al. 2010). It shows MC is a not a rigid value and it changes slightly along cell growth dynamically.

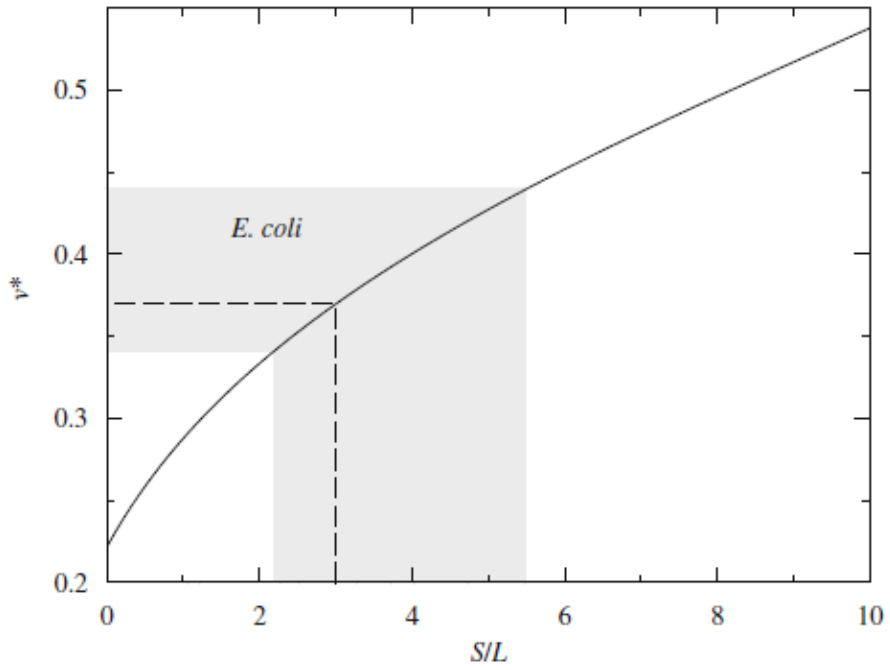

Figure 1.4 The optimal volume fraction.

The optimal volume fraction for α=5.8 as a function of the ratio S/L (solid line). The shadowed area was obtained using as input the volume fraction range0.34- 0.44 for *E.coli* (Zimmerman and Trach 1991) and computing the associated S/L range. The dashed line represents out prediction ν^*=0.37 assuming S/L=3. This figure is adopted from (Vazquez 2010)

Whether there is an optimal MC range for metabolic activities of a cell was the subject of another study, which varied cell density (MC) to achieve the highest metabolic rate in nutrient limited condition (Vazquez 2010). In this study, FBA modeling was applied to find the best solution of volume fraction of intracellular proteins to achieve the highest metabolic rate by obeying the constraints including flux balance at steady state, volume fraction restriction, and maximum substrate uptake capacity. The results of this study suggest that cells are only allowed to vary their intracellular MC within a narrow range to achieve the highest reaction rate to meet the needs for dynamic growth. Moreover, this study also suggests that this rearrangement of intracellular MC to the optimal range is also a must to achieve the maximum metabolic objective

in fast growing cell. As shown in Figure 1.4, the FBAwMC predicted optimal volume fraction value, ν^{*}=0.37 is within the experimentally measured range: 0.34~0.44 (Zimmerman and Trach 1991). This suggests the prediction is reasonable and there exits an optimal MC range for cells (Zimmerman and Trach 1991).

Taken together, it has been found that MC plays roles in metabolism pathway selection and cell growth optimization in *E. coli* cells, as given by the predictions of the FBAwMC model. The studies about MC's influence on cell physiology and its relationship with known molecular mechanisms, such as CCR will be discussed in the next chapter.

1.3 THESIS OUTLINE

E. coli can grow on a wide spectrum of carbon substrates, and CCR is a critical mechanism regulating carbon substrate catabolism to facilitate maximum cell growth in *E. coli* cells (Bettenbrock, Fischer et al. 2006; Deutscher 2008; Gorke and Stulke 2008). In our lab's previous study, the physical constraint of MC was included in a FBA modeling (FBAwMC) to predict substrate consumption kinetics in cells cultured in mixed media containing five carbon substrates. This modeling correctly predicted sequential substrate consumption kinetics without knowledge of CCR regulation. The microarray data of cell cultured in mixed substrate confirmed that CCR was present in the substrate consumption regulation (Beg, Vazquez et al. 2007). This suggests that MC is probably the boundary constraint to trigger CCR. However, the physiological meaning of CCR activation in the substrate consumption is not clear. The relationship between MC and CCR is not understood.

All machineries regulating cell biological processes have to adapt to the physico-chemical constraints of the cell in a long term evolution through metabolic network optimization. From this perspective, studying CCR may help us to better understand the role of underlying constraints such as MC (Seshasayee, Fraser et al. 2009).

To prove that the sequential substrate uptake observed previously (Beg, 2007) was regulated by CCR, in **Chapter 2** we carefully characterized CCR effects in regulating the sequential substrate consumption of *E. coli* cells in a mixed- and single substrate media, respectively. Cell growth, substrate consumption and transcription profile were examined. We confirmed that CCR was present both in mixed- and single substrate culture. The accelerated cell growth and substrate consumption kinetics observed in mixed substrate culture with CCR activate prompted us to study the relationship between CCR and cell growth rate. By using continuous feed chemostat experiments to control cell growth rate in mixed substrate culture, we found that CCR is a growth rate dependent regulatory mechanism, and its potency is positively correlated with the cell growth rate. Variations of MC corresponding to cell growth and substrate consumption were investigated. The essential function of CCR in fast cell growth under MC constraint is proposed and discussed.

As CCR is only activated in fast cell growth phase as found in **Chapter 2**, we hypothesized that CCR is critical for fast cell growth. Therefore, in **Chapter 3**, we aimed to study cell physiology upon CCR disruption by using inducers to overcome the repressive effects caused by CCR on the transporter genes of the secondary substrates, such as maltose in mixed substrate culture. We found that after the induced disturbance, cell growth and substrate consumption was hindered. Simultaneously, MC and cell volume variations occurred. This

shows that CCR is a maintenance mechanism responsible for maintaining optimal intracellular MC in fast growing cells.

Our results above implies optimal intracellular MC is critical for cell growth and our collaborator's modeling result also suggests the presence of optimal MC range required for cells to achieve high metabolic rate. Therefore, in **Chapter 4**, we tried to directly manipulate MC through the transient upregulation of intracellular protein content and genome modification as well as morphology disruption. MC was found to dynamically adjust upon transient protein expression and cell growth was affected accordingly. This result provides some preliminary insight into the relationship between MC constraint and protein synthesis during cell growth. The genome modification and morphology disruption also resulted in different MC levels and distinct cell growth and substrate consumption phenotypes.

Finally, in **Chapter 5**, we conclude the thesis with a perspective on how each of the four previous chapters contributes to the current understanding of CCR and the MC constraint. Improvements for future experimental designs and future studies are also proposed.

2.0 SUBSTRATE CONSUMPTION OF *E. COLI* CELLS IN MIXED SUBSTRATE CULTURE IS DETERMINED BY CCR UNDER MC CONSTRAINT

2.1 INTRODUCTION

Prior to my thesis study, , fermentor batch culture experiments with (wild type) *E. coli* MG 1655 cells were performed to study cell growth and substrate consumption in a carbon limited medium that contained five carbon substrates, including glucose, glycerol, galactose, lactate and maltose at a concentration of 0.04% (w/w) each (Beg, Vazquez et al. 2007). The sequential substrate uptake displayed three phases: glucose was exclusively consumed in phase I; glycerol was taken up in the last phase, and other three substrates were taken up in phase II. Both the sequential substrate uptake pattern and the transcription profile of transporter genes support that the substrate consumption was subjected to CCR regulation. However, FBAwMC (FBA with MC constraint) modeling correctly predicted the substrate consumption kinetics without including any prior knowledge of CCR. This strongly suggests that the biophysical constraint, MC is a crucial factor determining substrate consumption strategy in *E. coli* cells. However, the relationship between CCR and MC remained not fully understood.

In this section, we aim to understand the underlying mechanism of substrate utilization strategy under CCR regulation, the physiological significance of CCR in fast growing cells and fundamental limits defined by MC in CCR-regulated cell growth. Batch culture with carbon

substrates limited media and continuous feed chemostat experiments with varying growth rates were performed. Substrate consumption kinetics and MC variations were determined. We found that the substrate switch that appeared in the mixed substrate culture was stringently regulated by CCR only in fast growing cells. CCR potency is positively correlated with growth rate. MC level and cell volume are dynamically adjusted while growth rate varies.

2.2 RESULTS

2.2.1 Cell growth and substrate consumption kinetics of *E. coli* cells are accelerated in mixed substrate- compared to single substrate culture

We previously characterized the culture density-, growth rate - (Figure 2.1 A, B, black lines, respectively) and substrate uptake kinetics (Figure 2.1D) of *E. coli* cells in mixed substrate culture, and also determined the level of acetate, a well-known metabolic byproduct of rapidly dividing *E. coli* cells, in the culture supernatant (Figure 2.1C, black line) (Beg et al, 2007). The substrate consumption profiles we observed were compatible with the presence of CCR in the culture, in which the sole consumption of glucose preceded the concomitant utilization of all other substrates (Figure 2.1D) (Beg, 2007). To better understand the mechanism underlying the observed behavior, we have first examined these parameters in *E. coli* cells grown separately in the individual components of the mixed culture medium (i.e., in single carbon-limited media), the experiment being terminated upon substrate exhaustion from the growth media or when cells entered into stationary phase.

Compared with the mixed substrate culture, the culture density- (Figure 2.1A) and growth kinetics (Figure 2.1B) of *E. coli* cells in single carbon-limited media significantly differed, glucose-limited cultures showing the fastest- and lactate-limited cultures the slowest growth. In terms of their maximal biomass

glucose, maltose-, and galactose-limited cultures were comparable and slightly below the glycerol-limited culture that achieved the highest biomass, while lactate-limited growth resulted in about one half of that level (Figure 2.1A). As in the mixed culture, all growth rate kinetic curves displayed an initial rapid increase, peaked in the early exponential growth phase, and then decreased (Figure 2.1B). However, compared to the mixed substrate culture the curves were substantially flattened for the galactose-, lactate-, and glycerol-limited cultures and slightly less for the glucose- and maltose-limited cultures (Figure 2.1B), which correlated with their delayed substrate uptake rate from the culture media (Figure 2.1E).

Acetate (i.e., acetic acid) secretion by *E. coli* cells mirrored these trends, except that in contrast to that seen in the mixed substrate culture (Figure 2.1C, black tracing), on a population level there was no evidence for acetate reuptake in the single carbon cultures (Figure 2.1C). However, glycerol-limited cultures showed lower, while lactate-limited cultures displayed higher acetate levels than the other cultures (Figure 2.1C). Low acetic acid secretion in the glycerol-limited culture correlated with its highest final biomass, while the highest acetic acid secretion was associated with lowest final biomass in the lactate-limited cultures (Figure 2.1A).

The substrate consumption rate in the five single carbon-limited cultures (Figure 2.1E) correlate with their apparent substrate uptake order in mixed substrate culture (Figure 2.1D): in both cases glucose was taken up at the fastest (first)- and glycerol at the lowest (last) rate, while the other three substrates displayed slightly different rank order among the single substrate-limited- and mixed substrate cultures.

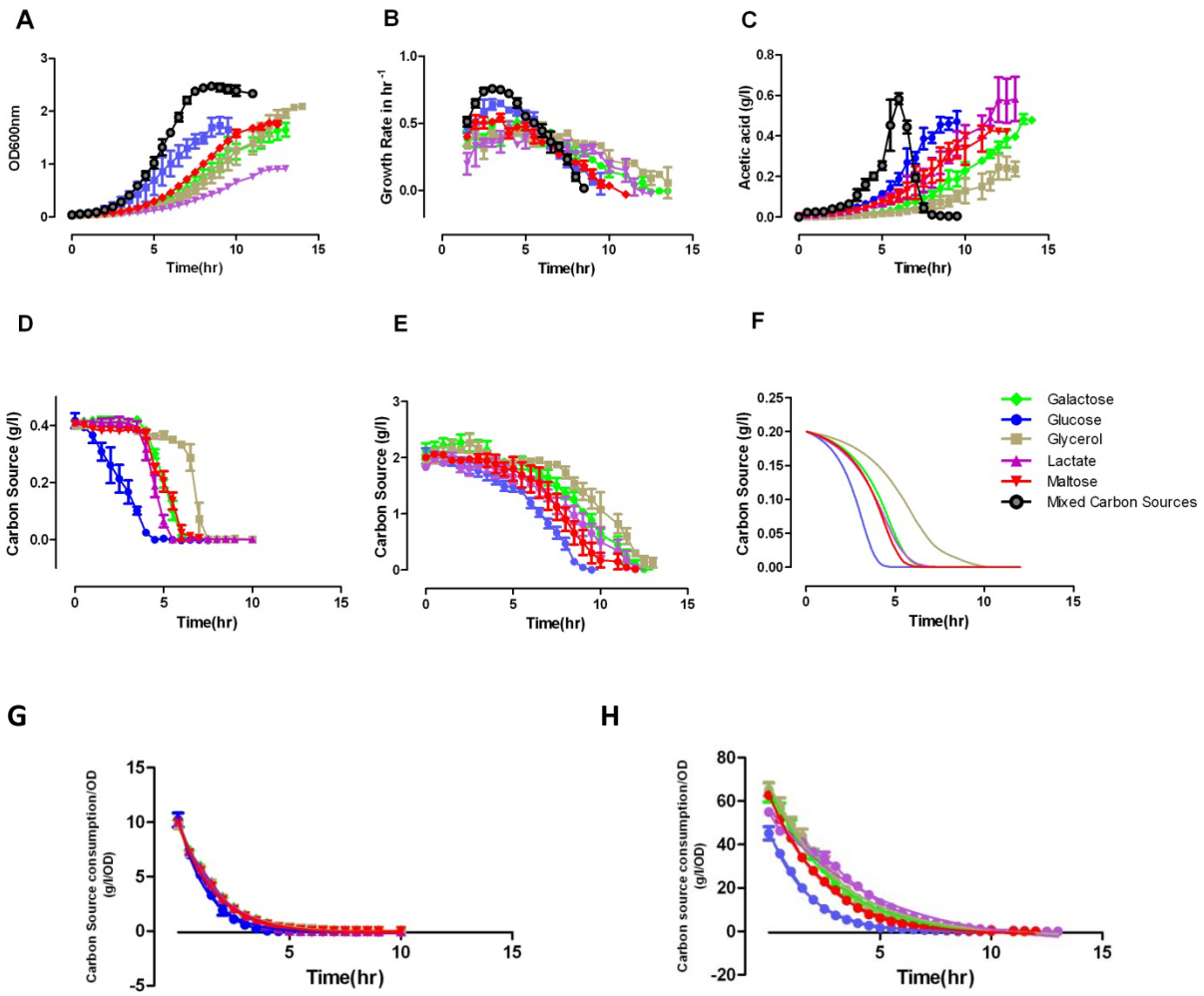

	Glucose	Maltose	Lactate	Galactose	Glycerol
K	.7847	.6194	.5905	.5893	.5813
Half life	.8834	1.119	1.174	1.176	1.192
Rank	1	2	3	4	5

	Glucose	Maltose	Lactate	Galactose	Glycerol
K	.5653	.4051	.2219	.3485	.3261
Half life	1.226	1.711	3.124	1.989	2.126
Rank	1	2	5	3	4

Figure 2.1 Batch culture experiments in single carbon-limited media

The O/N LB culture of MG1655 cells were inoculated into the fermenter tank containing 1.2 L of M9 media. The initial OD_{600} was ~0.02~0.04. Cells were cultured at 37°C, 400 rpm with air agitation. The oxygen probe was used to monitor the appearance of stationary phase of the culture (see Beg et al, P.N.A.S., 2009). In single substrate experiments, each carbon substrate concentration was at 0.2%. In the mixed substrate experiment, each carbon source concentration was at 0.04% and the total carbon source concentration was 0.2%; A. Culture growth rate as measured by tracing OD_{600}; B. Relative cell growth = $\ln(OD_{600t} - OD_{600t-1})$. C. measured acetic acid secretion and substrate consumption in D. Mixed substrate culture and E. Single substrate culture. F. the FBAwMC modeling prediction on substrate consumption in single substrate

culture conditions. The substrate consumption curves (D and E) were normalized to OD600nm data (Figure 1A) in individual culture conditions (shown in the dotted points). Curve fitting with one phase decay equation was applied to the normalized data in mixed substrate culture (G) and single substrate culture (H) (shown in the continuous lines). K is the rate constant and the higher K value indicates the faster substrate uptake. Half life shows the time points when the normalized substrates concentration drops to 50%.

To quantify the rate and order of substrate consumption kinetics independent of the growth rate, we normalized the measured substrate consumption (Figure 2.1D, E) to the biomass data (Figure 2.1A). It is evident that the order of intrinsic substrate uptake rate among the five single substrate cultures (Figure 2.1H) has varied from that seen in the mixed culture medium (Figure 2.1G). The rate of glucose and maltose uptake rates have displayed consistent consumption ranks in both culture types (first and second, respectively), while the other three substrates displayed different consumption orders. Of note, the consumption rates of all the substrates proved higher in the mixed substrate culture than in the single carbon-limited cultures.

Taken together these data indicate that the achievable culture density and growth rate is higher in mixed culture growth conditions than in single carbon cultures of its individual components, which in part may be related to the acetate reuptake observed only in the mixed substrate culture (Figure 2.1C). At the same time, the order of substrate consumption rates were similar among the mixed- and single substrate cultures indicating the intrinsic consumption kinetics of each individual substrate contributes significantly to the sequential uptake phenomenon in the mixed culture medium.

We previously developed a model of *E. coli* metabolism to investigate the origin of the substrate hierarchy consumption in mixed substrate cultures (Beg, 2007). This model obtains the steady-state metabolic flux distribution that result in the maximum proliferation rate given the available nutrients. In the absence of any further elements the FBA model would predict the

simultaneous uptake of all substrates present in the mixed culture. However, upon addition of the molecular crowding constraint (FBAwMC model), the model successfully predicts the hierarchy of substrate consumption. Here we also show that FBAwMC modeling successfully predicts the substrate uptake behavior in single substrate culture (Figure. 2.1F). Taken together, these results indicate that the FBAwMC model successfully recapitulates the substrate consumption curves of *E. coli* growing both in mixed and single substrate cultures, and suggesting molecular crowding as a potential cause of CCR.

2.2.2 Stronger transcriptional signature of CCR is seen in single carbon-limited- than in mixed substrate *E. coli* cultures

The observed difference in the substrate uptake kinetics in the mixed substrate culture (Figure. 2.1D) indicates that within the early exclusive glucose utilization phase where cells grew and proliferate very rapidly (Figure 2.1B) and the uptake of other substrates are inhibited (Figure 2.1D). To test if CCR is a general phenomenon in rapidly proliferating cells we examined if a signature of CCR is also evident in rapidly proliferating single carbon-limited *E. coli* cultures. To this end, we have reanalyzed our previously published microarray data collected from mixed substrate- or single substrate limited batch cultures in early exponential growth phase (at $OD_{600} \sim 0.2$)(also, see Figure 4 in Ref.(Beg, 2007). We find that all substrates upregulate their respective transporters' expression (Figure. 2.2 A). In glucose-limited cultures the mRNA expression of maltose-, galactose-, lactate- and glycerol transporter-encoding genes are downregulated (Figure. 2.2A, blue bars). In the other four single carbon-limited cultures the expression of the glucose transporter-encoding gene, ptsG, is largely unaffected. In the maltose-limited culture the expression of the galactose and glycerol transporters are downregulated, and

galactose has a similar effect on a subset of the maltose and lactate transporter subunits. However, lactate has mixed effects on the expression of maltose and galactose transporter genes (Figure. 2.2A).

We also examined the acetate pathway activities both in single and mixed substrate cultures, first comparing the gene activities of ackA and pta that are responsible for acetic acid production (Figure 2.2A). Consistent with its high acetate secretion rate, ackA and pta displayed the highest activities in lactate-limited media. The high pta activity also suggests that the flux from pyruvate toward acetate is the main contribution of high acetate concentration in lactate media. The reuptake of acetate by redirecting acetic acid flux back to the TCA cycle is facilitated by the gene products of acs, whose expression is lifted glycerol-, galactose- and maltose-limited media. This observation may explain the relatively slow acetate accumulation in these growth media (Figure 2.1C).

Of note, in the mixed-culture medium there is only limited mRNA expression level evidence for CCR: in spite of the presence of their respective substrates in the growth medium the expression of transporter-encoding genes of maltose and galactose are only upregulated at the time of their substrate uptake (Beg, 2007). However, the lactate transporter genes (lldp, dldD) are highly expressed on the mRNA level even before lactate uptake (Beg, 2007), potentially indicating the presence of (growth medium-specific) anticipatory regulation (Tagkopoulos, Liu et al. 2008; Selvarasu, Wong et al. 2009)

Taken together, in single carbon-limited cultures each substrate upregulates the mRNA expression of its own transporter gene(s) but downregulates the genes responsible for the other substrates' uptake, with glucose showing the strongest effect. Moreover, substrates that have faster uptake and provide faster initial growth (glucose, maltose) appear to have a stronger and

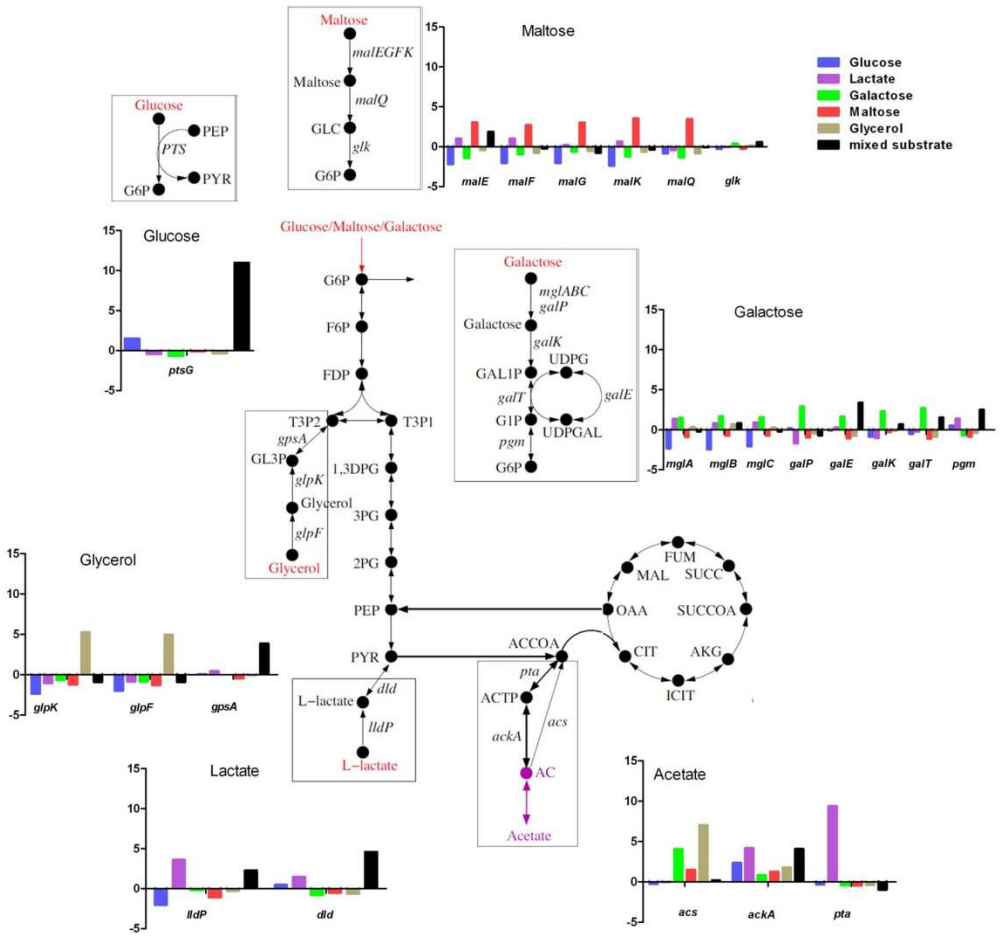

Figure 2.2. Cell metabolism gene expression profiles

The activities of the relative transporter regulon at OD_{600} ~ 0.2 in the single and mixed substrate experiment (obtained from Figure 4 Beg, et al, P.N.A.S., 2007). The six panels display the relative gene expression compared to the "average" expression level of all genes in the microarray experiments and the entry points and the activities of the transporter genes of different substrates in single and mixed substrate media are also shown.

more extensive suppressive effect on the expression level of transporters of other substrates than those that show slower uptake and provide slow initial growth (lactate, glycerol) (Figure 2.2A). In contrast, in the mixed substrate culture, beside the glucose transporter, ptsG, in the exclusive glucose utilization phase transporter genes' activation of some other substrates (e.g., lldP, dld,

malE, galE) is also evident. Thus, at least on a transcriptional level CCR is present in single substrate cultures, too, and its strength seems to correlate with the culture's initial growth rate. Moreover, stronger CCR is seen in single carbon-limited cultures than in the mixed substrate limited culture, perhaps indicating that the latter may be more primed for the activation of mixed substrate uptake upon the near exhaustion of glucose from the growth medium (Figure 2.1D) (Beg, 2007).

2.2.3 Cell growth rate determines the potency of CCR on substrate consumption regulation and positively correlates with MC

The mRNA expression profiles (Figure 2.2) and the substrate consumption kinetics in mixed- substrate culture (Beg, Vazquez et al. 2007) (Figure 2.1D) suggest that at least in their initial rapid growth phases all *E. coli* cultures activate CCR (even when only a single substrate is present). To formally test this hypothesis, we next studied the relationship between CCR and cell growth by examining substrate consumption behaviors in a mixed-substrate culture at various *E. coli* cell growth rates.

In continuous-feed culture of chemostat experiments the growth rate of *E. coli* cells can be manipulated by changing the culture's dilution rate, as to a stepwise increase in the exchange rate of the growth medium cells respond by increasing their rate of biomass synthesis and cell division, i. e., they divide faster and establish a new steady state of the culture until the maximal growth rate in a given growth condition is reached (Beg, 2007)(Vazquez et al, 2008). In our experiment, we sampled the mixed substrate culture 24 hr after increasing the dilution rate (i.e., after the culture has reached a new steady state growth rate), and we measured the culture

density (OD_{600nm}), the pH of the growth medium, and the *E. coli* cell volume and cell density. As has been shown before (Vazquez et al, 2008), the cell concentration in the culture media (i.e., the culture density) decreases with the increased exchange rate of the culture medium (Figure 2.3A, red curve). Also, the pH of the culture media decreases slightly to pH~6.8 at 0.2/hr dilution rate but returns to pH~6.9 and above at growth rates higher than 0.3/hr, probably due to the faster dilution rate of the pH 7.0 growth medium (Figure 2.3A, green curve).

The observed substrate consumption profiles clearly indicate a correlation between the rate of cell proliferation and the presence of CCR (Figure 2.3B). At the lowest growth rate (0.1/hr) CCR is absent, as glucose and the other four substrates are utilized fully and simultaneously. At a faster cell growth (0.2/hr) a limited CCR partially inhibiting the consumption of lactate and glycerol is clearly evident (Figure 2.3B). CCR is more widespread at 0.3/hr when the uptake of galactose and maltose are also partially inhibited (Figure 2.3B). Above this dilution rate there is extensive CCR with predominant glucose utilization while the concentration of the other four substrates in the growth medium remains high (0.2~0.42g/l) (Figure 2.3B). The uptake of maltose and galactose are further reduced at dilution rate 0.7/hr. This pattern indicates that CCR has mild control over secondary substrates' utilization in slow growing cells but it becomes increasingly more extensive in rapidly growing cells.

There is an increase in the volume of *E. coli* cells with increasing growth rate that reaches its peak (1.064fL) at 0.4/hr, and then decreases and reaches a plateau with ~0.98fL at the highest dilution rate of 0.7/hr (Figure 2.3A, purple tracing). *E. coli* cell density displays three different phases along the seven different dilution rates: it is lowest (1.11g/ml) at the lowest dilution/ growth rate at 0.1/hr, then reaches a medium density (~1.13g/ml) at growth rates 0.2 and 0.3/hr, respectively. Cell density reaches its highest value of ~1.14g/ml at 0.4/hr growth rate that is then

maintained till 0.7/hr. These data indicate that cell volume and cell density increases initially with an increasing cell proliferation rate to accommodate more biomass. However, above a threshold level (~1.05fL at 0.4/hr dilution rate) cell density cannot increase further, and the cells maintain a universal biomass density with smaller size cells perhaps to match the faster biomass accumulation rate brought on by faster cell growth.

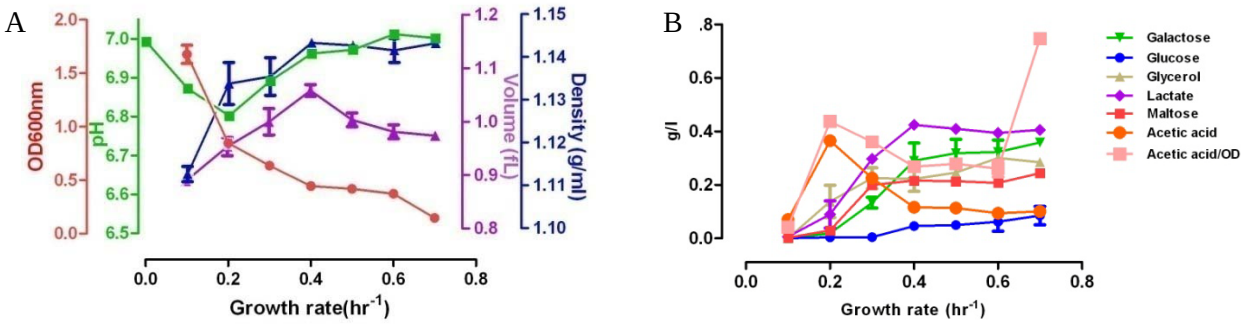

Figure 2.3 CCR effects observed in mixed substrate culture correlate with growth rates

The cells were inoculated in fermenter with initial OD~=0.04. Fresh media was pumped in and out of the reactor tank to replace the original cell culture at each specific flow rate. As a result cells grew at each specific growth rate to compensate the cell loss during the dilution. The flow rate was adjusted every 24 hrs and cells samples were sampled after growth rate has stabilized. Cells were collected to measure OD600nm, pH, cell volume, cell density (A) and substrate consumption (B) and gene profiles (Figure 2.4).

Of note, at the lowest proliferation rate the level of secreted acetate is minimal, indicating metabolism through oxidative phosphorylation (OxPhos) with mixed substrate uptake. However, with the initial appearance of CCR there is a sudden increase in acetate levels, indicating partial aerobic glycolysis in the culture. At maximal growth rate (0.7/hr) there is a second, larger peak in acetate secretion that may indicate the downregulation of OxPhos and a dominance of aerobic glycolysis in the culture. This observed acetic acid secretion is identical to that seen with

glucose-limited culture, and is in agreement with the predictions of the FBAwMC model (Vazquez, 2008).

Taken together, the utilizations of all the secondary substrates start to be significantly repressed when growth rate is 0.3/hr or higher while glucose is primarily utilized through all the growth rates. These results demonstrate that CCR is correlated with growth rates.

2.2.4 Transcriptome analysis of *E. coli* culture reveals several switches in physiological states

To further understand the consequence of CCR and growth rate change on *E. coli* physiology, we also collected samples at all dilution rates (except at 0.5/hr) for microarray experiments and subsequent transcriptome profiling.

Examining the transporter genes' expression at the various dilution/growth rates (Figure 2.4A) reveal that the expression of ptsG, the gene encoding the glucose transporter PtsG/Crr, is at a high level from the 0.2/hr growth rate (with a peak at 0.3/hr), while generally high level glucokinase (glk) peaks at the highest growth rate 0.7/hr. The low expression level of ptsG at 0.1/hr coincides with that high expression of glycerol transporter (glpK, F) and of the galactose transporter regulon genes (galE, K, T), the maltose transporter genes (malEFGK) and lactate gene (lld) (Figure 2.4A). This pattern indicates the minimum substrate concentration required to activate its transporter genes is different for each individual substrate. All the transporter genes, including ptsG, were very active at 0.2 and 0.3/hr growth rates indicating active and simultaneous substrate consumption at the slow growing phase. At 0.3/hr there is also an increased expression of the galEKPT whiose gene product is responsible for the transformation

of galactose to glucose intracellular (Figure 2.4A). Similar activations of wide spectrum of transporter genes were also seen in other studies when growth rate and/or substrate concentration was low (Ihssen and Egli 2005; Liu 2005). However, with growth rate increasing, most of the four substrates' regulon genes were turned off except that some of the individual genes displayed discontinuous activation in higher growth rate phase, such as glk and gpsA (glycerol transporters) at 0.7/hr growth rate.But there was no active glycerol uptake associated with the activation of glk and gpsA at 0.7/hr. This result indicates that only the activations of the whole regulon genes would result in active substrate consumption. In contrast, ptsG's expression was still maintained at a medium level from 0.3~0.7/hr. This corresponds with the lasting and active glucose consumption at all the growth rates (Figure 2.3B). These results are consistent with the observed substrate consumption kinetics (Figure 2.3B) and support the media that CCR is only widely activated when the growth rate is higher than 0.3/hr. Take together, the CCR effects are implemented by switching on and off the transporter genes in a growth-rate-dependent manner.

We next examined the correlation between preference of pathway utilization and growth rate (Figure 2.4B). Genes involved in the TCA cycle were expressed highly only at the slow growing phase (<0.3/hr). In contrast, the expressions of glycolysis pathway genes were initially repressed followed by a sudden increase at 0.3/hr growth rate and remained active through the high growth rate phase (0.3~0.7/hr) (Figure 2.4B). The metabolism shift from TCA cycle to glycolysis pathway utilization with growth rate increasing was observed previously in glucose-limited continuous chemostat experiments (Vazquez, Beg et al. 2008). This suggests that the selection of the metabolic pathways is growth rate dependent but not substrate dependent.

The activity of the glycolysis pathway is partially reflected by its metabolic byproduct, acetate, whose extracellular concentration is the consequence of a balance of its rate of secretion

(via pta and ackA) and re-uptake (acs). We find that acetate production genes (pta and ackA) are expressed highly between 0.2~0.4/hr growth rates (Figure 2.4B). However, both of these genes displayed attenuated expression at higher growth rates. The acs gene, whose gene product catalyzes acetate reuptake toward the citric acid cycle, displayed even lower activities at higher growth rates (0.4~0.7/hr). This suggests that the very high acetate concentration at 0.7/hr dilution rate may be due to the reduced acetic acid reuptake capability.

With increasing growth rate we observed cell volume and cell density adjustments (Figure 2.3A). As osmosensors are known to be associated with cell volume and density alteration in *E. coli* cells (Baldwin and Kubitschek 1984; Baldwin, Sheu et al. 1988; Baldwin, Myer et al. 1995), we also examined the osmosensor genes (osmYCBE), stress genes (rpoSE) and cell volume related genes (MreBCD). We find that osmosensor genes (Figure 2.4C) are highly expressed at slow growing phases (0.1~0.3/hr) but they are downregulated in the higher growth phase (0.4~0.7/hr). This implies that the osmosensors may be activated to cooperate with multiple transporter gene activation in the slow growing phase. As found previously (Notley-McRobb, King et al. 2002; Ihssen and Egli 2004), the hunger stress genes, rpoSE, is also expressed highly at low growth rates but not at high growth rates (Figure 2.4C). The results imply that at high culture density multiple substrate consumption phases without CCR regulation activate the hunger stress genes, while the stress level is lowered by growth rate increase with CCR activation. The nutrient uptake seems to be conducted more actively and efficiently to rescue cells from hunger stress with CCR activation. It is possible that the activation of CCR represses the unnecessary secondary transporter genes' activation to lower the demanding of cell resources allocation and intra volume that proteins commonly occupies. Correspondingly, cell morphology genes, mreBCD are also gradually upregulated with increasing growth rate, and

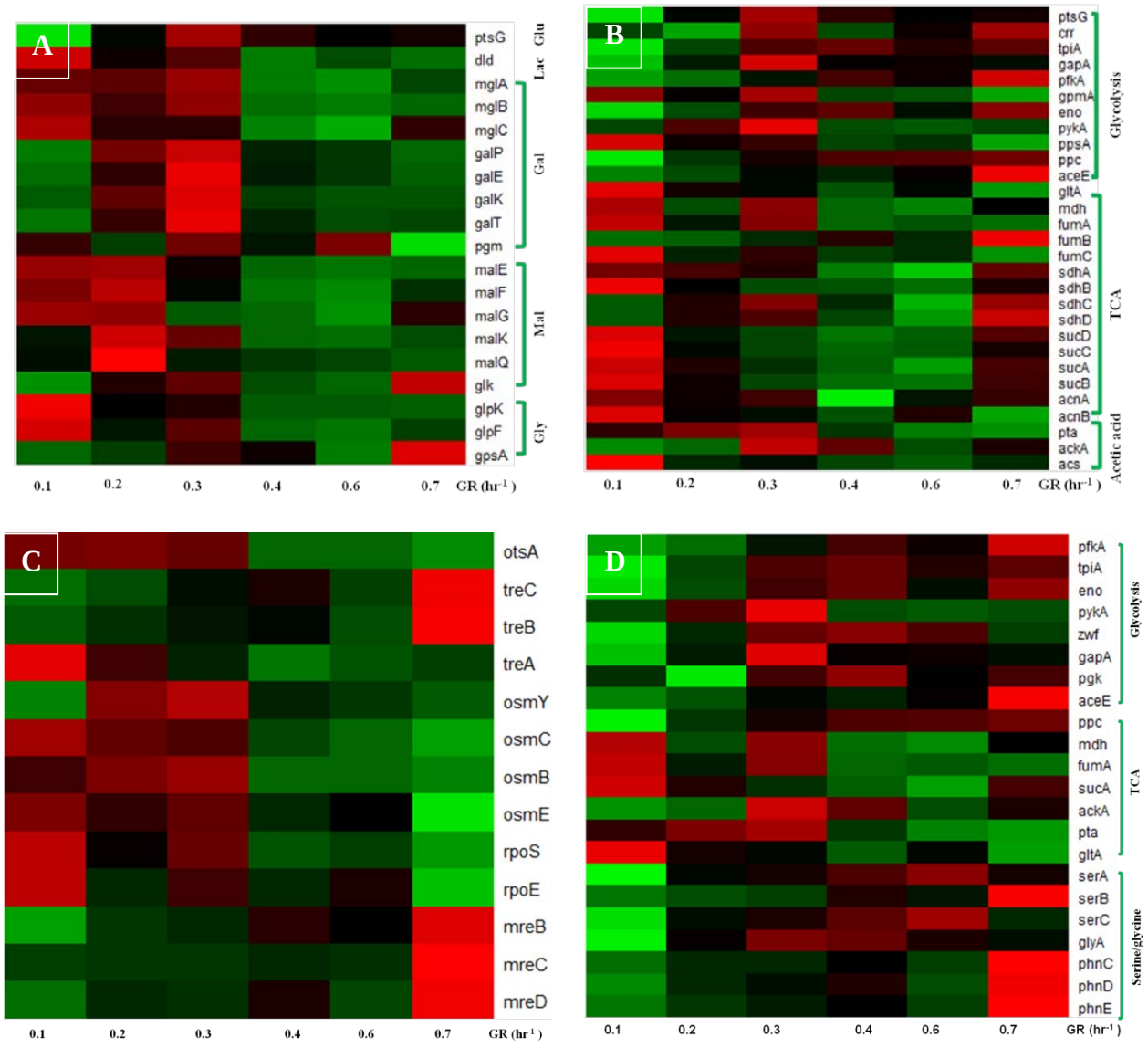

Figure 2.4 The microarray profile of MG1655 cells in mixed substrate media with growth rate variation.

Relative gene expression values from the highest (red) to the lowest (green) are shown. (A) Transporter regulon genes profile; (B) activities of TCA cycle and glycolysis pathway; (C) gene profiles of osmosensors, anti-stress and cell morphology related genes; (D) The activities of central metabolism network and serine/glycine pathway.

peaked at the highest dilution rate (0.7/hr). In light of the cell volume data (Figure 2.3A), this result suggests that active cell volume adjustment is coupled with higher MC and growth rate.

Finally, we examined the expression level of serine/glycine pathway genes, which represents an alternative pathway to provide efficient ATP generation with economical space occupancy of enzymes in rapidly proliferating mammalian cells (Vazquez, 2011). As shown in Figure 2.4D, the serine/glycine genes are upregulated at high dilution rates (0.4~0.7/hr). This data implies that a selection of metabolism pathway switch is present both in rapidly proliferating eukaryotic and prokaryotic cells (Vazquez, Liu et al. 2010; Vazquez and Oltvai 2011). Moreover, similar to what we found previously in glucose-limited culture (Vazquez, 2008), most of the genes in glycolysis are more expressed in the fast cell growth phase that coincides with the activation of CCR.

Taken together, the transcriptiom data indicate that CCR's activation is associated with the activation of the glycolysis pathway and the serine/glycine pathway activation. In fast growth phases, with a concomitant cell morphology and cell volume adjustments, MC changes are also associated with high activities of osmosensor genes (Figure 2.4C), implying that osmosensing may act as a potential cofactor of cell homeostasis.

2.3 DISCUSSION

CCR is one of the most important regulatory mechanisms in bacteria. It is the determining factor that ensures that the cell relies on its preferred substrates to achieve maximum (Muller, Petruschka et al. 1996; Liu, Durfee et al. 2005; Gorke and Stulke 2008). CCR was evident in the form of sequential substrate consumption in our previous study (Figure 2.1D).

More importantly, the mathematical modeling, FBA with MC constraint (FBAwMC) correctly predicted the hierarchy of substrate consumption without including any prior knowledge of CCR (Beg, Vazquez et al. 2007). This discovery prompted us to study the relationship between CCR and MC.

To confirm that sequential substrate uptake is due to intrinsic CCR regulation instead of the addition effects of single substrate consumption behavior, we conducted batch culture experiments with single substrates and compared to the results of the mixed substrate study. Firstly, much faster cell growth, substrate consumption and faster acetic acid secretion were observed in mixed substrate-than in the single substrate cultures (Figure 2.1). Moreover, the substrate consumption rate of each substrate in the single substrate culture did not recapitulate what was seen in the mixed substrate medium (Figure 2.1 G and H). This suggests the presence of repressive effects in mixed substrate culture. Additionally, microarray data of cells cultured in mixed substrate medium (Figure 2.2, OD_{600nm}=0.2) supports that CCR was governing the sequential substrate uptake by regulating the transporter genes. High activities of genes in the central metabolism pathway in mixed substrate were also observed. These data demostratesthat CCR is involved in the sequential substrate uptake regulation to achieve the highest growth rate, as predicted by FBAwMC (Beg, Vazquez et al. 2007).

However, the relationship between CCR and growth rate has still not been defined by these studies. We proposed that faster cell growth and substrate consumption is due to the derepression of transporter genes under CCR regulation in the mixed substrate media culture. It has been found that cells consume the same substrate faster in mixed culture- than in single carbon-limited growth media at the same growth rate (Kovárová-Kovar and Egli 1998; Covert and Palsson 2002). It suggests that cells under CCR regulation achieved growth advantage.

These findings prompted us to investigate the relationship between CCR governed substrate consumption behaviors and growth rates. Continuous feed chemostat experiments were conducted firstly to study the CCR effects at different growth rates, as shown in Figure 2.3. In the slow growth phase (0.1~0.3/hr), cells take up all the substrates simultaneously. With growth rate increasing, cells start to consume glucose preferentially followed by a limited utilization of maltose, glycerol, galactose and lactate. The inhibition on the secondary substrates' uptake stabilized at 0.4/hr growth rate. CCR effects become more and more stringent as growth rate increases. The microarray data in Figure 2.4A also shows that the transporter genes were more tightly repressed at higher growth rates (>0.3/hr) except for the glucose transporter gene, *ptsG*. In contrast, most of the transporter genes of the secondary substrates, such as malEK (maltose), galEK (galactose), glpK (glycerol) and dld (lactate) were very active at the slow growth rates, a result that is consistent with the findings of previous studies (Tseng, Hansen et al. 1994; Ihssen and Egli 2005; Liu, Durfee et al. 2005). We therefore reasoned that in slow growth phase, as a carbon foraging strategy, cells activate multiple transporter genes to facilitate substrate catabolism. CCR is only activated in fast growth phase to prevent simultaneous multiple transporters activation while achieving fast cell growth. However, it is not understood why CCR is indispensible for fast cell growth and what is the boundary condition to activate CCR.

As FBAwMC correctly predicted substrate consumption kinetics regulated by CCR in the batch culture of mixed substrate media, we propose that CCR resulted sequential substrate consumption is the best solution under MC constraint to satisfy the needs for fast cell growth (Beg, Vazquez et al. 2007). But the role played by MC in the CCR regulated cell growth is unknown. To study the relationship between MC and CCR, we measured MC at different growth rates. As shown in Figure 2.3A, MC increased with faster cell growth and cell volume expansion

was also observed. Cell volume was found to decrease while cell density was maintained at the highest level of 1.14g/ml after growth rate exceeded 0.4/hr. It seems cells maintain an optimal MC by dividing faster with smaller volume at higher growth rates. Cell density augmentation with growth rate increase had been observed previously in *E. coli, B. subtilis, S. cerevisiae* and mouse lymphoblast (Godin, 2010 ,Bryan, 2010). Cell volume expansion within cell cycle associated with cell density increase was found in *S. cerevisiae* (Godin, 2010). These data indicate that cells are able to sense MC, and cell volume is dynamically adjusted during cell growth. Cell growth rate and buoyant density was previously found to be determined by the osmolarity of the culture media. In those studies, it was proposed that cell volume was regulated by osmosensing and transporter adaptive regulation. (Kubitschek, 1984; Baldwin, 1988; Baldwin, 1995). Although the osmolarity of the mixed substrate culture media in our study was not determined, the microarray data (Figure 2.4C) showed osmoregulation was more active in the slow growth phase. Also cell stress level (or stringent response) was negatively correlated with CCR activation. Taken together, we deduced that with increasing mass accumulation from faster cell growth, cells tend to expand cell volume to accommodate the extra biomass. CCR is activated to prevent unnecessary protein synthesis and substrate uptake to maintain an optimal MC level.

However, the consumption of secondary substrates were under less rigid CCR in the continuous feed chemostat culture than in substrate limited batch culture of mixed substrate media. The secondary substrates, such as glycerol and maltose were still consumed at fast cell growth rates (>0.3/hr) in the chemostat culture. The less restrictive CCR effects on second substrate consumption was also observed in the chemostat experiments with other combinations of carbon substrates culture media (Lendenmann, 1996). CCR potency is stronger in limited

substrate culture than in chemostat culture because glycerol and maltose were not consumed at all at growth rate ~ 0.7/hr at 4^{th} hr as shown in Figure 2.1B and D. It shows the potency of transient CCR activation is more stringent than stabilized CCR observed in the chemostat culture. We propose that with more potent CCR, cells maximizes nutrient uptake at maximum rate when substrates are limited.

Of note, as one of the indexes of glycolysis pathway activity, the kinetics of acetic acid secretion upon growth rate variation (Figure 2.3B) is different from that of previous reports that the acetic acid overflow starts after the growth rate is higher than ~0.3/hr in glucose culture (Nakano, 1997,Valgepea, 2010). This might be due to a difference in the culture media. Compared to the kinetics of acetic acid secretion observed in batch culture of mixed substrate medium, as shown in Figure 2.1 B and C, the highest growth rate, 0.7/hr was not accompanied with the highest acetic acid concentration. It shows that acetic acid concentration may reflect the synergetic effects of acetic acid production and consumption. In the chemostat culture (Figure 2.3B), acetate production potential, acetic acid concentration/OD increased at 0.2/hr and 0.7/hr respectively and the highest acetic acid production potential appeared at the highest growth rate, 0.7/hr. The microarray data (Figure 2.4 B) also supports that acetic acid pathway is highly active at the slow growth phase, 0.2~0.4/hr, while its uptake is repressed in fast growth phase which might be due to CCR.

Taken together, our study advances a novel interpretation of CCR in fast growing cells: CCR is activated to achieve an optimal MC in fast growing phase. As a physical constraint, the threshold of optimal MC is more susceptible to be exceeded at high growth rates. To prevent excessive MC level from curbing cell growth, CCR is necessarily activated to prevent simultaneous activations of a wide spectrum of transporter genes and substrate consumption.

Cell volume also dynamically adjusted to ensure optimal MC level at corresponding growth rate. We propose that CCR acts as a protective mechanism that prevents the intracellular MC from exceeding the threshold that would interfere with physiological processes in fast growing cells. Further support for MC regulated CCR will be provided by studying the physiological responses of cells with disrupted CCR or/and manipulated MC. These results are introduced in the following chapters.

2.4 MATERIALS AND METHODS

Bacterial strains and growth conditions

In this study, the wild-type *E. coli* MG1655 strain was used. The growth experiments used M9 minimal medium containing individually are of the five carbon sources including glucose, maltose, galactose, L-lactate, and glycerol or mixed-substrate medium. Before inoculation, *E. coli* cells were routinely cultured with agitation at 200rpm, 37°C in Luria-Bertani broth (Teknova) O/N from a glycerol stock, or from an LB-agar plate. Cell inoculation was carried out in a 2-liter bioreactor with 1.2-liter working volume (Labfors, Infors, Switzerland) with initial OD600nm~=0.035. The 1 x M9-minimal salts media was supplemented with $MgSO_4$ and $CaCl_2$ to final concentrations of 2mM and 0.1mM, respectively. In single substrate culture experiments, the concentration of substrates was 0.2% w/vol. In mixed substrate culture experiments, five substrates were added (glucose, glycerol, galactose, lactate and maltose) and each of the substrates had the final concentration of 0.04% w/vol. All the carbon sources (used in equal ratios) were filter sterilized and added to the growth medium at a final concentration

equivalent to total of 0.2%. For these growth experiments, the dissolved oxygen was set at 100% initial value, and sterile air was continuously sparged into the medium. Growth parameters, such as pH, pO2, temperature, and agitation were continuously monitored through microprocessor probes. Samples were collected at 30-min intervals to document various growth phases and extracellular substrate concentrations and to assess the transcriptome state. For chemostat experiments with growth rate variations, sterile mixed substrate media was continuously pumped in and out of the reactor tank at different rates to keep the growth rate at each specific value ranging from 0.1 to 0.7/hr. The growth rate was adjusted every 24 hr and samples were collected for OD, cell size, cell density and microarray analysis.

Cell growth and growth rate calculation

The cell growth data were collected at 30min intervals and 150µl aliquot of the cell cultures were measured by a photometer (Eppendorf) at OD_{600nm}. The growth rate was calculated as:

$$GR = {\ln\left({OD_t}/{OD_{t-1}}\right)}/{\Delta t}$$

Where GR denotes the growth rate at t (hr^{-1}), OD_t: the OD_{600nm} measured at t, and Δt: the sampling interval (hr).

Microarray Sample Collection

For the chemostat culture experiments, cells were sampled at every 24 hrs after the dilution ratewass adjusted. The whole cell culture volume (45 ml) was mixed with 5 ml of ice-cold stop-solution (5% water-saturated phenol in absolute ethanol), and a cell pellet was obtained by centrifugation at 4,500 × *g* for 10 min at 4°C, followed by flash freezing of pellets with liquid

nitrogen. The pellets were stored at –80°C until further use. RNA was isolated from the frozen cell pellets by using Epicenter's Masterpure RNA isolation kit (using the manufacturer's product manual). The samples were also treated with DNase for 1hr at 37°C to remove DNA contamination in the RNA samples. Ten micrograms of all RNA samples was processed for transcriptome analysis using *E. coli* Affymetrix microarray chips by the Microarray Resource Centre, Department of Genetics and Genomics at Boston University School of Medicine (www.gg.bu.edu/microarray/index.htm).

Microarry data processing

The individual arrays were also normalized with MAS5 procedure, which is Affymetrix's recommended then followed by qspline; and cross-array normalization is done using R's version of dchip. Relative gene expression values from the highest (red) to the lowest (green) are shown.

Cell density measurement with Ficoll gradient

The Ficoll gradient was prepared by dissolving the Ficoll 400 powder (GE Healthcare) in 1×PBS to achieve ~ 60%w/v concentration. The density of the solution was measured with a densitometer, Densito 30PX (Mettler Toledo). The most condensed Ficoll solution prepared for the experiments was 1.19g/ml (ρ_0). The lower density solutions (ρ_1~ ρ_7) were prepared from ρ_0 solution by diluting the dissolved Ficoll solution with PBS. The densities of the gradient used for the cell separation were, ρ_0- 1.19g/ml, ρ_1- 1.18g/ml, ρ_2- 1.16g/ml, ρ_3- 1.14g/ml, ρ_4- 1.12g/ml, ρ_5- 1.10g/ml, ρ_6- 1.08g/ml, ρ_7- 1.06g/ml. 0.5ml of each individual gradient solution were gently layered into a 4.5ml centrifuge tube (Beckman, 344062) from the heaviest to the lightest solution, respectively. The interface of each two layers was marked on the tube before centrifugation.

In each set of Ficoll gradient experiment, all the cells in the culture media were used for cell density determination and cell growth measurement. 30ml and 20ml of cell culture were

collected at T3 and T6, respectively. The OD_{600}s of the two time points were documented also. The cells were centrifuged at 4,500g x 15min in Beckman Coulter Allegra 15R at 4°C. The supernatant was removed until only ~0.1ml culture media was left in the tube. 0.1ml PBS was added into each tube and the cells were resuspended. The cells were then transferred into the 4.5ml tube with 8 layers of Ficoll gradient. More PBS solution was added into the 4.5ml tube to fill the rest space to prevent cracking during the high speed centrifugation. The prepared tubes were loaded into a SW60 Ti rotor and subjected to centrifugation at 16,000g × 1hr at 4°C in an L8 Ultracentrifuge (Beckman Coulter). The cells distributed into each of the layer that has had the most similar density to the cells. 0.5ml of each layer was transferred into a 70µl UV-Cuvette (BRAND) and the solution was mixed through pipetting. The OD was measured at 600nm with a Photometer (Eppendof) and the background of the same Ficoll gradient solution was subtracted from the readout. The cell density distribution (CDD) was calculated as:

$$CDD_{\rho_i} = \frac{OD_{\rho_i}}{\sum_{i=0}^{7} OD_{\rho_i}}$$

Cell volume measurement

After adjusting the dilution rate of the feeding medium, cells in chemostat culture were sampled several times a day, until after the growth rate has been stabilized. Cells culture media was vortexed for 5 seconds then 20µl cell suspension for each sample was measured by diluting in 20ml suspension solution (Beckman Couldter) then loaded into Multisizer 3 for measurements (Beckman Coulter). Each sample was measured twice to determine cell volume and cell number by Beckman Coulter Multisizer 3.

Statistics

Values are expressed as the mean ± SEM. Data are plotted in Graphpad Prism5 (Graphpad Scientific). Intergroup differences were assessed by one-way ANOVA or t-test. * : $p<0.05$ represents significant difference between groups or samples.

2.5 ACKNOWLEDGEMENT

The chemostat experiments could not have been finished without the help from Krin Kay, Jiangxia Liu and Emily Ostrin. Qasim Beg also helped me to set up the initial fermenter experiments. Figure 2.2 data was obtained from the previous study, (Beg, 2007 #234) and my thanks go to Qasim Beg who performed the microarray experiments in mixed substrate culture.

3.0 INHIBITING CELL GROWTH AND SUBSTRATE CONSUMPTION BY INTERFERING WITH CCR

3.1 INTRODUCTION

As we have discussed in Chapter 2, CCR has been found to regulate substrate consumption in batch culture experiments. The CCR controlled sequential substrate uptake enables cells to achieve the maximum cell growth, as indicated e.g., by the precise activation of transporter genes to facilitate the observed substrate consumption switch. Therefore, we next aimed to study the physiological significance of CCR in cell growth by interfering with it.

In previous mixed substrate batch culture, there were glucose-, mixed substrate and glycerol consumption phases (Figure 2.1D). Maltose started to be consumed after glucose was used up by the end of the 4^{th} hr of growth. Maltose transport and catabolism are dependent on the maltose operon genes. As introduced in 1.1.5, maltose regulon genes can be activated by the universal transcription factor, cAMP-Crp through its binding to the operon's promoter sequence and/or by maltotriose, a more specific inducer which only activates the maltose regulon transcription factor, MalT.

We hypothesize that CCR under MC constraint results in the maximum cell growth in mixed substrate media. By disrupting CCR through the inappropriate activation of maltose regulon, we aim to investigate: firstly, if CCR in the mixed substrate culture can be relieved to

activate the maltose regulon genes; secondly, how CCR disturbance affects cell physiology including cell growth and substrate consumption; lastly, whether MC alteration is associated with CCR interference.

3.2 RESULTS

3.2.1 Establishing a GFP reporter system for maltose regulon activity measurements

3.2.1.1 Maltose regulon genes

The Crp origon is the largest external signal sensitive topological module in *E. coli* (Balázsi, Barabási et al. 2005) which contains feed-forward loops in the *E. coli* transcriptional regulatory network (TRN). It comprises numerous genes and operons. Operons include the arabinose-, maltose-, melobiose-, fucose-, and galactose regulon genes. The intracellular level of cAMP regulates the expression of many genes in this origon. Those genes and operons are controlled either positively or negatively by the *crp* gene product, the cAMP-sensitive transcription factor, CRP. The transcription of *crp* gene is also under self-regulation by the CRP-cAMP complex that binds to a specific site located downstream from its transcriptional start site (Okamoto and Freundlich 1986; Hanamura and Aiba 1991). The activation or repression of transcription by CRP requires its binding to cAMP and undergoing allosteric conformational change, which is essential for its binding to DNA at CRP binding sites (Mukhopadhyay, Sur et al. 1999).

The maltose operon is one of the operons that can be activated by cAMP. In the operon, the maltose transporter genes MalKFGE, constitute a maltose transport system that is a member

of the ATP-Binding Cassette (ABC) superfamily of transporters (Wu and Mandrand-Berthelot 1995; Schneider 2001; Böhm, Diez et al. 2002). MalE (also called MBP, maltose binding protein) is the periplasmic maltose-binding protein. MalF and MalG are the integral membrane components. MalK is the ATP-binding component of the ABC transporter. The hydrolysis of ATP on MalK is associated with maltose being transported crosses the membrane (Böhm, Diez et al. 2002; Joly, Bohm et al. 2004; Orelle, Ayvaz et al. 2008). The mutations in the *malK* gene resulted in loss of transport activity without affecting protein stability (Panagiotidis, Reyes et al. 1993).

As shown in Figure 3.1 A, the expression of the *malE* and *malK* operons is activated by MalT and cAMP-CRP (Hofnung 1974; Chapon 1982; Vidal-Ingigliardi and Raibaud 1991). Inactive (ATP-bound) MalK inhibits the activation of MalT by competing with the binding of the inducer, maltotriose, to MalT (Hofnung 1974; Böhm, Diez et al. 2002; Joly, Bohm et al. 2004). MalK with hydrolysed ATP no longer associates with and inhibits MalT (Panagiotidis, Boos et al. 1998). MalY and Aes also inhibit activation of MalT by competing with maltotriose (Reidl and Boos 1991; Schreiber, Steegborn et al. 2000; Schlegel, Danot et al. 2002). MalK activity is also subject to inducer exclusion by $EIIA^{Glc}$ through protein-protein interaction (Dean, Reizer et al. 1990). Besides the activity regulation at protein level, malT is also repressed by Mlc (Decker, Plumbridge et al. 1998; Lengsfeld, Schonert et al. 2009) and activated by cAMP at transcriptional level (Alonzo, Heyde et al. 1998; Chagneau, Heyde et al. 2001). Both maltotriose and cAMP activates the maltose regulone genes, and the detailed functions of each maltose gene are listed in **Table 1 (extracted from www.Ecocyc.org).**

Table 1 The functions of maltose regulon genes

Gene Name	Functions
male	ATP-binding component of transport system for maltose. MalK inhibits the activation of MalT by competing with the binding of the inducer maltotriose to MalT
malK	ATP-binding component of transport system for maltose. MalK inhibits the activation of MalT by competing with the binding of the inducer maltotriose to MalT
malS	Gene encoding the periplasmic α-amylase. The periplasmic alpha-amylase degrades maltooligosaccharides with chain lengths longer than 6 glucose units, which can then be transported through the cytoplasmic membrane. The enzyme hydrolyzes internal 1,4-glucosidic linkages. The enzyme is thought to contain Ca^{++} binding sites
malt	Positive regulator of MAL-regulon. This regulator participates in controlling several genes involved in maltose utilization. It binds maltotriose and ATP. It activates the transcription of the *malS* gene and the *malEFG*, *malK-lamB-malM*, and *malPQ* operons
malI	MalI belongs to the GalR/LacI family of the transcriptional regulators. It is a negative DNA-binding transcriptional regulator member of maltose regulon. *malI* regulates the expression of *malXY* adjacent and divergently operon. It binds maltose as an inducer
malX	MalX, the maltose-glucose PTS permease, belongs to the functional superfamily of the phosphoenolpyruvate (PEP)-dependent, sugar transporting phosphotransferase system (PTS). The PTS transports and simultaneously phosphorylates its sugar substrates in a process called group translocation. MalX presumably takes up exogenous sugar, releasing the phosphate ester into the cell cytoplasm in preparation for metabolism. The MalX (Enzyme $IICB^{Mal}$) use glucose and maltose as substrate
malZ	Maltodextrin glucosidase is the product of the *malZ* gene. This enzyme catalyzes the degradation of short malto-oligosaccharides, ranging from maltotriose to maltoheptaose. The enzyme also play a role in regulating the intracellular level of maltotriose
malP	Codes for enzyme maltodextrin phosphorylase. The maltodextrin phosphorylase has a high affinity for short, linear alpha-1,4 linked oligoglucosides. The shortest maltodextrin which can be readily phosphorylyzed is maltopentaose. The enzyme is dependent on pyridoxal phosphate for activity

3.2.1.2 Constructing a GFP reporter system of maltose regulon genes

As introduced in 2.1.1, maltose was taken up in the second consumption phase, after glucose has been used up from the mixed substrate batch culture. CCR regulation in the sequential substrate uptake has been proven. To understand the importance of CCR in fast growing cells, we aimed to perturb CCR by activating the transporter genes of the secondary substrate with inducers when these genes are supposed to be repressed by CCR in a mixed

substrate culture. To meet this purpose, we constructed a GFP reporter system that tracks the activities of maltose regulon genes (Figure 3.1A) upon induction.

The GFP reporter system was constructed by integrating the promoter sequences of maltose regulon genes upstream of the GFP in the low copy vector, pCS21 (Figure 3.1B) (Zaslaver, Mayo et al. 2004). As a result, GFP synthesis is positively correlated with promoter activities. To achieve an optimal response, we built two separate sets of constructs. One is referred to as the 'LF' or long form, and the other as the 'SF' or short form. The L forms contain the promoter regions of operons T, P, Z, S, E, and K from 100bp 5' upstream from the TF binding site to 100bp into the first ORF. The S forms end at the beginning of the first ORF. The commercially available constructs (Alon Zaslaver 2006) for promoters of malE, S, I and X were purchased from Open Biosystem and were referred as 'OB'. Subsequently, we transformed the cells with the constructs and established *E. coli* MG1655 clones that stably harbor the various promoter-GFP constructs.

To examine their sensitivity upon induction, inducers (4mM cAMP and 200μM maltotriose) were applied to examine how the 'LF', 'SF' and 'OB' constructs perform in 0.2% glucose. malE, K, S, T, I, X, P and Z were tested and the GFP signal was compared between the groups with or without the inducers. Upon induction, maltose transporter malEKGS are supposed to be significantly activated by cAMP-CRP due to their positions in the regulon as shown in Figure 3.1A (Vidal-Ingigliardi and Raibaud 1991). In contrast to expectation, we found that only 'LF' malE, K, S and T responded to inducers (the solid lines) with significant activation of GFP signal compared to the controls without inducers treatment (the dotted lines) (Figure 3.3 A, C, E, G). The GFP fluorescence signal was also confirmed with flow cytometry (data not shown). The difference of GFP response implies that the length of the promoter sequence is correlated with

promoter activities. It can be expected that the required concentration of inducers to activate each individual gene may differ. Also, no significant GFP upregulation was observed in pCS21 (empty vector containing) cells upon induction. As a low basal GFP level is desirable for promoter activity measurements, we only used the 'LF' constructs for subsequent experiments.

Next, to fine tune the inducers concentration and to study the dynamics of the GFP reporter system upon induction, we applied different concentrations of inducers to the GFP reporter system in 0.2% glucose culture. Glucose media was used because we aimed to find the optimal concentrations of inducers by monitoring the relief of stringent repression on maltose transporter genes caused by glucose. As shown in Figure 3.3, panel A and B represent the responses calculated as GFP/OD upon the stimulations of various concentrations of cAMP and maltotriose, respectively. In general, the response to maltotriose appeared later (~at 150min) than in response to cAMP (~at 100min). This is due to the indirect activation of maltose transporter genes through malT by maltotriose. The transporter genes malE and malK respond to the concentrations of maltose and cAMP positively in both low (0.05%) and high (0.2%) concentration of glucose. 4mM cAMP and 200μM maltotriose induced significant GFP signal in malE and malK in 0.2% glucose concentration. As a transcription factor, malT was mildly activated by the inducers in higher glucose concentration, implying that glucose may facilitate malT's activation. It also suggests that malT has a narrow dynamic range of activation. The combination of inducers didn't induce any significant GFP signal in empty vectors pCS21, as shown in black lines in Figure 3.3C. Therefore, we chose 4mM cAMP and 200μM maltotriose as the inducer concentration in all the subsequent experiments.

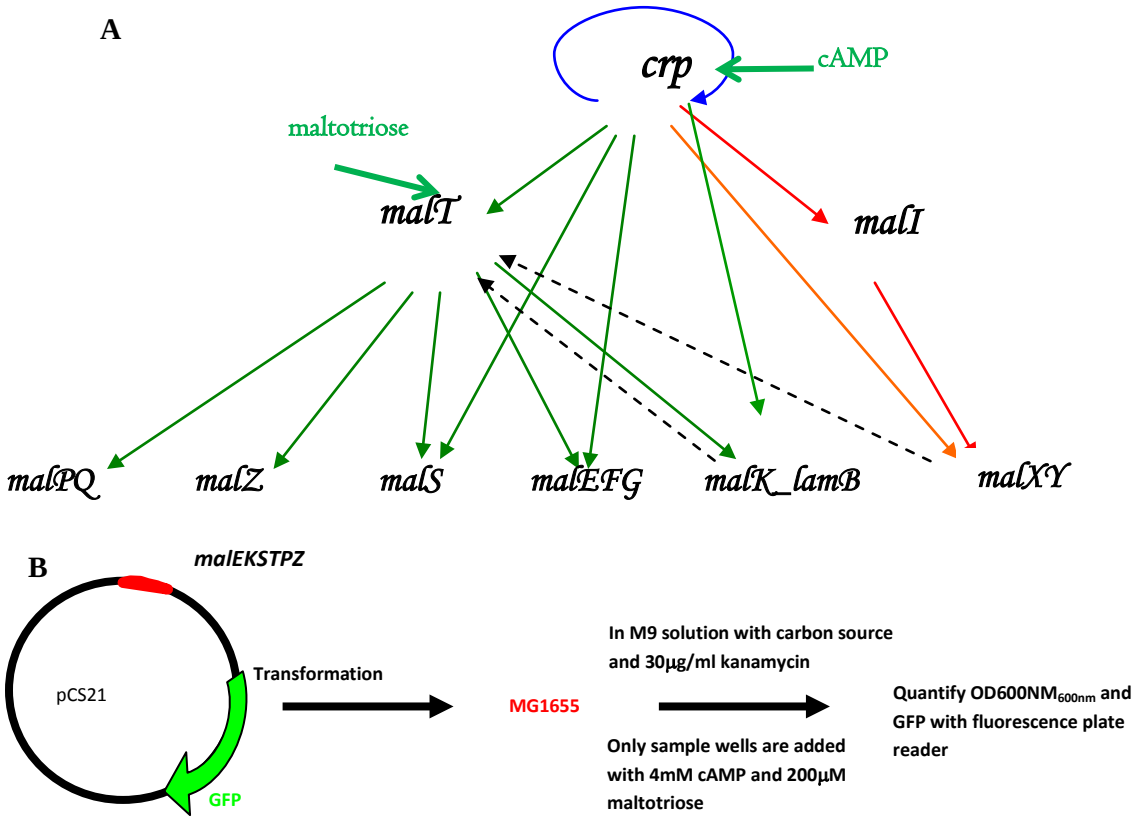

Figure 3.1 The GFP-reporter system for mal-gene activity study

A. In the maltose regulon, upon the activation of crp and malT, downstream genes will be activated including the transporter genes malEFG and malK; green lines: activation; black lines: inhibition through proteins-protein contact; red lines: transcriptional inhibition. **B.** Constructing the reporter strains by integrating the promoter sequences of malEKSTPZ to the upstream of GFP sequence in vector pCS21. The 100 μl O/N cell cultures were added into 1ml M9 solution containing wells. The cells were then cultured for 6 hr at 37°C, 200rpm, and the gene's activity was recorded as the GFP signal collected from the 24 well-plate at different time frequency.

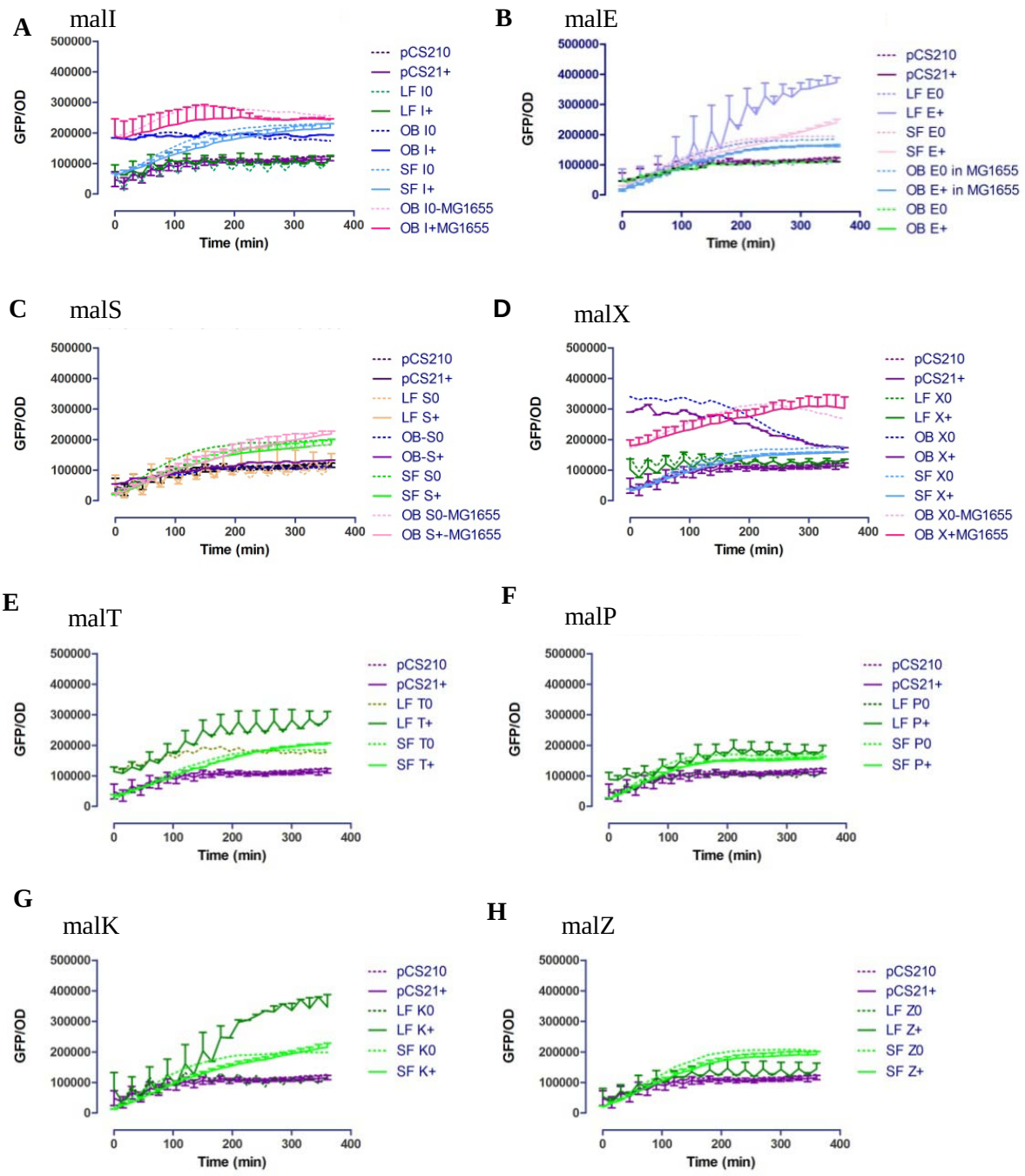

Figure 3.2 Assessing the GFP response of the promoter constructs to be used in glucose 0.2% culture.

The promoters cloned and tested were as follows: OpenBiosystem (OB): the regions between two adjacent ORFs with an extension of 50-100bp into each of the two ORFs (Zaslaver, Mayo et al. 2004); Long form (LF) reporter strains: extension of ~100 bp before the first TF binding site in each case and ~50bp into ORFs; Short form (SF): extension of ~100 bp before the first TF binding site in each case and until the beginning of the ORF. OB constructs were transformed into to two strains: JM109 (OB) and OB-

MG1655 (MG1655) respectively. Induction was induced with 4mM cAMP and 200μM maltotriose in glucose 0.2% and GFP/OD were recorded for 6hr.

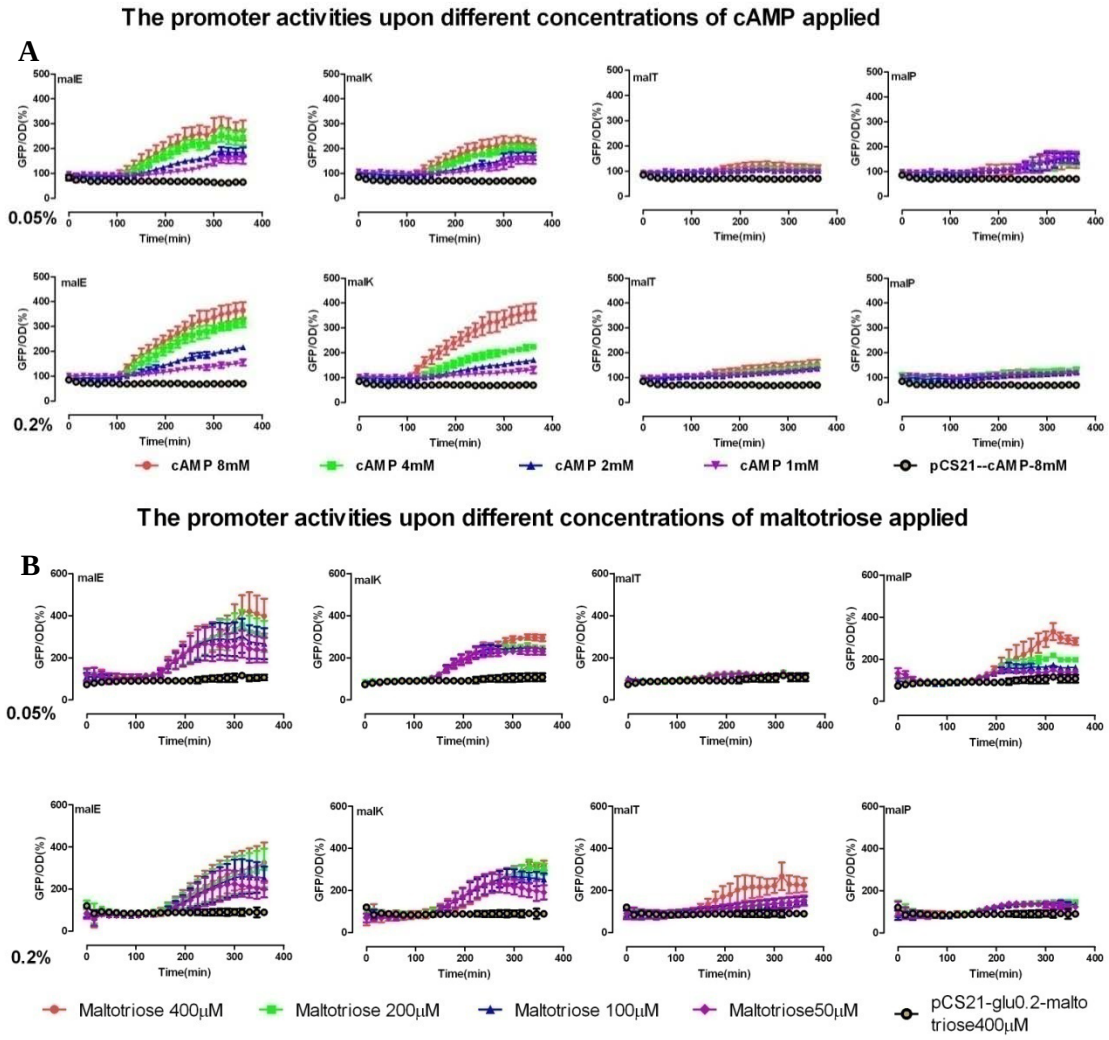

Figure 3.3 Maltose genes' responses to inducer stimulations

A. malEKTP respond to different concentrations of cAMP (A) and maltotriose (B) in 0.05% and 0.2% glucose media. malE and malK respond to cAMP and maltotriose positively. malP and malT respond to cAMP mildly. malK and malT's activation is associated with higher glucose concentration. malP's activation upon cAMP addition is repressed in higher glucose concentration media.

3.2.2 The repression of maltose regulon genes is relieved by inducer to a lesser extent in mixed substrate- than in single substrate-limited growth media

The sequential substrate uptake observed in Figure 2.1D is a result of strict CCR regulation, which is found to be associated with fast cell growth in mixed substrate cultures. Therefore, we hypothesized that the repressions caused by CCR should be more stringent in mixed substrate- than in single substrate-limited cell cultures. To test this hypothesis, we examined the gene activities of the maltose regulon upon their induction in single- and mixed substrates cultures. GFP and OD_{600nm} were measured with plate reader. As shown in Figure 3.4, the ratio of GFP/OD between the cells with or without induction was calculated to evaluate gene activities. We found that promoters of the maltose regulon genes, such as malE and malK, responded actively to the inducers in glucose-, galactose-, and glycerol-limited cultures with 0.2 % w/w concentration (Figure 3.4 A-C). Yet, milder response was seen in lactate- and maltose-limited cultures (Figure 3.4 D, E). malP responded strongly to inducers after 5 hr in lactate unexpectedly (this could be a measurement error because the GFP/OD base line dropped significantly at nearly 5hr culture for unknown reasons). As expected, a delayed and repressed plasmid activation response is evident in a mixed substrate culture, indicating the presence of strict repression against maltose uptake (Figure 3.4F). Of note, the repressed gene activities in mixed substrate cannot be interpreted as higher basal gene activity because the GFP/OD levels in mixed substrate culture were similar to that in the maltose culture (data not shown). As the transporter genes can be activated by the presence of their substrates, cells without inducers might have been induced by maltose in maltose single substrate and mixed substrate media. This may partially explain the milder response observed in maltose (Figure 3.4E) and mixed substrate media (Figure 3.4 F).

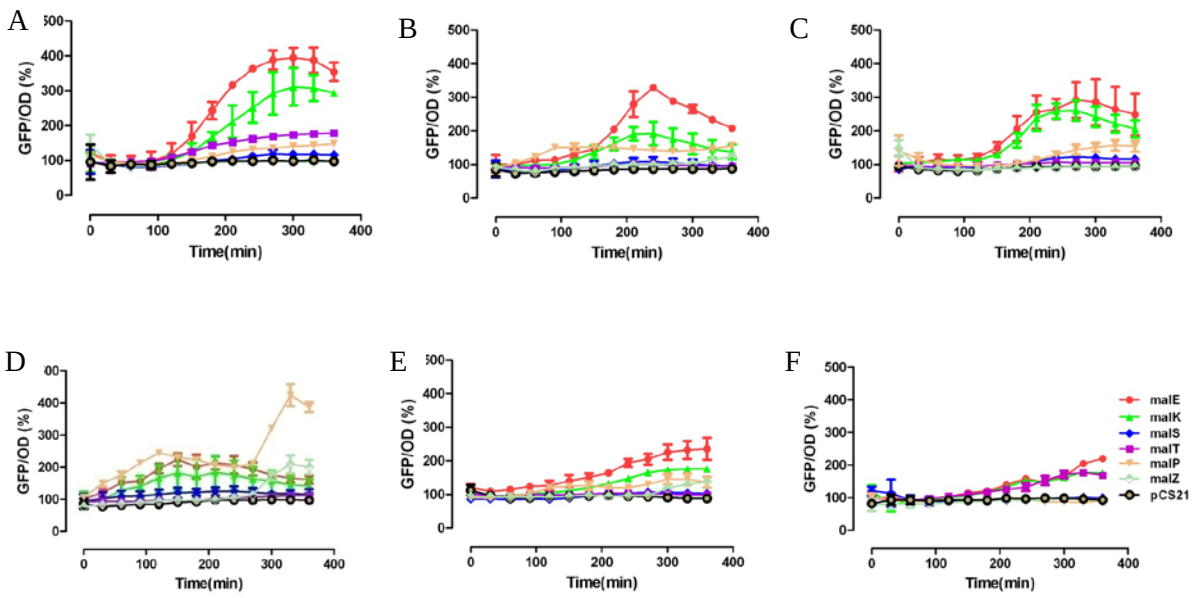

Figure 3.4 Maltose regulon responses to its inducers in different growth media

Response of the maltose regulon genes to induction with 200 μm maltotriose and 4 mM cAMP in (A) glucose-, (B) galactose-, (C) glycerol-, (D) lactate-, and (E) maltose-limited cultures and (F) in mixed substrate culture, all with 0.2% w/w substrate concentration.

These inducer experiments provide clues about the different mechanisms of the maltose regulon repression. For example, in glucose and glycerol-limited cultures, GFP signal upregulation was seen after the 2nd hr and reached their peak values by the 5th hr. It suggests that the repression on maltose regulon exerted by the presences of the two substrates can be overcome by elevation of intracellular cAMP level. However lactate might exert repression on maltose regulon through cAMP-Crp independent mechanisms, which are reflected by the flattened response (Figure 3.4D). Consequently, the synergetic repressions that exist in the mixed substrate culture couldn't be fully relieved by inducers (Figure 3.4F). More stringent and delayed repression on maltose regulon genes appeared in mixed substrate culture, e. g., significant upregulation of malE activity didn't appeared until ~200min after induction in mixed substrate

media while it occurred at 150min in maltose culture. Interestingly, the activation kinetics of malT in the mixed substrate culture was similar to that in the glucose-limited culture. This might be due to glucose sequestering of the MalT's inhibitor, Mlc, and as a result more MalT could bind to maltotriose to be activated. These results conclusively show that a more stringent repression on maltose regulon genes is present in the mixed substrate culture than in single substrate-limited media, and the repression cannot be fully relieved by the inducers.

3.2.3 Induction by inducers inhibits cell growth of malE strain in mixed substrate and glucose-limited medium but not in other single substrate-limited cultures

It has been found that intracellular cAMP is negatively correlated with cell growth rate in glucose culture (Valgepea, Adamberg et al. 2010). Also, the gene transcript levels of ptsG (the glucose transporter gene) and cyaA (coding adenylate cyclase to synthesize cAMP) are positively and negatively correlated with growth rates, respectively (Yao, Hirose et al. 2011). CCR is also found to be activated at higher growth rates in our study (Figure 2.3B). Therefore, we hypothesized that intracellular cAMP would interfere with CCR and would be detrimental to cell growth.

In order to provide support the for the hypothesis, first we assessed the rate of cell growth in malE construct containing *E. coli* strain upon induction with 4mM cAMP and 200μM maltotriose in mixed substrate- and single carbon-limited cultures. As shown in Figure 3.4, GFP

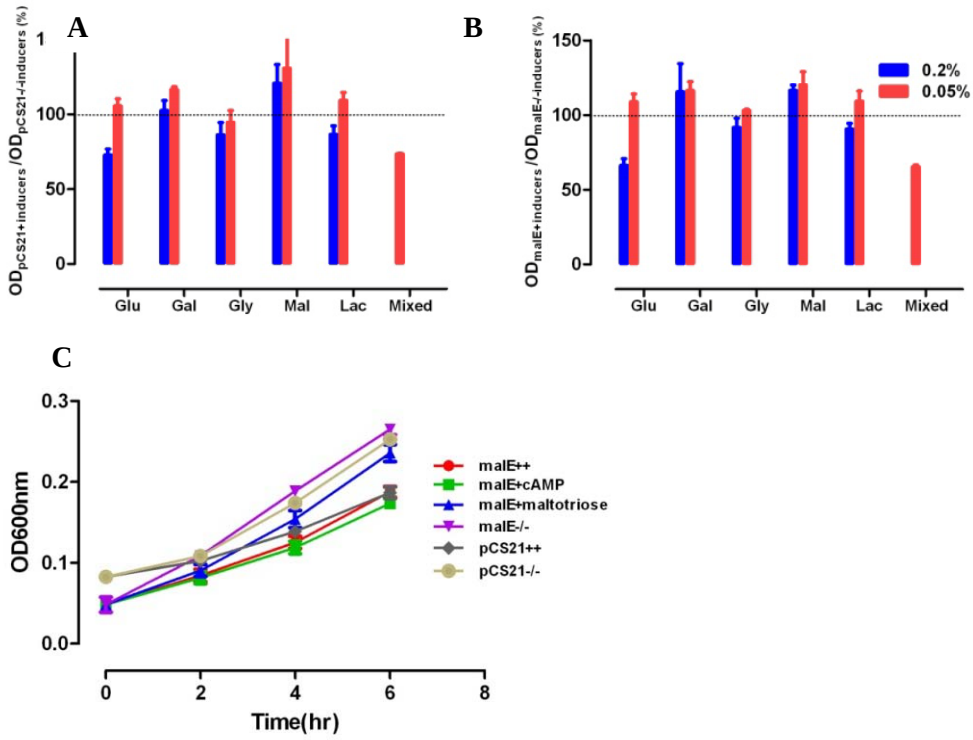

Figure 3.5 Cell growth of GFP reporter strain malE and pCS21 cultured in different substrates.

The OD ratios between cells with and without inducers at 6th hr culture are calculated in (A) empty vector strain, pCS21 and (B) malE. It indicates that significant growth inhibition is present only in glucose (0.2%) and mixed substrate culture for both the control strain, pCS21 and the reporter strain, malE. Cell growth in mixed substrate culture upon inducers addition was determined in malE (C). ++: cAMP+maltotriose; -/-: without treatment. The empty and GFP integrated strains have similar response to inducers. It shows GFP synthesis has no interference on inducers' effects.

signal was determined by a plate reader to verify the activation of maltose regulon genes, including that of malE's activation. Cell growth was represented as the ratio between OD_{600nm} of cells with and without inducer treatment at T6 (Figure 3.5 A and B). We found that malE (promoter-GFP) and pCS21 (empty vector) plasmid-containing cells displayed very similar growth in all the culture conditions upon induction (Figure 3.5 A and B). This finding supports that the growth phenotypes produced by induction were not due to GFP synthesis. However, the induction induced a mild growth inhibition in low concentration of glycerol and lactate, but not

in high substrate concentration-limited media, except in glucose. Interestingly, cell growth was even enhanced in galactose and maltose upon induction in both concentrations. This implies that the activation of maltose regulon genes facilitated maltose utilization in maltose media. The inducers also activated galactose transporter genes to increase galactose uptake (Ferenci 1996).

In contrast, cell growth in 0.2% glucose-limited and mixed substrate cultures were significantly lower compared to that seen in the other 0.2% substrate-limited culture (Figure 3.5 A and B). The growth inhibition disappeared in 0.05% glucose medium upon induction, implying that the inhibition is positively correlated with glucose concentration (Figure 3.3A). In conclusion, cell growth of the malE *E. coli* strain was significantly inhibited upon maltose regulon induction in mixed substrate media even with possible growth benefits gained from the uptake of maltose and galactose. It is probably due to the inhibition on cell growth caused by glucose after CCR is disrupted.

To further characterize the effects of inducers on cell growth observed in the mixed substrate culture, a cell growth study was conducted by treating cells with the inducers individually. As shown in Figure 3.5C, growth inhibition in mixed substrate culture was mainly due to cAMP because growth arrest only appeared in cAMP or cAMP plus maltotriose (++) treated cells. The empty vector strain, pCS21 responded to inducers similarly as the malE strain, supporting the notion that the growth inhibition was caused by inducers and not by GFP synthesis. Collectively, the observations show that the addition of cAMP hinders malE cell growth in mixed substrate, probably mainly by interfering with glucose uptake by the cells.

3.2.4 Inducers inhibits glucose, maltose and glycerol uptake in malE cells cultured in mixed substrate media

To further investigate the hypothesis that the cell growth delay in mixed substrate culture upon induction is mainly due to the inhibition of glucose uptake, substrate consumption was determined in the malE strain. The culture media of malE strain cultured in 24-plate culture with induction was collected to determine the substrate consumption kinetics. There are five substrates in the mixed substrate media but only glucose, glycerol and maltose were subjected to concentration measurements. As shown in Figure 2.1D, these substrates were consumed in each of the three phases of the sequential substrate uptake. By studying their consumption kinetics, the level of disruption of CCR can be evaluated. In Figure 3.6, the left column (Figure 3.6 A, C and E) represents normalized (to OD) substrate concentrations, while the right column (Figure 3.6, B, D and F) displays the absolute concentration results. The two sets of data also displayed similar inhibitory effects on substrate consumption by inducers. As expected, cAMP plus maltotriose or cAMP alone were observed to significantly inhibit glucose consumption from 2^{nd} hour on (Figure 3.6 C and D). Interestingly, the consumption of maltose was also inhibited from the 2^{nd} hr (Figure 3.6 A and B) while glycerol's consumption attenuation was observable at the 4^{th} hr time point (Figure 3.6 E and F). To perform a clear comparison, the substrate concentration in fermenter batch culture experiment (Figure 2.1 D) was plotted in Figure 3.6 B, C and D. As shown in Figure 3.6 B, maltose consumption in fermenter batch culture experiments was held till the 4^{th} hour. Yet, in 24-well plate culture, which display slower cell growth rate, maltose was consumed from the 2^{nd} hr on (malE -/-). This is also consistent with our previous discovery that CCR's potency is positively correlated with growth rate (Figure 2.3B). Glycerol and glucose consumption seemed not to be affected by growth rate as much as maltose consumption (Figure

3.6 D and F). These results demonstrate that the attenuated cell growth observed in the mixed substrate culture upon induction is due to a hindered uptake of glucose, glycerol and maltose. The inhibition on substrate uptake may also equally exist for galactose and lactate. In short, disrupting CCR by activating the secondary substrate' transporter genes in mixed substrate culture results in attenuated cell growth and substrate consumption in malE cells.

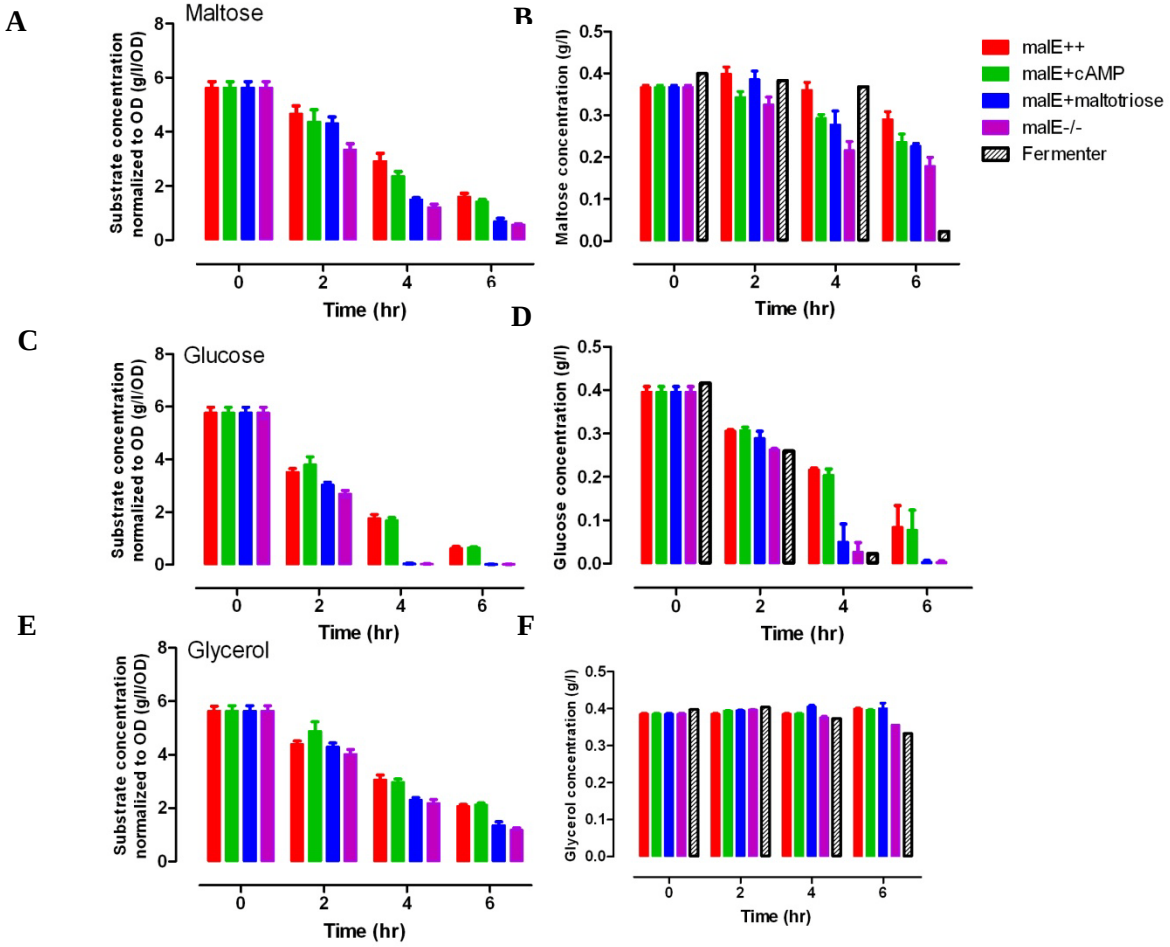

Figure 3.6 Substrate consumption of malE in mixed substrate culture upon inducers' addition in 24-well plate culture.

Glucose, maltose and glycerol consumption were determined by substrate kit experiments. The substrate concentrations were normalized to OD as shown in A, C, E. The absolute substrate concentration has been shown in B, D and E.

3.2.5 Inducers affect cell physiology in fast growing MG1655 cells upon CCR disruption in mixed substrate media

It has been observed that substrate consumption and cell growth inhibition of malE cells were caused by the inducers in the mixed substrate culture. To further inspect whether this inhibition was caused by the interaction between inducers and the plasmid pCS21, we repeated the experiments with MG1655 cells in mixed substrate culture. Cells were cultured in plate and flasks respectively. Cell growth both in flask and 24-well plate cultures were examined upon inducer treatment. As shown in Figure 3.7 A, cell growth of MG1655 upon induction recapitulated the kinetics observed in malE cells (Figure 3.5C) in that cAMP or cAMP plus maltotriose caused attenuated cell growth. It shows the growth inhibition upon inducers addition is not due to inducer-plasmid interaction in malE cells. Moreover, no observable growth inhibition upon induction was detected in MG1655 cells cultured in 24-well plate (data not shown).

We reasoned that interfering with CCR is detrimental in fast growing cells only in which substrate consumption is under a rigid CCR control. To test this hypothesis, we determined substrate consumption of MG1655 cells in 24-plate and flask culture and plotted the results together with the batch culture results (Figure 2.1D). The substrate consumption kinetics (Figure 3.7B) demonstrated that the strictest hierarchy of substrate consumption occurred in fermenter batch culture because of the most delayed maltose uptake was only initiated after 4^{th} hr (0.368g/l at T4). Similarly, in flask culture, maltose consumption was restrained until the 4^{th} hr (0.342g/l). Yet in a plate culture, maltose uptake started from 2^{nd} hr (0.29g/l by 4^{th} hr) and glycerol was

taken up gradually from the 2nd hr (0.363g/l). Combined with the cell growth data (Figure 3.7A), it can be inferred that interfering with CCR with inducers can cause more significant cell growth inhibition in cells displaying sequential substrate uptake. This is also supported by the discovery of the correlation between CCR potency and cell growth rate (Figure 2.3B). We reasoned that fast growing cells rely on CCR more than slow growing cells to govern optimization of substrate uptake and to achieve maximum cell growth. Therefore, detrimental effects will occur if CCR is disrupted.

Next, we examined the substrate consumption of MG1655 cells cultured in flask with growth inhibition caused by inducers (Figure 3.7A). Significant repressive effects were observed in the uptake of maltose and glucose but only mild retardation was observed for glycerol consumption (Figure 3.7C). This may be due to glycerol's intrinsic slow consumption. Inducers have evidently inhibited maltose consumption by the 6th hr and glucose consumption from the 2nd hr. The substrate consumption kinetics also coincides with the results of the substrate uptake study in the malE strain (Figure 3.6). Therefore, cell growth retardation caused by CCR disruption with inducers is resulted from the inhibition of substrate consumption. Taken together, we found that CCR is critical to fast growing cells but not for slow growing cells. It can be inferred that interfering with the more stringent CCR in faster growing cells will cause more severe growth- and substrate consumption inhibition.

As observed before, activations of maltose regulon genes with inducers in mixed substrate culture didn't result in accelerated maltose consumption (Figure 3.6 and 3.7B). It is unknown whether this is due to the repression on transporters' protein levels. To determine the transporter protein level upon induction, we determined the expression of the maltose transporter protein MalE (MBP) by western blot analysis (Figure 3.7 E). MBP level was found to be

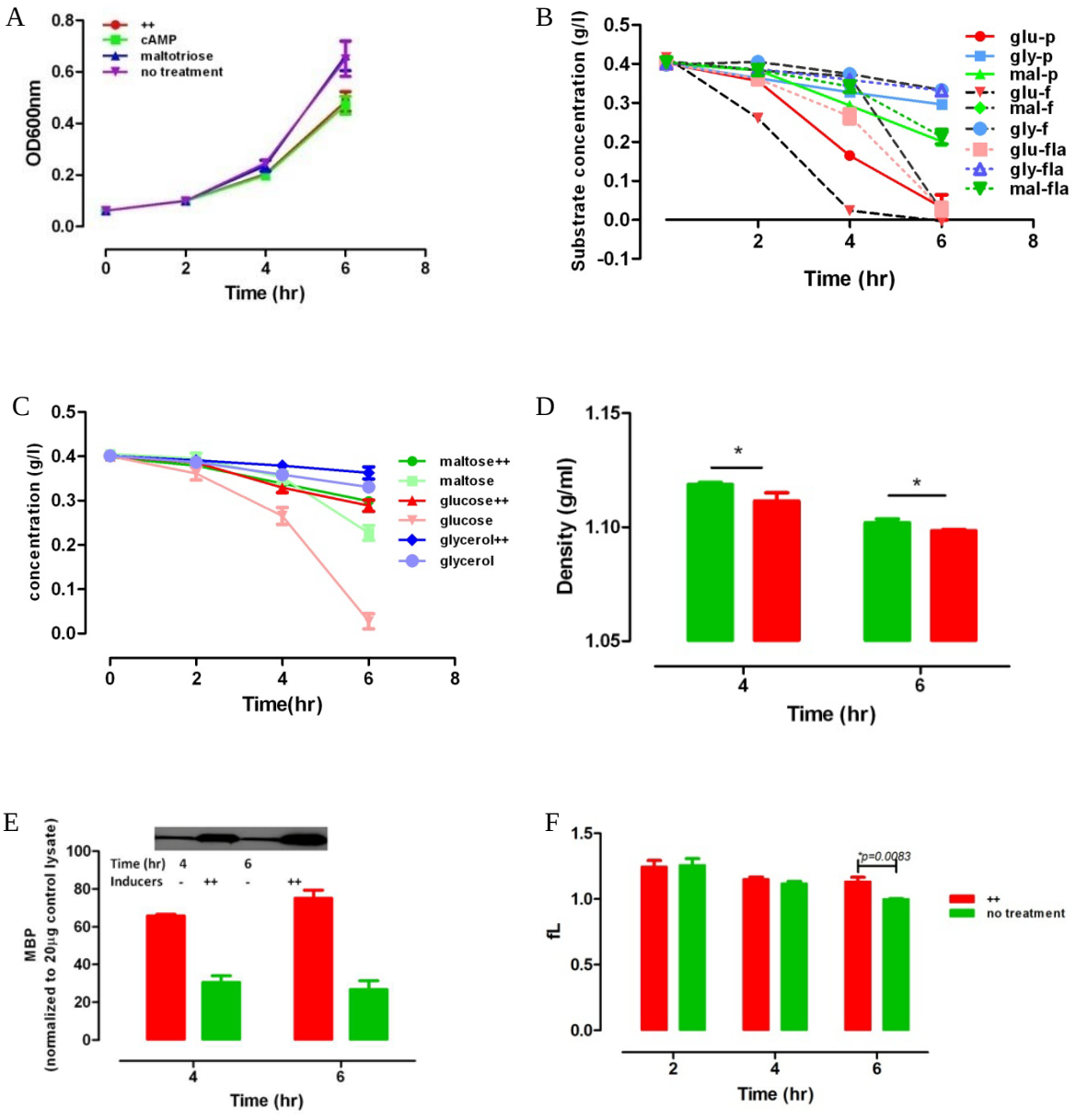

Figure 3.7 Cell growth and substrate consumption are inhibited by inducers in flask culture of MG1655 cells in mixed substrate.

The O/N LB cultures of cells were inoculated into 125ml flask with 15ml M9 media with 0.2% mixed substrate. The initial OD_{600} was ~0.03~0.04 and cells were cultured for 6 hr on a shaker with 200rpm at 37°C. The inducers, 4mM cAMP and 200μM maltotriose were added after 15min culture. Cell growth (A) and substrate consumption (B) were sampled every 2 hr. p: plate culture; f: fermenter culture; fla: flask culture. Cell density (C) and maltose transporter MBP (MalE) level (D) were measured at 4^{th} and 6^{th} hr by Ficoll gradient and western blot respectively. The protein expression level was determined with ImageJ. Cell volume (E) was measured by Beckman Coulter.

significantly increased upon induction at 4^{th} and 6^{th} hrs, respectively. We suspect that the protein levels of other transporter proteins may also be increased upon the induction of the maltose regulon. However, due to the paucity of antibodies against the other transporter subunits, we could not further assess this hypothesis.

As demonstrated in Figure 2.4, transporter synthesis is subjected to CCR regulation in fast growing cells and CCR is activated to prevent sub-optimal MC level. Thus, we hypothesized that a wide spectrum of transporter activation upon CCR disruption deviates MC from the optimal level. To test whether MC and cell volume alteration is associated with CCR disruption, we measured cell density and cell volume of MG1655 cells upon induction of the maltose regulon. The results in Figure 3.7 D proved that MC variation was caused by the induction protocol. Inducers enhanced transporter protein synthesis and cell volume expansion, and decreased cell density (Figure 3.7 D, E and F). Combining these observations, we propose that upon induction synthesizing the transporter proteins of secondary substrates, which were originally repressed by CCR, causes the wasting of the cell's resources, pathway competition and MC variations. All the bio-processes, including substrate consumption are affected to a certain degrees when MC is not maintained within an optimal range. As a result, cells adjust cell volume to accommodate the biomass fluctuation and regain optimal MC. However, before the optimal MC is restored, cell growth is inhibited.

3.3 DISCUSSION

CCR plays an important role in regulating cell growth when multiple substrates are available. The strategy of using the preferred substrate to ensure the maximum cell growth is determined by CCR (Blencke 2003; Liu 2005; Gorke and Stulke 2008). As we discussed in 2.3, CCR is found to be activated when growth rate is high. In this chapter, we focused on studying the physiological consequences of CCR interference, including the influences on MC.

To interfere with CCR, the inducers which activate maltose regulon genes were applied to cells that harbor a GFP reporter system. These results showed that the GFP reporter system responds to cAMP and maltotriose positively even in the presence of glucose (Figure 3.3). Subsequently, we investigated the responses of maltose regulon genes in each of the five single substrates (glucose, galactose, glycerol, lactate and maltose) and in mixed substrate media. Upon induction (Figure 3.4), the GFP signals of maltose regulon genes showed that the repressive effects on maltose regulon genes caused by glucose, galactose and glycerol are more inducer dependent than that on maltose and lactate. This is supported by previous studies (Chapon 1982; Dean, Reizer et al. 1990; Vidal-Ingigliardi and Raibaud 1991; Szabolcs, Sandeep et al. 2007). The milder response observed in maltose media might be due to the fact that the maltose regulon has already been activated by maltose; therefore, the effect of further activation is limited.

Interestingly, a more stringent repression of the maltose genes in mixed substrate was observed upon induction (Figure 3.4 F). The activation of the maltose transporter genes, malE and malK, were delayed and more attenuated in mixed substrate culture than in single substrate cultures. The upregulation in malT activation was similar to that observed in glucose-limited culture, and this might be due to the derepression of Mlc repression by EIIB with the presence of

glucose (Nam, Cho et al. 2001; Seitz, Lee et al. 2003). The studies above show that the repressive effects on maltose regulon genes in mixed substrate can't be fully relieved upon the addition of inducers. Moreover, the repressive effects seem to be more stringent in mixed substrate- than in the single substrate-limited cultures.

We hypothesized that cell growth is affected by disrupting CCR when substrate consumption is under CCR regulation in fast growing cells. We found that cell growth of male construct containing cells was inhibited by inducers in glucose-limited- and mixed substrate cultures (Figure 3.5 B and Figure 3.7 A). In contrast, the inhibitory effects were milder in other single substrates and inducers even enhanced cell growth in galactose- and maltose-limited media (Figure 3.5 A and B). This suggests that the affected cell growth in mixed substrate culture might be due to the repression on glucose uptake by elevated cAMP level (Figure 3.5 C). To further test this hypothesis, substrate consumption kinetics were determined in the MalE expressing and the wt MG1655 cells upon induction, as shown in Figure 3.6 and Figure 3.7 C. It was found that the repression on substrate consumption caused by CCR disruption is not glucose specific. cAMP significantly delayed the consumption of all three measured substrates (glucose, glycerol and maltose) while maltotriose did not. Additionally, without the influence caused by plasmid, inducers didn't inhibit cell growth and substrate consumption in plate cultured MG1655 cells (data not shown) but significant inhibitory effects were seen in flask cultured cells (Fig 3.7A and C). The most potent CCR effects were observed in fermenter batch culture, as shown in Fig 3.7 B. This result is supported by the growth rate-related CCR effects, as shown in Figure 2.3B. The repressive effects on substrate consumption are not glucose specific. In conclusion, interfering with CCR regulation causes cell growth defects by suppressing substrate uptake for

all the substrates to a different degree. It can be expected that the significance of the detrimental effects on cell growth is determined by the potencies of CCR.

The discovery that cell growth inhibition resulted from CCR disruption is in agreement with other studies that discovered that simultaneous substrate consumption hampered cell growth instead of accelerating it (Silver and Mateles 1969). For industry application purposes, various mutants can be constructed to disrupt CCR in order to promote simultaneous substrate consumption; however, further modifications are necessary to circumvent cell growth inhibition (reviewed in (Gosset 2005)). Cell growth inhibition caused by CCR disruption can be understood as the interference on intracellular cAMP level, which expedites the corresponding substrates' consumption (Bettenbrock 2007). But it can't explain why maltose uptake was also hindered upon the activation of maltose transporter genes (Figure 3.6 B and Figure 3.7 C).

As we proposed in 2.3, optimal MC maintenance is a critical constraint under which CCR evolves to optimize cell growth. Therefore, we hypothesized that disruption of CCR should result in MC variation, and cell growth is affected when MC exceeds an optimal range (Vazquez 2010). We assayed the protein level of the maltose transporter subunit, MalE, and found significant maltose transporter synthesis was seen upon induction (Figure 3.7 E). It is likely that the regulation of other substrate transporter protein subunits were also induced as well by cAMP-Crp (Chapon 1982; Dean, Reizer et al. 1990; Vidal-Ingigliardi and Raibaud 1991; Szabolcs, Sandeep et al. 2007) leading to increased intracellular biomass. We also found cell density decrease and cell volume expansion upon induction (Figure 3.7 D and F). Consequently, it is unavoidable that the instant transporter synthesis alters cell resource allocation and cell growth optimization (Dekel and Alon 2005; Scott, Gunderson et al. 2010). To maintain an optimal MC level, cells expanded their volume to accommodate the extra biomass (Fig 3.7F). This volume

expansion is similar to “overshoot” in cell size when cells are transferred from a poor media to a richer media. Usually, growth arrest is followed by growth rate change during volume alteration (Cooper, 1989). Volume adjustment was found to be coupled to osmosensing (Roth, 1985). Although it is not determined yet if inducers induced osmostress to cells, the repression of substrate membrane transporters was observed when the osmo-response was activated (Roth, Porter et al. 1985; Houssin, Eynard et al. 1991; Culham, Henderson et al. 2003). Moreover, MC was found to influence cell volume regulation through affecting activities of membrane transporters in a modeling study (Minton, 1992). Based on these results, we proposed that CCR disruption upon induction might mimic the slow growth phase with transporter synthesis of multiple substrates. Osmosensors and stress genes are active (Figure 2.4C) to activate MC optimization through volume regulation. The lower MC and bigger cell volume may be the result of overshoot of transient adjustment upon induction. It would be more informative if the MC optimization process was monitored in an evolutionary experiment by transient induction. Yet, we can confirm that MC is altered when CCR is disrupted.

As shown in Fig 2.3B, with the presence of the preferential substrate and the needs of fast growth, CCR is activated. The ways of optimization of cell resource allocation, such as the transcription of substrate transporters, precursor synthesis, ATP production, ribosome occupancy and dynamic external substrate sensing, determine the phenotypes of substrate consumption to meet the growth rate needs (Goelzer and Fromion ; Furusawa and Kaneko 2008; Molenaar, Van Berlo et al. 2009; Tsuru, Ichinose et al. 2009). We reasoned that activating the transporter genes without discrimination when CCR is active causes unnecessary resource competition and optimal MC is disrupted. Distorted MC level might hinder many critical biological processes, such as PTS activities (Rohwer, 1998) and polymerization of FtsZ (Rivas, 2001). As a result, cell

growth retardation is observed due to disrupted physiologies such as metabolism and cell cycle. Taken together, CCR is implemented to ensure that cell growth is within an optimal MC environment. Disruption of CCR in fast growing cells generates detrimental effects on cell physiology associated with MC alteration.

3.4 MATERIALS AND METHODS

Western Blotting

The protein lysates were prepared as above. For each sample, 20µg protein mixed with 1 × sample buffer was boiled for 5min. The samples were loaded onto 15% SDS-PAGE, 100V for 2 hr. The gel was transferred on a nitrocellulose membrane (Bio-Rad) at 25V for 2 hr. The membrane was blotted with monoclonal MalE antibody (purchased from NEB) (1:1x3000, NEB) O/N at 4°C. The membrane then was washed for 3 times and 5min each time with TBST buffer. The secondary antibody HRP-anti mouse (1:10000) was used to blot the membrane for 1hr at RT. The membrane was washed 3 times with TBST then processed with film development.

24-well plate culture and flask cell culture

Before inoculation into 24-well plate culture, *E. coli* cells (malE and MG1655) were routinely cultured with agitation at 200rpm, 37°C in Luria-Bertani broth (Teknova) for O/N from a glycerol stock, or from an LB-agar plate. In flask culture, LB O/N cultured cells were inoculated into a 125ml flask with 15ml 1x M9-minimal salts medium (Sigma) with various

carbon substrates. In 24-well plate culture,1:50 dilution to make OD_{t0} ~=0.06 measured on the plate reader, Beckman Coulter DTX880. The 1 x M9-minimal salts media was supplemented with $MgSO_4$ and $CaCl_2$ to final concentrations of 2mM and 0.1mM, respectively. In single substrate culture experiments, the concentration of substrates was 0.2% w/vol. In mixed substrate culture experiments, five substrates were added (glucose, glycerol, galactose, lactate and maltose) and each of the substrates had the final concentration of 0.04% w/vol. The cells were cultured in the flasks for 6hr continuously at 200rpm, 37°C. Inducers were added after 15mins culture and cell culture was monitored for 6hr. Cell culture media was sampled to determine OD_{600nm} , GFP and substrate consumption.

Cell density measurement with Ficoll gradient

The Ficoll gradient was prepared by dissolving the Ficoll 400 powder (GE Healthcare) in 1×PBS to achieve ~ 60%w/v concentration. The density of the solution was measured with a densitometer, Densito 30PX (Mettler Toledo). The most condensed Ficoll solution prepared for the experiments was 1.19g/ml (ρ_0). The lower density solutions (ρ_1~ ρ_7) were prepared from ρ_0 solution by diluting the dissolved Ficoll solution with PBS. The densities of the gradient used for the cell separation were, ρ_0- 1.19g/ml, ρ_1- 1.18g/ml, ρ_2- 1.16g/ml, ρ_3- 1.14g/ml, ρ_4- 1.12g/ml, ρ_5- 1.10g/ml, ρ_6- 1.08g/ml, ρ_7- 1.06g/ml. 0.5ml of each individual gradient solution were gently layered into a 4.5ml centrifuge tube (Beckman, 344062) from the heaviest to the lightest solution, respectively. The interface of each two layers was marked on the tube before centrifugation.

In each set of Ficoll gradient experiment, all the cells in the culture media were used for cell density determination and cell growth measurement. 30ml and 20ml of cell culture were

collected at T3 and T6, respectively. The OD_{600}s of the two time points were documented also. The cells were centrifuged at 4,500g x 15min in Beckman Coulter Allegra 15R at 4°C. The supernatant was removed until only ~0.1ml culture media was left in the tube. 0.1ml PBS was added into each tube and the cells were resuspended. The cells were then transferred into the 4.5ml tube with 8 layers of Ficoll gradient. More PBS solution was added into the 4.5ml tube to fill the rest space to prevent cracking during the high speed centrifugation. The prepared tubes were loaded into a SW60 Ti rotor and subjected to centrifugation at 16,000g × 1hr at 4°C in an L8 Ultracentrifuge (Beckman Coulter). The cells distributed into each of the layer that has had the most similar density to the cells. 0.5ml of each layer was transferred into a 70µl UV-Cuvette (BRAND) and the solution was mixed through pipetting. The OD was measured at 600nm with a Photometer (Eppendof) and the background of the same Ficoll gradient solution was subtracted from the readout. The cell density distribution (CDD) was calculated as:

$$CDD\rho_i = \frac{OD_{\rho_i}}{\sum_{i=0}^{7} OD_{\rho_i}}$$

Plasmids, strains and chemicals

Low-copy reporter plasmids (pCS25 with a destabilizing ssrA tag, and a more stable pCS21 vector without destabilizing tag), in which an inserted promoter can control the expression of green fluorescent protein (*gfp*) gene were obtained from Dr. M. Surrette, University of Calgary, AB, Canada. The genomic DNA of *E. coli* K-12 strain, MG1655 ($F^- \lambda^-$ *ilv*G *rfb*50 *rph*1) was used as template for PCR. The pGEMT easy kit and *E. coli* JM109 strain was purchased from Promega. The primers were from Invitrogen®. The kits used for routine

plasmid and genomic DNA isolation were from Qiagen and Epicenter, respectively. T4 DNA ligase and restriction enzymes were from New England Biolabs. All other chemicals and antibiotics (ampicillin and kanamycin) used in the study were either from Sigma-Aldrich or Fisher Science.

Primer design

The promoter regions and the binding sites for the individual genes that participate in maltose biosynthesis in *E. coli* MG1655 were PCR amplified using *E. coli* genomic DNA from the sequenced *E. coli* genome (http://ecocyc.org). The primers were designed using Invitrogen® custom design software to amplify the sequences that contain the promoter region with CRP and all other transcription factor binding sites for the gene of interest, with an extension of ~100 bp before the first TF binding site in each case. Both the forward and reverse primers were designed with either XhoI or BamHI restriction site tails.

PCR and cloning strategy

The genomic DNA of *E. coli* MG1655 was extracted and purified using the Epicenter kit and was used as template for PCR of all promoter regions. The PCR conditions were as follows: 95°C for 5 min; followed by 25 cycles of 94°C for 30 sec., 60°C for 1 min., 72°C for 1 min.; and a final step of 72°C for 15 min. The PCR products were run on gel to check their size and those products which are expected to be of correct size were ligated and transformed into pGEMT easy vector system (Promega) in *E. coli* JM109 competent cells (as per the manufacturer protocol) followed by plating on LB-Amp plates (100µg/ml ampicillin) containing X-gal and IPTG for

blue-white screening. After overnight incubation of plates at 37°C, ~6 white colonies expected to contain the insert were picked and grown in 3-ml LB-Amp cultures for 12-14 hrs at 37°C under shaking (250 rpm). These cultures were subjected to plasmid isolation using Qiagen Miniprep kit followed by digestion with the respective restriction enzyme for 1 hr at 37°C to confirm presence of insert (XhoI and BamHI were the two restriction enzymes used in all the cases, except *araC* and *araB*, where XhoI and BglII were used for restriction digestion). Plasmids that showed the presence of insert of correct size on gel were extracted and purified using Qiagen gel extraction kit, and subjected to DNA sequencing at Genomics and Proteomics core laboratory at University of Pittsburgh (ABI 3100 or ABI 3730 sequence analyzer). The inserts which showed the 100% match (Table 2) were further selected for second round of sub-cloning into a site upstream of a promoter-less low-copy reporter plasmids, pCS21 and pCS25-containing GFP (Figure 4). The selected gene inserts were then grown in large batches of 150 ml LB-Amp cultures, followed by plasmid purification using Qiagen Midiprep kit. These plasmids were again digested by the suitable restriction enzyme followed by gel extraction and purification of the insert.

Promoter-less, low-copy pCS 21 and pCS25 GFP vectors

The pCS21 vector was purified from *E. coli* JM109 cells using the Qiagen Midiprep kit followed by double digestion with BamHI (6-8 hrs at 37°C) and XhoI (6-8 hrs at 37°C). In between the double digestion steps, after the first cut using BamHI, the plasmid was run on gel, and was extracted and purified using Qiagen gel extraction kit. Thereafter, the purified plasmid was subjected to second round of digestion with XhoI followed by plasmid extraction and purification from the gel.

Sub-cloning of insert containing promoter region into pCS 21

The purified insert was ligated individually into pCS21 vector overnight at 4°C, followed by transformation into *E. coli* JM109 competent cells and plating on selective LB-Kan plates (containing 30μg/ml kanamycin). As controls, following self-ligation, digested vectors were also transformed into *E. coli* JM109 competent cells. For screening of positive colonies that contain the ligated product, ~5-10 colonies from each plate were picked and cultured overnight at 37°C and 250 rpm in 3-ml LB-Kan cultures (containing 30μg/ml kanamycin). The presence of correct size insert was checked on the gel after plasmid extraction and double digestion with the suitable restriction enzyme for 1 hr at 37°C. The clones that showed the correct insert size after restriction digestion were selected and stored at -80°C in glycerol stocks till further use.

3.5 ACKNOWLEDGEMENT

The GFP constructs have been constructed by Krin Kay in the Oltvai lab, and I thank Krin for helping me with setting up the initial experiments to test GFP response to inducers.

4.0 MANIPULATION OF MC IN *E. COLI* CELLS

4.1 INTRODUCTION

In our previous study, MC variation has been observed at different growth rates (Figure 2.3). Therefore, cells adjust cell volume and cell density at each specific growth condition to achieve optimal cell growth. Theoretically, whether the MC adjustment is contributing to the cell's metabolic has been addressed by a recent modeling study by Vazquez (Vazquez 2010) . In this study, the enzyme molecules' volume fraction is taken as a variable. In a simplified diffusion model, the diffusion coefficients of the molecules are used to calculate the reaction rate. To achieve the highest reaction rates, cells adjust the molecules' volume occupancy by changing their concentration and as a result achieve the highest reaction rate. By solving the equations, the maximum substrate uptake rate and flux balance with constraints at the steady state, the best solution for v, volume fraction is found for the best MC prediction. The calculation predicts that cells can achieve the highest metabolic rate when the volume fraction is close to 0.37, which is within the measured MC range in volume fraction, 0.34~0.44 (Zimmerman, 1991). Therefore, the work predicts that cells have to adjust MC to ensure that it is within an optimal range that meets the needs for fast cell growth.

Therefore, we hypothesized that cell growth is correlated with optimal MC *in vivo*, and we aimed to study cell physiology upon MC alteration .To transiently alter MC, we used three

different systems: to test this hypothesis: 1) the genetic modification system, which creates cells with different MCs with genome reduction; 2) endogenous protein expression system, which alters MCs by transient protein expression upon induction; 3) morphology mutant, which has altered morphology and cell volume.

In the genetic modification system, we used the two strains, the parent strain, *E. coli* MG1655 and the strain MDS42 (Posfai, Plunkett et al. 2006), which has up to 15% of genome deleted. We examined their MC and cell growth in the glycolytic substrates, including mixed substrate, glucose, maltose culture and non-glycolytic substrate, glycerol. The results answer whether DNA mass modification can achieve different MC steady states in cells. Yet, the genetic background difference also should be considered when interpreting the results.

To transiently increase MC, we aimed to use IPTG to induce a non-functional, non-toxic protein in *E. coli* cells. Previous studies have already shown that protein overexpression results in an attenuated cell growth (Andrews KJ 1976; Dekel and Alon 2005). However, whether this phenomenon is also associated with cell MC alteration is not known. Therefore, the transient MC variation induced by protein expression was studied with BL21 cells upon IPTG induction. Other protein expression system was also tested to examine the growth inhibitory effects.

Lastly, a morphology mutant was used to study if morphology alteration can induce volume and MC change in cells. The mutant, rodZ$^-$ was found to form sphere instead of rod shape cells (Alyahya, Alexander et al. 2009). The deletion of rodZ interferes the location of the peptidoglycan synthesis sites. More than that, it also induced MC alteration, which suggests that MC maintenance is coupled with cell volume and cell morphology regulation. Cell growth was resumed after MC was restored.

4.2 RESULTS

4.2.1 MC study in genome reduced strain MDS42 vs the parent strain MG1655

4.2.1.1 Cell growth and MC studies in different substrate culture

To study how increased MC affects growth rate, we utilized two *E. coli* strains with predicatively different intracellular MC. One is the parent strain *E. coli* MG1655 and the other is strain MDS42 (Posfai, Plunkett et al. 2006), which has ~15% of genome deletion. It supposes to contain less DNA, RNAs as well as proteins compared to its parent strain, MG1655. We examined their MC and cell growth in five single substrates and mixed substrate. The results are shown in Figure 4.1.

We first examined the cell growth in the glycolytic substrate (Figure 4.1A) and the non-glycolytic substrates (Figure 4.1B). It was found that in all the single glycolytic cultural conditions, MDS42 grew faster than MG1655 but the trend was reversed in the mixed substrate culture condition (Figure 4.1B). Significant difference in ODs at the 6^{th} hr culture was detected between the two strains in glycolytic but not in glycerol, a non-glycolytic substrate. In glycerol culture (Figure 4.1B), both strains displayed comparable growth kinetics through the 6hr culture period.

Cell density (MC) of the two strains in different substrates was determined using Ficoll gradient method. We found MDS42 had higher MC in glucose, maltose, glycerol and mixed substrate culture conditions (Figure. 4.1C). MDS42 had significantly higher cell density in all 6^{th} hr samples. By the end of 6^{th} hr culture, MDS42 increased cell density in all culture conditions

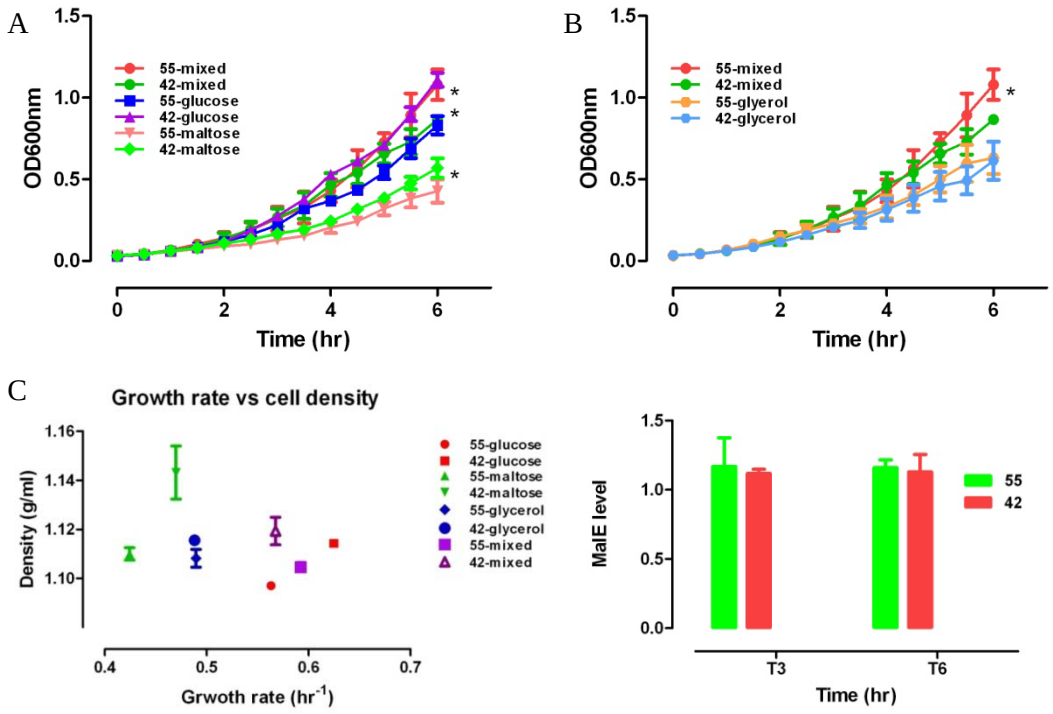

Figure 4.1 Cell growth MG1655 (55) and MDS42 (42) in flask experiments.

The O/N LB cultures of cells were inoculated into 125ml flask with 15ml M9 media with different substrates with 0.2% concentration. The initial OD_{600} was ~0.03~0.04 and cells were cultured for 6 hr in shaker with 260rpm at 37°C. A./ Cell growth in 0.2% of mixed substrate, glucose and maltose culture; B./ Cell growth in 0.2% of mixed substrate and glycerol culture; C. Cell density measured by Ficoll gradient experiments; D. Average cell growth rate vs cell density in different substrate cultures.

except in glycerol in which attenuated cell density was seen. In contrast, MG1655 maintained density in glucose and maltose culture but increased in mixed substrate and decreased in glycerol culture. It seemed MDS42 tended to increase MC while MG1655 tended to maintain or slightly upregulate its MC level in glycolytic and mixed substrate culture. In non-glycolytic substrate culture, both strains demonstrated a decreased MC along the culture.

We also investigated the relationship between cell density and average cell growth rate in different substrates for MG1655 and MDS42 cells (Figure 4.1D). It was found that in all the glycolytic substrates and mixed substrate culture, different MC levels were observed with different growth rates. However, similar growth rates were found with distinct MC levels in glycerol culture. It suggests that glycolytic pathway dependent cell growth might be more sensitive to MC changes or it prefers relatively higher MC level. On the other hand, we also found higher MC cells displayed slower cell growth in mixed substrate culture. This result indicates that metabolism of multiple glycolytic substrate is different from single substrate. Excessively high MC has the restriction effect on sharing glycolysis pathway. Therefore, an optimal MC environment is critical for glycolysis pathway utilization while non-glycolytic substrate metabolism seems to have more resilient requirement for MC.

4.2.1.2 Biomass and cell volume study in different substrate cultures

It has been confirmed that the genome reduced strain, MDS42 has higher MC than its parent strain, MG1655. It conflicts with the expectation that DNA reduction should result in less biomass content inside the cell. Therefore, we studied the biomass and cell volume in the two strains. The total protein concentration (Figure 4.2A) was consistent with dry weight (Figure 4.2B) in that both of them decreased along the culture time. The 3rd hr protein concentration is higher than that of 6th hr in all culture conditions for both strains. Interestingly, MG1655 cells contained significantly more proteins than MDS42 cells in maltose but not in other conditions at 3rd hr (Figure. 4.2A). This was not reflected in dry weight because both strains had similar dry weight for all the conditions except in maltose (Figure 4.2B). The inconsistence between MC (Figure 4.1C) and the total protein implies that MC level is not simply reflected by the total protein concentration. MDS42 cells contained slightly less dry mass compared to MG1655 cells

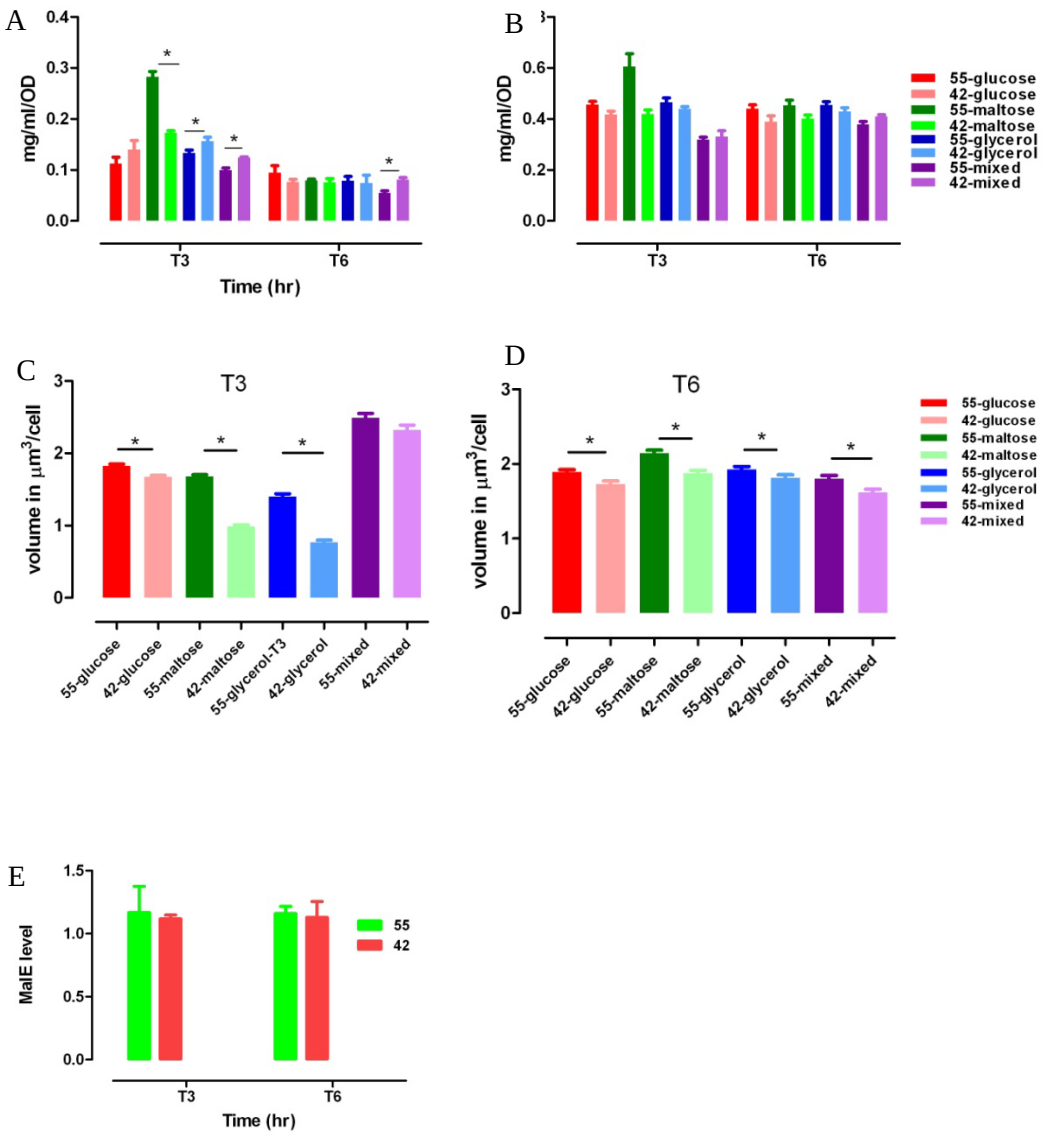

Figure 4.2 The biomass and cell volume study with MG1655 (55) and MDS42 (42) in flask experiments.

The O/N LB cultures of cells were inoculated into 125ml flask with 15ml M9 media with different substrates with 0.2% concentration. The initial OD_{600} was ~0.03~0.04 and cells were cultured for 6 hr in shaker with 260rpm at 37°C. A/ The total protein concentration; B./ Dry weight; Cells were stained with FM464 on cytoplasm member and imaged with confocal microscope. The total cell volume was estimated by taking the cells as rod shape cylinder. Cells were sampled for volume analysis at 3rd hr (C) and 6ht hr (D). The protein level of malE (E) was determined in mixed substrate.

except in mixed substrate culture. But no significant difference was seen. It shows dry mass is not an accurate measurements for MC neither.

To understand why MDS42 has higher MC, we measured cell volume in different culture conditions (Figure 4.2 C and D). In general, MDS42 cells had similar cell length compared to MG1655 cells but they had smaller diameter of the rod shape (data not shown). Cell volume difference between the two strains became smaller along the culture due to the gradually decreased growth rate. As a result, MDS42 cells have higher cell density because its smaller cell volume contained similar biomass compared to MG1655 cells. But how this high MC environment enabled MDS42 cells to grow faster in the glycolytic substrates is still not clear. We hypothesized that this growth advantage is due to the higher level of the substrate transporters. To test this hypothesis, we assayed the maltose transporter MalE in both cells at 3^{rd} and 6^{th} hr in mixed substrate culture. Due to the availability of the antibodies, we only tested maltose transporter MalE's protein level in maltose. However, the result (Figure 4.2 E) showed that there wasn't significantly difference in the transporter's protein level in the two strains. It implies that cell growth advantage is not gained from higher protein levels of transporters. But the high MC might benefit cell growth from higher surface/volume ratio of the smaller cell volume, more concentrated transporters on the membrane and other thermodynamically enhanced activities of PTS system (Kholodenko, Rohwer et al. 1998; Rohwer, Postma et al. 1998) or/and transporters on the membrane (Minton, Colclasure et al. 1992).

In summary, the two strains with different MC levels display different cell growth in glycolytic and non-glycolytic substrate culture. The high MC cells, MDS42 grow faster in the glycolytic substrate culture but not in mixed substrate media. No detectable difference is seen in single non-glycolytic substrate culture. MDS42 cells have smaller cell volume but similar total

biomass content compared to MG1655 cells. However, the modified genetic background of the MDS42 prevents us from fully attributing the growth phenotypes to different MC difference.

4.2.2 MC study in protein overexpressing strains

4.2.2.1 Directly altering MC by transiently overexpressing an exogenous protein

As shown in Figure 2.3 A, MC (cell density) is different for cells under different growth rate. It indicates that cells might need to adjust their intracellular MC to facilitate cell growth. To understand the relationship between MC and cell growth rate, we altered MC by transiently overexpressing an exogenous protein in *E. coli* cells. Human heat shock proteins (Hsp27) and ubiquitin carboxy-terminal hydrolase-L1 (UCH) were used in the pilot study. The two proteins were chosen because of their good solubility, medium protein size (~25kD), and low toxicity. More importantly, they are not supposed to interfere with signaling pathways in *E. coli* cells (e.g., UCH proteins are mostly distributed in neuron cells) (Day and Thompson 2010).

As shown in Figure 4.3A, upon IPTG induction, rat UCH and human Hsp27 proteins were successfully overexpressed 3 hr after induction. The protein expression level could be controlled by IPTG concentration, as shown by the western blot data. Moreover, higher expression level of proteins slowed down cell growth more significantly in both Hsp27 and UCH cells , as reflected in OD600nm readout along the 6hr culture observed in both protein expressing cells (Figure 4.3A). Note that a high basal expression level was seen in 3rd hr cell samples but not in 6hr sample. It might be due to the intracellular cAMP level variation, which relieves the repression of lacI in the pET vector containing cells. After considering that Hsp27 might be

conserved as an anti stress protein in *E. coli* cells (Takeuchi 2006), we decided to use UCH cells only in the subsequent studies.

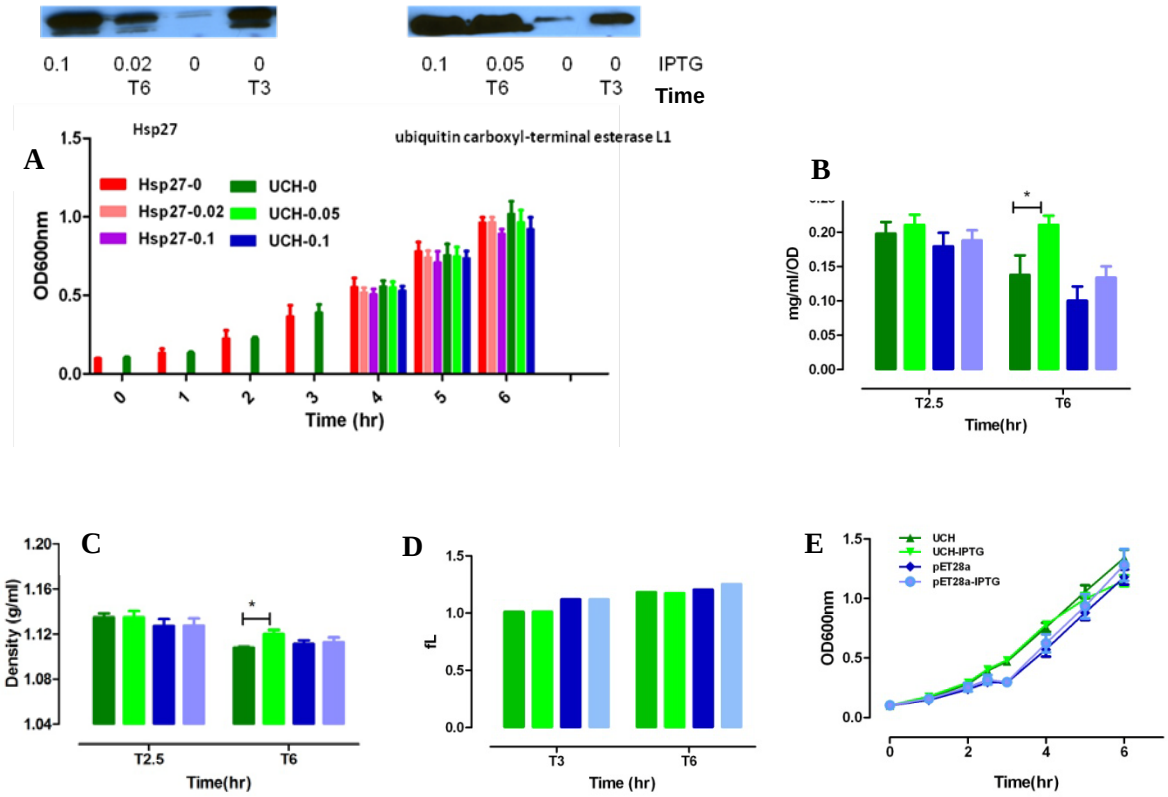

Figure 4.3 Protein expressions with pET 28 upon IPTG induction in BL21 cells.

The O/N LB cultures of cells were inoculated into 125ml flask with 15ml M9 media with 0.2% glucose. Hsp27 and UCH cells were subjected to 3hr induction and the protein expression's was examined in western blot and cell growth was recorded in A. UCH and the empty vector cells, pET28a were induced with 0.1mM IPTG for 3.5 hr. total protein level (B), Cell density (C), Cell volume (D) and cell growth (E) upon IPTG induction were determined.

In 0.2% glucose culture, the empty vector containing cells, pET28a and UCH cells were subjected to 3.5 hr IPTG induction. As shown in Figure 4.3B, IPTG induction significantly increased total protein concentration in UCH cells by 6th hr but only mildly in pET28a cells.

Ficoll gradient assay showed that UCH protein expression was associated with dramatic MC increase (Figure 4.3C). This MC increase was not seen in the control, empty vector containing cells. The protein expression also mildly increased dry weight in UCH cells (data not shown). As shown in the Beckman Coulter counter result there is no significant volume increase upon IPTG induction in UCH cell (Figure 4.3D) but mild cell volume expansion was still seen. Therefore, it seems that transient protein expression can increase MC with instant protein synthesis without dramatic cell volume expansion. Slower growth rate was observed in UCH expressing cells from 5^{th} hr. This growth inhibition wasn't observed in pET28a cells. Growth inhibition wasn't seen in lower protein expression condition such as for Hsp27 0.02mM IPTG (Figure 4.3A). It indicates an optimal MC window might exist for cells to accommodate the biomass accumulation. The growth arrest will be resulted once MC threshold is reached. But sufficient amount of transient protein expression did transiently increase MC in cells.

4.2.3 MC study in the morphology mutant, Δ *rodZ*

MC alteration has been observed during cell growth (Figure 2.3), after genome modification (Figure 4.1C), or in protein expression (Figure 4.3C). Cell volume change has been observed to be coupled with MC variation (Figure 2.3A). To study how cell volume disruption affects MC as well as cell growth, we used the morphology mutant, Δ *rodZ,* which contains single gene deletion and examined in mixed substrate culture.

It has been found that loss of RodZ protein (Δ *rodZ*) leads to misassembly MreB and giant spheres-shape of cells (Alyahya, Alexander et al. 2009; Bendezu, Hale et al. 2009). It was also found that cell growth was delayed in deletion strain cultured in M9 medium and no

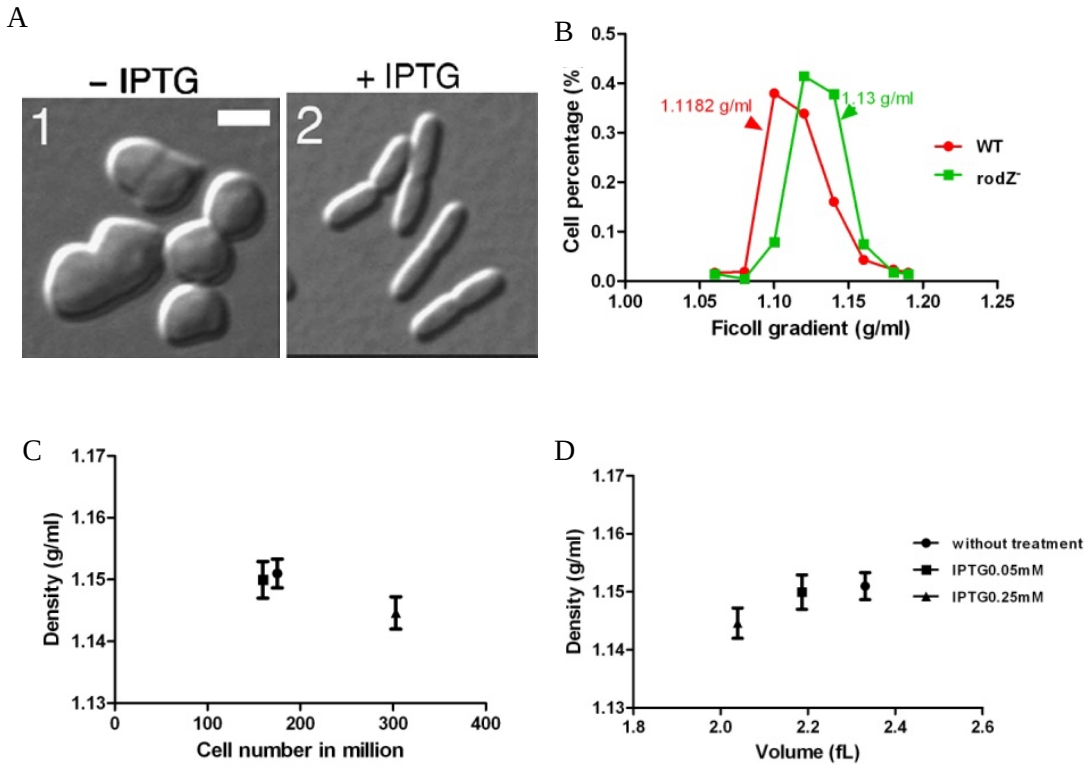

Figure 4.4 MC and cell growth alteration upon morphology restoration in *rodZ*⁻ mutant.

A. Morphology restoration with IPTG induction in *rodZ*⁻ cells. Adopted from (Bendezu, Hale et al. 2009). B. Cell density distribution of wild type cells, TB28 and the *rodZ*⁻ cells in glucose 0.2% M9 culture media. In mixed substrate culture, *rodZ*⁻:: rodZ cells were induced with 0.05 and 0.25 mM IPTG at 37°C for 3.5 hr in 6hr culture experiments. Cell density vs cell number (C) and cell density vs cell volume (D) were determined with Ficoll gradient and Beckman coulter.

chromosome segregation was affected (Bendezu, Hale et al. 2009) .Therefore, it has no direct defects in cell proliferation. This prompted us to study the relationship between MC and cell growth in the morphology altered Δ *rodZ* cells. As shown in Figure 4.4 A1, *rodZ*⁻ cells displayed giant sphere shape. The rod shape was restored upon the expression of RodZ (Figure 4.4 A2). The wild type cells, TB28 cells have significant lower MC (1.118g/ml) compared to Δ *rodZ* cells (1.13g/ml) in glucose culture as shown in Figure 4.4 B. This result indicates RodZ facilitates cells to not only maintain rod shape but also the optimal MC. The maintenance of normal MC

level might also be critical to cell growth because cell growth defects were observed in the deletion strain (Bendezu, Hale et al. 2009).

To further study how morphology affects cell density (MC) as well as cell growth, we cultured cells in mixed substrate and tried to restore cell morphology by inducing RodZ expression upon IPTG induction. Cell shape restoration has been confirmed previously (Bendezu, Hale et al. 2009), as shown in Figure 4.4A. Cells were subjected to Ficoll gradient and cell volume analysis after 3.5 hr induction with IPTG. It was discovered that cells decreased cell density upon higher IPTG induction (0.25mM) while the lower IPTG concentration didn't induce cell density change. Moreover, cells accelerated growth when MC decreased because cell number almost doubled upon 0.25mM IPTG treatment (Figure 4.4 C).

Induction with 0.05mM IPTG restored cell shape to rod shape cells with decreased cell volume (Figure 4.4D). However, MC alteration was much milder in 0.05mM than in 0.25mM IPTG. Volume decrease alone didn't restore cell growth only MC decrease was associated with the rescued cell growth in *rodZ*$^-$ cells.

Taken together, MC alteration can be realized by cell morphology alteration/volume adjustment and cell growth is affected by lowering MC and cell volume of *rodZ*$^-$ cells in mixed substrate culture resulted in fast cell growth. The MC constraint might not be the only cause for cell growth defects in Δ *rodZ* cells, but it is possible that MC is the necessary condition for cell growth restoration.

4.3 DISCUSSION

In this chapter, we studied MC alteration in three different systems: the genomic deletion strains, the inducible protein expression strains, and the morphology gene deletion strains. We aimed to understand how DNA mass and protein content as well as cell morphology contribute to MC homeostasis.

In the genomic deletion system, although the total genomic DNA has been decreased up to 15% by deleting the non-essential genes in MDS42 strains (Posfai, Plunkett et al. 2006), cells reorganized cell structure to form smaller cells with higher MC compared to its parent strain. Even with the central metabolism network integrity, it is probably thatthe genes deleted in MDS42 cells are mostly known or predicted membrane proteins, or membrane-associated proteins, all of which could influence membrane composition as well as the intracellular molecule density (Posfai, Plunkett et al. 2006; Wood 2006). The genes of membrane protein, which are deleted in MDS42 might be involved in osmolarity sensing and volume regulation. Loss of the genes may cause volume regulation defects and result in failure of dynamic volume adjustment to maintain optimal MC. Moreover, as we introduced in Chapter 1.2.3, the genome modification resulted high MC may also change DNA replication and the activities of DNA related enzymes to produce a growth and morphology phenotype. Nevertheless, in all the culture conditions, MDS42 displayed a higher MC level consistently and it implies that the DNA reduction modification has resulted a permanent MC alteration.

In the 6 hr culture experiments, high MC cells didn't display growth difference in glycerol culture, or even grew slower in mixed substrate culture. As a contrast, high MC cells grew faster in glycolytic substrates, such as glucose or maltose. In mixed substrate culture, the

potential defects in volume regulation in MDS42 might be critical for cell growth phenotypes because: firstly, as shown in Figure 2.3 A, cell volume dynamically adjusts along cell growth rate change (Waldegger, Matskevitch et al. 1998; Pasantes-Morales, Lezama et al. 2006). Failure of volume regulation will result biomass accumulation and MC might exceed the optimal range. As a result, cell growth is affected. Secondly, corresponding MC adjustment is seen in Figure 4.1 C when cells were cultured in different substrates for both MG1655 and MDS42 cells. Each substrate may have the preferential MC level requirement to facilitate the maximum substrate metabolism. As we studied previously (Figure 3.7 B), CCR can't fully repress the secondary substrates' consumption in flask culture. It implies substrate transporter genes and proteins are actively transcribed and translated during culture. From this perspective, osmolarity and volume sensing is critical to the flexibility of MC adjustment in mixed substrate culture as shown in Figure 2.4 C. Therefore, volume and osmosensing related genes should be re-screened from the deleted gene list to understand the physiological result of MDS42.

On the other hand, growth advantage is observed in glycolytic substrate culture in high MC cells. This prompts us to think that glycolysis pathway utilization may prefer relatively higher MC environment. In our previous study and observation, the oncogenic cell lines, which have glycolysis addiction, have higher MC and smaller cell volume compared to the control cells (Vazquez, Liu et al. 2010). MC was observed to increase with upregulated glycolysis pathway in mixed substrate culture (Figure 2.4B). However, given the genomic modification background, conclusive conclusion can't be drawn about the relationship between MC levels and the preference on glycolysis pathway utilization. To further prove this, glycolytic strains which preferentially use glycolysis pathway can be used to examine if MC level has been adjusted to adapt the metabolism pathway utilization (Koebmann, Westerhoff et al. 2002; Holm, Blank et al.

2010). ATP synthesis rate (Vazquez, Beg et al. 2008; Vazquez, Liu et al. 2010) PTS flux (Kholodenko, 1998 ; Rohwer, 1998) and EI activity (Patel, 2006 ;Patel, 2006) can be examined with different MC background to understand the effects of MC on cell growth and metabolism in *E .coli* cells.

Compared to the genome deletion strain system, IPTG inducible system is more controllable in that the expression of protein can be fine tuned. As studied before, protein expression in cells is under the control of cost-benefit to maximize cell metabolism (Goelzer and Fromion ; Dekel and Alon 2005; Goelzer and Fromion 2011; Poelwijk, Heyning et al. 2011). Cell growth inhibition and accelerated ribosome degradation were found to be associated with protein overexpression under induction (Dong, Nilsson et al. 1995; Hoffmann, Weber et al. 2002; Poelwijk, Heyning et al. 2011). On the other hand, cells tend to constitutively synthesize some non-functional proteins without growth arrest (Andrews KJ 1976). Our results suggest the transient protein overexpression did increase MC. It also suggests that MC has been dynamically adjusted given the protein production during the fast cell growth. To ensure fast cell growth, protein expression has to be regulated under MC constraint or growth arrest will appear.

In an IPTG-protein-overexpression system, upon proteins being synthesized, cell metabolism including respiratory activity as well as biosynthetic rate for metabolic enzymes has been proven (Hoffmann, Weber et al. 2002; Weber, Hoffmann et al. 2002). Therefore, it is difficult to differentiate the effects caused by MC alteration. However, still, some improvements can be done. Firstly, we could overexpress a secretory protein in cells with or without inhibiting its secretion (Wang, 2011 #1250). The comparisons between the two conditions might give us more clues about MC effects with the same protein synthesis burden. Secondly, a more sensitive inducible system that produces a large amount of protein expression should be used. By

shortening the induction time from 3.5 hr, we may be able to minimize the influences caused by the basal protein synthesis in empty vector containing cells. Thirdly, in mammalian cell system, specially formulated bubbles can be loaded to study MC alteration effects. This will be introduced in Chapter 5.

To study MC's effects on cell growth, we also examined the morphology mutant, *Δ rodZ*. RodZ (YfgA) has no direct functional correlation with cell growth and metabolism. It links another morphology actin molecule, MreB protofilament in the cytoplasm to form spiral structure along cell membrane to support the rod shape of *E. coli* cells (Alyahya, Alexander et al. 2009; Bendezu, Hale et al. 2009; van den Ent, Johnson et al. 2010). Without RodZ, *E. coli* cells have defects in elongation for cell biomass accumulation during cell growth (Shiomi, Sakai et al. 2008). The morphology defects were found to be restored after RodZ expression under induction (Bendezu, Hale et al. 2009). However in all the previous studies, whether MC in the mutant has been altered wasn't investigated.

In the morphology mutant study, as shown in Figure 4.4A and B, cells with RodZ depletion displayed bigger size with higher cell density in glucose culture. To further study how MC is correlated with cell growth in mixed substrate, we cultured cells with and without IPTG induction. Lower IPTG concentration at 0.025mM only induced volume expansion but not MC alteration. Volume expansion induced by IPTG wasn't associated with cell growth change which was measured as the cell number counted by Beckman Coulter counter (Figure 4.4 C and D). However, higher IPTG induction generated sufficient cell morphology and MC alteration. MC decrease was observed with accelerated cell growth for the mutant cells. Cell division was accelerated after MC decrease due to the expression of RodZ. It is probably that cell division is through sensing the intracellular molecule concentration or MC instead of cell volume. Cell

cycle molecules such as FtsZ (Weart, 2003), DnaA (Chiaramello, 1989) and the stress factor, ppGpp (Zyskind, 1992) could be further investigated to understand if the growth phenotypes are caused by the disruption of those molecules' spatial distributions in high MC environment. To further confirm MC is the key factor contributing to cell cycle regulation instead of volume, we can screen Keio collection (a single gene deletion library for *E. coli* cells) (Baba, 2006) for more morphology mutants to study MC levels and cell growth.

Taken together, MC as a physical constraint has been found to be associated with many physiological parameters such as genomic DNA amount, intracellular protein content and cell morphology. Disturbance in those parameters produces MC alteration and growth phenotypes. Although the checkpoint of bacterial cell division is not clear, it has been proposed that bio-mass increase is the driving force of the division cycle (Cooper 1991; Koch 2002; Cooper 2006). Therefore, MC might be the potential constraint which governs cell growth by interacting with the checkpoint sensors to maintain MC homeostasis. Moreover, constant MC monitoring and optimal MC maintenance is a necessary condition for fast cell growth.

4.4 MATERIALS AND METHODS

Bacterial strains and growth conditions

Information on the strains and plasmids used is provided in Table 1. Before inoculation, *E. coli* cells were routinely cultured with agitation at 200rpm, 37°C in Luria-Bertani broth (Teknova) for 48 hr from a glycerol stock, or 24 hr from an LB-agar plate. After the pre-culture in LB, cells were inoculated into a 125ml flask with 55ml 1x M9-minimal salts medium (Sigma)

with various carbon substrates. The 1 x M9-minimal salts media was supplemented with $MgSO_4$ and $CaCl_2$ to final concentrations of 2mM and 0.1mM, respectively. In single substrate culture experiments, the concentration of substrates was 0.2% w/vol. In mixed substrate culture experiments, five substrates were added (glucose, glycerol, galactose, lactate and maltose) and each of the substrates had the final concentration of 0.04% w/vol. The cells were cultured in the flasks for 6hr continuously at 260rpm, 37°C. For all the experiments, the initial OD of the cells was at OD_{600nm}~0.035.

Table 2 Bacterial strains and vectors

Cell Strains	**Containing vectors or modifications**	**Source**
MDS42	15% genome deletion from MG1655 strain, K12.	Purchased from scarabgenomics
BL21		Invitrogen
UCH	pET28a	Obtained from Hao Liu's lab at Neurology Department, University of Pittsburgh
Hsp27	pET151	Invitrogen
UCH	pASK-IBA35plus	BioTAGnology， Germany
TB28	MG1655 LacIZYA<>frt	Obtained from Dr. Piet AJ de Boer, Case Western Reserve University (Bendezu, Hale et al. 2009)
Δ rodZ::*rodZ*	TB28/pFB290	(Bendezu, Hale et al. 2009)

Average growth rate calculation

The OD_{600nm} measurements along the culture were converted to ln scale. The slope of the ln curves of each sample was taken as the average growth rate.

Cell dry weight measurement and total protein determination

During the 6hr culture, cells were sampled at 3 and 6 hour of growth (T3 and T6) for dry weight and total protein concentration measurements. Cells were harvested at different time points as described after induction. The sampled cell culture (for dry weight measurement, 20ml at T3 and 10ml at T6; for total protein concentration measurement, 10ml at T3 and 5ml at T6) was centrifuged at 4,500g x 15min in Beckman Coulter Allegra 15R at 4°C. The supernatant was removed until only ~0.5ml culture media was left in the tube. For dry weight measurement, the cells were resuspended and transferred into 1.5ml tubes that were pre-baked at 80°C for 48hrs and weighted on a XS105 DualRange Analytical Balance (Mettler Toledo). For protein concentration determination, the resuspended cells were transferred into 1.5ml tubes. The tubes were centrifuged at 13,000rpm for 10 min (Microfuge 18 centrifuge, Eppendof). Cell pellets were dissolved in 100µl lysis buffer. Prior to protein concentration determination cell pellets were stored in -80°C. The lysis buffer contained 10mM tris-HCl (pH 8.3), 500mM NaCl, 10% Glycerol, 0.1% Igepal CA-630, 5mM β-mercaptoethanol. To lysis the cells, 100µl lysis buffer containing 1:100 dilution lysozyme and protease inhibitor (Sigma) were added into each tube. The cells were suspended in the lysis buffer and incubated on ice for 30min. After the incubation, the cells were subjected to five cycles of “freeze and thaw” from dry ice (-80°C) to water bath (37°C). The cells were then centrifuged at 13,000rpm on a desktop centrifuge (Fresco, Sovall) at 4°C for 30min. The supernatants were assayed with Bradford kit (Bio-Rad) to determine protein concentration. The protein lysates were prepared as above. For dry weight measurement, the supernatant was removed and all the tubes were placed on a heatblock (VWR) with temperature set at 80°C. The tubes were heated for 48hr and weighted on the analytical balance. The cell dry weight was calculated as:

$$DW_t = {DW_{tube}}/{(OD_t \times Vol_t)}$$

where DW_t denotes the dry weight of cells at t (mg per OD_{600nm} per ml of cell culture), DW_{tube}: the weight of the cells inside the weighted tube (mg), OD_t: the OD_{600nm} at t, and Vol_t: the volume of the cell culture sampled for dry weight measurement at t (ml);

Cell density measurement with Ficoll gradient

The Ficoll gradient was prepared by dissolving the Ficoll 400 powder (GE Healthcare) in 1×PBS to achieve ~ 60%w/v concentration. The density of the solution was measured with a densitometer, Densito 30PX (Mettler Toledo). The most condensed Ficoll solution prepared for the experiments was 1.19g/ml (ρ_0). The lower density solutions ($\rho_{1\sim}\ \rho_7$) were prepared from ρ_0 solution by diluting the dissolved Ficoll solution with PBS. The densities of the gradient used for the cell separation were, ρ_0- 1.19g/ml, ρ_1- 1.18g/ml, ρ_2- 1.16g/ml, ρ_3- 1.14g/ml, ρ_4- 1.12g/ml, ρ_5- 1.10g/ml, ρ_6- 1.08g/ml, ρ_7- 1.06g/ml. 0.5ml of each individual gradient solution were gently layered into a 4.5ml centrifuge tube (Beckman, 344062) from the heaviest to the lightest solution, respectively. The interface of each two layers was marked on the tube before centrifugation.

In each set of Ficoll gradient experiment, all the cells in the culture media were used for cell density determination and cell growth measurement. 30ml and 20ml of cell culture were collected at T3 and T6, respectively. The OD_{600}s of the two time points were documented also. The cells were centrifuged at 4,500g x 15min in Beckman Coulter Allegra 15R at 4°C. The supernatant was removed until only ~0.1ml culture media was left in the tube. 0.1ml PBS was added into each tube and the cells were resuspended. The cells were then transferred into the 4.5ml tube with 8 layers of Ficoll gradient. More PBS solution was added into the 4.5ml tube to fill the rest space to prevent cracking during the high speed centrifugation. The prepared tubes

were loaded into a SW60 Ti rotor and subjected to centrifugation at 16,000g × 1hr at 4°C in an L8 Ultracentrifuge (Beckman Coulter). The cells distributed into each of the layer that has had the most similar density to the cells. 0.5ml of each layer was transferred into a 70µl UV-Cuvette (BRAND) and the solution was mixed through pipetting. The OD was measured at 600nm with a Photometer (Eppendof) and the background of the same Ficoll gradient solution was subtracted from the readout. The cell density distribution (CDD) was calculated as:

$$CDD_{\rho_i} = \frac{OD_{\rho_i}}{\sum_{i=0}^{7} OD_{\rho_i}}$$

Confocal imaging and image processing

E. coil cells were precipitated and suspended in 4% PFA for 20min at room temperature (RT). The cells were washed with 1xPBS. The slides were coated with poly-l-lysine preparation at RT for 30min. Then cells were subjected to FM4-64 (Sigma) staining at 1:500 dilution with PBS for 1min at RT and 5min on the slides at 4°C. Slides were washed 1x with sterile PBS and mounted for imaging. Olympus 1000 Fluoview was used to image the cells with excitation wavelength of 543 nm and emission filter HQ660LP. Images were processed using ImageJ and 150 cells for each sample were analyzed.

Competent cells

Inoculate one colony from LB plate into 2ml LB liquid medium and shake at 37 C° overnight. Then inoculate 100µl O/N cell culture into 10ml LB medium and shake vigorously at 37 C° till OD_{600nm} ~0.25-0.3. Cells were chilled on ice for 15min and centrifuged for 10min at 3300g at 4 C°. The supernatant was discarded and cells were resuspended in 3~4ml chilled 0.1M $CaCl_2$ followed by incubation on ice for 30min. Cells were centrifuged again as above the

resuspended in 0.6ml 0.1M $CaCl_2$ solution plus 15% glycerol then divided into sterile 1.5 ml tubes and kept in -80 C°.

Transformation of competent cells

200 µl competent cells were thawed on ice. 10ng DAN was added to the competent cells and mixed gently by swirling the pipette tip. Then cells were incubated on ice for 30mins followed by in 42 °C for 45-60 seconds then on ice for 2mins. 3ml of LB medium was added and cells were incubated for 45 mins at 37 °C with shaking at 150rpm. Cells were plated onto selection plates and incubated at 37 °C for O/N to get recognizable clones.

Primer design

The primers of UCH were designed using Invitrogen® custom design software to amplify the sequences of UCH gene of interest: the forward primer sequence (5' to 3'): ATCAGAATTCATGCATGCAGCTGAAACCGATG and the reverse primer sequence (5' to 3'): ATAATGCGGCCGCTTAGGCTGCTTTGC. Both the forward and reverse primers were designed with either XbaI or BamHI restriction site tails. T4 DNA ligase and restriction enzymes were from New England Biolabs. All other chemicals and antibiotics (ampicillin, kanamycin Anhydrotetrocycline) used in the study were either from Sigma-Aldrich or Fisher Science.

PCR and cloning strategy

The PCR conditions were as follows: 95°C for 5 min; followed by 25 cycles of 94°C for 30 sec., 60°C for 1 min., 72°C for 1 min.; and a final step of 72°C for 15 min. The PCR products were run on gel to check their size and those products which are expected to be of correct size were ligated and transformed into pASK-35plus in *E. coli* MG1655, BL21 and one shot competent cells (as the transformation protocol above) followed by plating on LB-Amp plates

(100µg/ml). After overnight incubation of plates at 37°C, ~6 white colonies expected to contain the insert were picked and grown in 3-ml LB-Amp cultures for 12-14 hrs at 37°C under shaking (250 rpm). These cultures were subjected to plasmid isolation using Qiagen Miniprep kit followed by digestion with the respective restriction enzyme for 1 hr at 37°C to confirm presence of insert (XhoI and BamHI were used for restriction digestion). Plasmids that showed the presence of insert of correct size on gel were extracted and purified using Qiagen gel extraction kit, and subjected to DNA sequencing at Genomics and Proteomics core laboratory at University of Pittsburgh (ABI 3100 or ABI 3730 sequence analyzer). The inserts which showed the 100% match were further induced with ATc induction with different concentrations.

Western Blotting

Cells were harvested at different time points as described after induction. Cell pellets were dissolved in 100µl lysis buffer. Prior to protein concentration determination cell pellets were stored in -80°C. The lysis buffer contained 10mM tris-HCl (pH 8.3), 500mM NaCl, 10% Glycerol, 0.1% Igepal CA-630, 5mM β-mercaptoethanol. To lysis the cells, 100µl lysis buffer containing 1:100 dilution lysozyme and protease inhibitor (Sigma) were added into each tube. The cells were suspended in the lysis buffer and incubated on ice for 30min. After the incubation, the cells were subjected to five cycles of “freeze and thaw” from dry ice (-80°C) to water bath (37°C). The cells were then centrifuged at 13,000rpm on a desktop centrifuge (Fresco, Sovall) at 4°C for 30min. The supernatants were assayed with Bradford kit (Bio-Rad) to determine protein concentration. The protein lysates were prepared as above. For each sample, 20µg protein mixed with 1 × sample buffer was boiled for 5min. The samples were loaded onto 15% SDS-PAGE, 100v for 2 hr. The gel was transferred on a nitrocellulose membrane (Bio-Rad) at 25v for 2 hr.

The membrane was blotted with monoclonal MalE antibody (1:1x3000, NEB) or UCH antibody (1:1000, Cellsignaling) O/N at 4°C.

Statistics

Values are expressed as the mean ± SEM. Data are plotted in Graphpad Prism5 (Graphpad Scientific). Intergroup differences were assessed by one-way ANOVA or t-test. * : $p<0.05$ represents significant difference between groups or samples.

4.5 ACKNOWLEDGEMENT

I would like to thank the staffs in CBI with the confocal imaging assistance and Dr. Jianjun Wang for providing kind help with cell size measurements.

5.0 CONCLUSIONS AND FUTURE WORK

The main goal of this thesis is to investigate the role of MC in CCR-regulated sequential substrate uptake in the growth of *E. coli* cells. This goal suggested from the finding of a previous study, in which MC was the crucial boundary condition in a modified FBA model that correctly predicted the sequential substrate order in a mixed substrate culture of *E. coli* without including any prior knowledge of CCR (Beg, Vazquez et al. 2007). This study suggests that the sequential substrate uptake activated by CCR is the best solution under MC constraint to achieve the fastest cell growth. Other than addressing the intrinsic mechanisms in CCR, we proposed a novel interpretation of its function in fast growing cells: CCR is only activated in fast growing cells to ensure that cells maintain a maximum growth within an optimal MC range.

The work described in this thesis provides experimental support for the validity of the hypothesis. Firstly, (Figure 2.3) there is a positive correlation between the strength of CCR and the growth rate. CCR is activated at high growth rates but not at low growth rates. Our study (Figure 2.4) also showed that the mRNA expression level of transporter genes is high when the growth rate is low and substrates are consumed simultaneously, and this finding is in agreement with the findings of other studies (Silver and Mateles 1969; Ihssen and Egli 2005; Liu, Durfee et al. 2005). In contrast, *E. coli* cells display substrate consumption preference when their growth rate is increased (Figure 2.3 and 2.4). The expression of transporter genes were lower and was associated with lowered osmostress and higher glycolysis pathway activation at higher growth

rates (Figure 2.4). Disruption of CCR in rapidly growing cells but not in slowly growing cells caused detrimental effects on cell growth and substrate consumption (Figure 3.7) Thus, CCR is critical for fast growing cells with obeying MC constraint.

Secondly, a previous studying suggested a narrow MC range that is compatible with the presence of a narrow dynamic of optimal MC has been proposed from the modeling result (Vazquez 2010). In our study, MC was experimentally proven to increase with growth rate till the growth rate reached 0.4/hr then plateaued (Figure 2.3A). At the same time, cell volume also peaked at 0.4/hr but decreased thereafter. An increase in cell density increasing with growth rate was also observed in other species, including *B. Sutilis, S. cerevisae* and mouse lymphoblast (Bryan, Goranov et al. 2010; Godin, Delgado et al. 2010). In those studies, cell density was measured by microchannel resonator (SMR) measurements (Godin, Delgado et al. 2010). MC alteration was also observed upon CCR disruption with cell growth arrest (Figure 3.7D). Taken together, our data and previous findings support the notion that limited increase in MC is closely correlated with the cell growth rate in different species.

Finally, the direct MC perturbation experiments suggest that MC increases through transient protein overexpression interferes with *E. coli* cell growth. It is known that there is a trade-off between the protein synthesis and metabolic rate (Dekel and Alon 2005; Poelwijk, Heyning et al. 2011; Poelwijk, de Vos et al. 2011). A strong correlation between RNA/protein and growth rate has been found (Scott, 2010). Our data implies that the MC constraint drives the optimization of protein synthesis and further suggests the necessity of optimal MC maintenance. Other modifications such as genome depletion and morphology alteration also result MC disruption. Therefore, it indicates that MC homeostasis is maintained through regulating intracellular mass accumulation and cell volume.

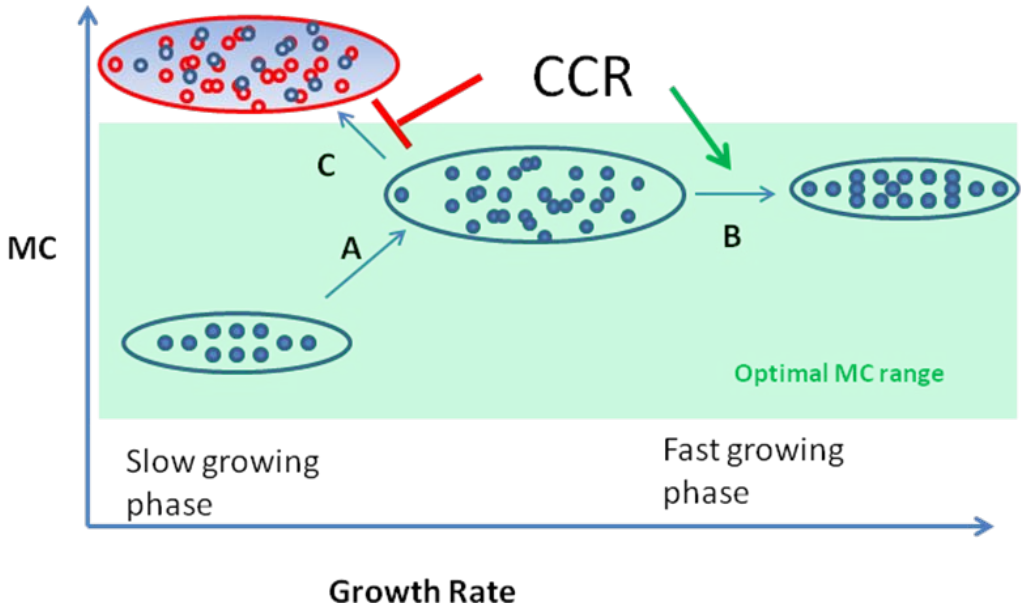

Figure 5.1 CCR activation facilitates optimal MC maintenance and fast cell growth with a high metabolic rate.

Cells expand cell volume to accommodate the biomass accumulation increase caused by faster growth rate (transition A). However, excessive MC due to the indiscriminate synthesis of transporter proteins would cause growth defects (transition C). To ensure that MC is always within an optimal range (shown in the shaded area) in the fast cell growth phase, CCR is activated to prevent unnecessary transporter regulons' activation (transition B).

As we have found, altered MC is always associated with cell growth phenotypes. To sense intracellular biomass and determine cell cycle initiation, cells need to coordinate cell volume to optimize intracellular protein synthesis (Cooper 1989; Marr 1991; Cooper and Denny 1997). However, by certain point, volume regulation cannot fully dilute the crowding effects cause by higher growth rates and MC disruption appears. Our experimental data already show that cells with excessively high and display growth defects in mixed substrate (the genome reduced strain MDS42, the RodZ mutant) and in single substrate (the transient protein overexpressing strain). As summarized in Figure 5.1, these discoveries support that CCR can be understood as a protective mechanism to maintain optimal intracellular MC with the variations

of growth rate (as shown in the shaded area of Figure 5.1) because CCR attenuates target gene transcriptions and protein synthesis (Gorke, 2008; Josef, 2008; Rojo, 2010). By including MC as a constraint, enzyme concentrations and metabolic network flux related to cell growth rate were correctly predicted (Vazquez, Beg et al. 2008; Vazquez, De Menezes et al. 2008; Vazquez, Liu et al. 2010; Vazquez and Oltvai 2011). It shows MC is a necessary molecular mechanism to ensure the proper functioning enzymes and the optimal enzyme concentrations in fast growing cells. Therefore, it can be postulated that CCR is activated to circumvent excessive MC level in fast growing cells. Moreover, the optimal MC level is within a narrow-range (Vazquez 2010) and this is shown by the dynamic change of MC in to different culture media (Figure 4.1) and growth needs (Figure 2.3).

To adapt the changing environment, cells need to adjust cell growth smoothly with high sensitivity and efficiency. As an enabler of physiological condition for fast cell growth, MC acts as a dynamic threshold that govern the evolution of switches among different metabolism pathways such as those regulated by CCR. MC physically changes the signaling molecules' concentration and spatial distribution and the restoration is easily implemented once the biomass accumulation is adjusted back to an optimal level. Therefore, MC might work similarly as a stringent response regulatory mechanism (Jin, 2011) in that being sensitive to detect the growth needs (the availability or the lack of nutrient) and turn on/off the metabolism pathway by facilitating or repressing the necessary molecules of the pathway to achieve the optimal cell growth.

We think the critical biophysical constraints for cell growth should be simple, robust and sensitive to the changes to the nutrients and MC is one of them. The constraint-based systematic analysis with FBA may provide the novel potential targets to introduce perturbation into a known

regulatory mechanism, such as CCR. Simultaneous substrate consumption without CCR activation might be achieved by in-silico gene knock out study with FBAwMC. Those potential gene knockout targets can be further tested in experimental conditions to search the genes which are responsible for CCR activation by obeying MC constraint. As we have shown in the data (Figure 2.4), the morphology and osmosensing as well as other gene targets that involved in MC homeostasis maintenance might exert critical functions in metabolism regulation. Therefore, the constraint based study can provide a novel method to search for potential targets of metabolism network and the targets, which reside probably outside of the network itself. These results will contribute to antibiotics development as well as industry applications such as fermentation. Moreover, as the similarity shared in the metabolism network, MC-constrained metabolism is shared by eukaryotic cells as well. Therefore, the potential targets found in *E. coli* metabolism network can also contribute to the studies of drug targeting fast growing eukaryotic cells, such as cancer cells.

Future work

However, there is still a significant amount of work need to be done to understand MC's role in cell metabolism. Firstly, MC perturbation experiments could be more convincing if they were conducted in an evolutionary experimental set-up (>300 generations culture) (Brown, 1991;Lenski, 1991). The evolutionary experiments eliminate the effects of transient MC alteration and demonstrate the optimization along the evolution. Cell growth, morphology and protein expression should be studied to understand how cells progressively adapt to MC perturbation with a systematic optimization. Secondly, the molecular mechanisms that are sensing and determining MC are still undefined. Potentially, the Keio collection of *E. coli* single

gene deletion mutants (Baba, 2006) could be used for this purpose. Since MC adjustment in mixed substrate culture has been observed, the strains with single deletion of the critical genes related to MC regulation may display defects in cell growth and MC adjustment. This study can be conducted under the guidance of FBA modeling (Covert, 2002). Thirdly, the potential factors which are closely related to cell growth and susceptible to be affected by MC variation, such as PTS (Rohwer, Postma et al. 1998), EI (Patel, Vyas et al. 2006; Patel, Vyas et al. 2006), DNA structure and cell cycle related molecules, such as FtsZ (Weart, 2003; Rueda, 2003) and RelA (English, 2011) should be investigated to understand the influences exerted by MC. As those molecules activities and spatial distribution can be measured easily, they can be characterized when MC is transiently altered.

In the transient MC alteration experiment, protein expression has been found to contribute to MC alteration (Figure 4.1) but the crowding of membrane proteins might alter MC differently than cytosolic proteins do, as suggested previously (Zhuang, 2011). To test this, we can overexpress the membrane protein and the cytosol proteins respectively to examine their contribution to MC perturbation (Stoebel, 2008). Moreover, ribosomes' contribution to MC can also be determined to study the influence of protein load on cell growth. But for MC alteration in mammalian cells, another feasible strategy to alter the cells MC is to load cells with inert particles by endocytosis. Such strategy could be realized by either pinocytosis, phagocytosis, or ligand mediated endocytosis, depending on the nature of the actual particles and cells involved. The crowding effects will be determined by the effective volume of the endocytosed particles. Such particles could be inert metal particles like gold nanoparticles or polymers, such as those made of polystyrene. Cells can also uptake polymeric microbubbles that are around 3 microns in diameter. Such microbubbles are made with biodegradable polylactide and crosslinked human

serum albumin as the shell and nitrogen or perfluorobutane as the gas core. In one recent study it was shown that the effects of microbubble endocytosis on the viability, proliferation and differentiation of human mesenchymal stem cell were very limited (Fu, 2011). The advantage of the particle endocytosis strategy is that the MC could be easily tuned by choosing the size and loading amount of particles. The inert particles taken up by cells may also have much less direct effects on the metabolic pathways than other schemes, such as gene deletion or cell morphology alteration. However, the duration of particles staying inside the cytosol and actual cell volume after particle endocytosis remain to be determined to verify the feasibility of such way of MC alteration.

At last, different metabolism pathway utilization has been found to be selected under MC constraint. Therefore, we want to study whether MC adjustment is a necessity for cells to preferentially using certain metabolism pathway, such as glycolysis pathway. To further prove this, glycolytic strains which preferentially use glycolysis pathway can be used to examine if MC level has been adjusted to adapt the metabolism pathway utilization (Koebmann, Westerhoff et al. 2002; Holm, Blank et al. 2010). Moreover, the FBAwMC modeling used in sequential substrate study should be improved by updating dynamic cell volume and cell density constraints suggested by the experimental results (Figure 2.3 A). Cell volume and cell density should be the functions of cell growth rate. This will provide more accurate cell physiology parameters in *E. coli* study. Other biophysical or biochemical constraints may also be involved in shaping the strategy of substrate consumption for the benefit of optimal cell growth, such as cell volume, cell membrane and ribosome concentration. The comprehensive studies above will provide better understanding about the necessary physiological conditions for fast cell growth. As a result, novel drug targets for cell metabolisms in both bacteria and mammalian cells may be found.

BIBLIOGRAPHY

Aiba, H. (1985). "Transcription of the Escherichia coli adenylate cyclase gene is negatively regulated by cAMP-cAMP receptor protein." Journal of Biological Chemistry **260**(5): 3063-3070.

Al-Habori, M., M. Peak, et al. (1992). "The role of cell swelling in the stimulation of glycogen synthesis by insulin." Biochemical Journal **282**(3): 789-796.

Allen P, M. (1997). "Influence of excluded volume upon macromolecular structure and associations in 'crowded" media." Current Opinion in Biotechnology **8**(1): 65-69.

Almaas, E., Z. N. Oltvai, et al. (2005). "The Activity Reaction Core and Plasticity of Metabolic Networks." PLoS Computational Biology **1**(7): 0557-0563.

Alon Zaslaver, A. M., Michal Ronen and Uri Alon (2006). "Optimal gene partition into operons correlates with gene functional order." Physical Biology **3**(3): 183.

Alonzo, S., M. Heyde, et al. (1998). "Analysis of the effect exerted by extracellular pH on the maltose regulon in Escherichia coli K-12." Microbiology **144**(12): 3317-3325.

Alyahya, S. A., R. Alexander, et al. (2009). "RodZ, a component of the bacterial core morphogenic apparatus." Proceedings of the National Academy of Sciences **106**(4): 1239-1244.

Andrews KJ, H. G. (1976). "Selective disadvantage of non-functional protein synthesis in Escherichia coli." J mol Evol **8**(4): 11.

Balázsi, G., A.-L. Barabási, et al. (2005). "Topological units of environmental signal processing in the transcriptional regulatory network of Escherichia coli." Proceedings of the National Academy of Sciences **102**(22): 7841-7846.

Baldwin, W., R. Myer, et al. (1995). "Buoyant density ofEscherichia coli is determined solely by the osmolarity of the culture medium." Archives of Microbiology **164**(2): 155.

Baldwin, W. W. and H. E. Kubitschek (1984). "Evidence for osmoregulation of cell growth and buoyant density in Escherichia coli." J. Bacteriol. **159**(1): 393-394.

Baldwin, W. W., M. J. Sheu, et al. (1988). "Changes in buoyant density and cell size of Escherichia coli in response to osmotic shocks." J. Bacteriol. **170**(1): 452-455.

Beard, D. A., S. D. Liang, et al. (2002). "Energy balance for analysis of complex metabolic networks." Biophysical Journal **83**(1): 79-86.

Beg, Q. K., A. Vazquez, et al. (2007). "Intracellular crowding defines the mode and sequence of substrate uptake by Escherichia coli and constrains its metabolic activity." Proceedings of the National Academy of Sciences **104**(31): 12663-12668.

Beg, Q. K., A. Vazquez, et al. (2007). "Intracellular crowding defines the mode and sequence of substrate uptake by Escherichia coli and constrains its metabolic activity." Proceedings of the National Academy of Sciences of the United States of America **104**(31): 12663-12668.

Bendezu, F. O., C. A. Hale, et al. (2009). "RodZ (YfgA) is required for proper assembly of the MreB actin cytoskeleton and cell shape in *E. coli*." EMBO J **28**(3): 193-204.

Bettenbrock, K. (2007). "Correlation between growth rates, EIIACrr phosphorylation, and intracellular cyclic AMP levels in Escherichia coli K-12." J. Bacteriol. **189**: 6891-6900.

Bettenbrock, K., S. Fischer, et al. (2006). "A quantitative approach to catabolite repression in Escherichia coli." J Biol Chem **281**: 2578 - 2584.

Bettenbrock, K., T. Sauter, et al. (2007). "Correlation between Growth Rates, EIIACrr Phosphorylation, and Intracellular Cyclic AMP Levels in Escherichia coli K-12." J. Bacteriol. **189**(19): 6891-6900.

Blencke, H. M. (2003). "Transcriptional profiling of gene expression in response to glucose in Bacillus subtilis: regulation of the central metabolic pathways." Metab. Eng. **5**: 133-149.

Böhm, A., J. Diez, et al. (2002). "Structural Model of MalK, the ABC Subunit of the Maltose Transporter of Escherichia coli." Journal of Biological Chemistry **277**(5): 3708-3717.
Brown, G. C. (1991). "Total cell protein concentration as an evolutionary constraint on the metabolic control distribution in cells." Journal of Theoretical Biology **153**(2): 195-203.
Bruckner, R. and F. Titgemeyer (2002). "Carbon catabolite repression in bacteria: choice of the carbon source and autoregulatory limitation of sugar utilization." FEMS Microbiol. Lett. **209**: 141-148.
Bryan, A. K., A. Goranov, et al. (2010). "Measurement of mass, density, and volume during the cell cycle of yeast." Proceedings of the National Academy of Sciences **107**(3): 999-1004.
Busby, S. and R. H. Ebright (1999). "Transcription activation by catabolite activator protein (CAP)." J. Mol. Biol. **293**: 199-213.
Cai, M., D. C. Williams, et al. (2003). "Solution Structure of the Phosphoryl Transfer Complex between the Signal-transducing Protein IIAGlucose and the Cytoplasmic Domain of the Glucose Transporter IICBGlucose of the Escherichia coli Glucose Phosphotransferase System." Journal of Biological Chemistry **278**(27): 25191-25206.
Cases, I., F. Velazquez, et al. (2007). "The ancestral role of the phosphoenolpyruvate-carbohydrate phosphotransferase system (PTS) as exposed by comparative genomics." Res. Microbiol. **158**: 666-670.
Chagneau, C., M. Heyde, et al. (2001). "External-pH-Dependent Expression of the Maltose Regulon and ompF Gene in Escherichia coli Is Affected by the Level of Glycerol Kinase, Encoded by glpK." J. Bacteriol. **183**(19): 5675-5683.
Chapon, C. (1982). "Role of the catabolite activator protein in the maltose regulon of Escherichia coli." J. Bacteriol. **150**(2): 722-729.
Chen, C. C. H., H. Zhang, et al. (2002). "Degradation Pathway of the Phosphonate Ciliatine: Crystal Structure of 2-Aminoethylphosphonate Transaminase†,‡." Biochemistry **41**(44): 13162-13169.
Chen, J., G. Lu, et al. (2003). "A Tweezers-like Motion of the ATP-Binding Cassette Dimer in an ABC Transport Cycle." Molecular Cell **12**(3): 651-661.
Chen, J., S. Sharma, et al. (2001). "Trapping the transition state of an ATP-binding cassette transporter: Evidence for a concerted mechanism of maltose transport." Proceedings of the National Academy of Sciences **98**(4): 1525-1530.
Chou, C., G. Bennett, et al. (1994). "Effect of modulated glucose uptake on high-level recombinant protein production in a dense Escherichia coli culture." Biotechnol Prog **10**: 644 - 647.
Contesse, G., M. Crépin, F. Gros, A. Ullmann, and J. Monod. (1969). "On the mechanism of catabolite repression." In J. R. Beckwith and D. Zipser (ed.) The lactose operon: 14.
Cooper, S. (1991). "Bacterial growth and division : biochemistry and regulation of prokaryotic and eukaryotic division cycles / Stephen Cooper." San Diego : Academic Press, c1991.
Cooper, S. (2006). "Regulation of DNA synthesis in bacteria: analysis of the Bates/Kleckner licensing/initiation-mass model for cell cycle control." Molecular Microbiology **62**(2): 303-307.
Cordaro, J., T. Melton, et al. (1976). "Fosfomycin resistance: selection method for internal and extended deletions of the phosphoenolpyruvate:sugar phosphotransferase genes of Salmonella typhimurium." J Bacteriol **128**: 785 - 793.
Courcelle, J. and P. C. Hanawalt (2001). "Participation of recombination proteins in rescue of arrested replication forks in UV-irradiated Escherichia coli need not involve recombination." Proceedings of the National Academy of Sciences **98**(15): 8196-8202.
Covert, M. W. and B. Ø. Palsson (2002). "Transcriptional regulation in constraints-based metabolic models of Escherichia coli." Journal of Biological Chemistry **277**(31): 28058-28064.
Covert, M. W., C. H. Schilling, et al. (2001). "Regulation of gene expression in flux balance models of metabolism." Journal of Theoretical Biology **213**(1): 73-88.

Crasnier, M., V. Dumay, et al. (1994). "The catalytic domain of Escherichia coli K-12 adenylate cyclase as revealed by deletion analysis of the cya gene." Molecular and General Genetics **243**(4): 409-416.
Culham, D. E., J. Henderson, et al. (2003). "Osmosensor ProP of Escherichia coli responds to the concentration, chemistry, and molecular size of osmolytes in the proteoliposome lumen." Biochemistry **42**(2): 410-420.
Dai, J., S. H. Lin, et al. (2004). "Interplay between site-specific mutations and cyclic nucleotides in modulating DNA recognition by Escherichia coli cyclic AMP receptor protein." Biochemistry **43**(28): 8901-8910.
Day, I. N. M. and R. J. Thompson (2010). "UCHL1 (PGP 9.5): Neuronal biomarker and ubiquitin system protein." Progress in Neurobiology **90**(3): 327-362.
DE, B. (2000). "Can cytoplasm exist without undergoing phase separation?" Int. Rev. Cytol. **192**: 9.
Dean, D. A., J. Reizer, et al. (1990). "Regulation of the maltose transport system of Escherichia coli by the glucose-specific enzyme III of the phosphoenolpyruvate-sugar phosphotransferase system. Characterization of inducer exclusion-resistant mutants and reconstitution of inducer exclusion in proteoliposomes." Journal of Biological Chemistry **265**(34): 21005-21010.
Decker, K., J. Plumbridge, et al. (1998). "Negative transcriptional regulation of a positive regulator: the expression of malT, encoding the transcriptional activator of the maltose regulon of Escherichia coli, is negatively controlled by Mlc." Molecular Microbiology **27**(2): 381-390.
Dekel, E. and U. Alon (2005). "Optimality and evolutionary tuning of the expression level of a protein." Nature **436**(7050): 588.
Deutscher, D., I. Meilijson, et al. (2006). "Multiple knockout analysis of genetic robustness in the yeast metabolic network." Nature Genetics **38**(9): 993-998.
Deutscher, J. (2008). "The mechanisms of carbon catabolite repression in bacteria." Current Opinion in Microbiology **11**(2): 87.
Deutscher, J., C. Francke, et al. (2006). "How Phosphotransferase System-Related Protein Phosphorylation Regulates Carbohydrate Metabolism in Bacteria." Microbiol. Mol. Biol. Rev. **70**(4): 939-1031.
Deutscher, J., U. Kessler, et al. (1985). "Streptococcal phosphoenolpyruvate: sugar phosphotransferase system: purification and characterization of a phosphoprotein phosphatase which hydrolyzes the phosphoryl bond in seryl-phosphorylated histidine-containing protein." J. Bacteriol. **163**(3): 1203-1209.
Dong, H., L. Nilsson, et al. (1995). "Gratuitous overexpression of genes in Escherichia coli leads to growth inhibition and ribosome destruction." J. Bacteriol. **177**(6): 1497-1504.
Dubois, J. M. and B. Rouzaire-Dubois (2004). "The influence of cell volume changes on tumour cell proliferation." European Biophysics Journal **33**(3): 227-232.
Edwards, J. S., M. Covert, et al. (2002). "Metabolic modelling of microbes: The flux-balance approach." Environmental Microbiology **4**(3): 133-140.
Edwards, J. S., R. U. Ibarra, et al. (2001). "In silico predictions of Escherichia coli metabolic capabilities are consistent with experimental data." Nature Biotechnology **19**(2): 125-130.
Ehrt, S., X. V. Guo, et al. (2005). "Controlling gene expression in mycobacteria with anhydrotetracycline and Tet repressor." Nucleic Acids Research **33**(2): e21.
Ellis, R. J. (1997). "Molecular chaperones: Avoiding the crowd." Current Biology **7**(9): R531-R533.
Ellis, R. J. (1998). "Steric chaperones." Trends in Biochemical Sciences **23**(2): 43-45.
Ellis, R. J. (2001). "Molecular chaperones: Inside and outside the Anfinsen cage." Current Biology **11**(24): R1038-R1040.
Elowitz, M. B., M. G. Surette, et al. (1999). "Protein Mobility in the Cytoplasm of Escherichia coli." J. Bacteriol. **181**(1): 197-203.

Eppler, T. and W. Boos (1999). "Glycerol-3-phosphate-mediated repression of malT in Escherichia coli does not require metabolism, depends on enzyme IIAGlc and is mediated by cAMP levels." Molecular Microbiology **33**(6): 1221-1231.
Eppler, T., P. Postma, et al. (2002). "Glycerol-3-Phosphate-Induced Catabolite Repression in Escherichia coli." J. Bacteriol. **184**(11): 3044-3052.
Fell, D. A. and J. R. Small (1986). "Fat synthesis in adipose tissue. An examination of stoichiometric constraints." Biochemical Journal **238**(3): 781-786.
Ferenci, T. (1996). "Adaptation to life at micromolar nutrient levels: the regulation of Escherichia coli glucose transport by endoinduction and cAMP." FEMS Microbiology Reviews **18**(4): 301-317.
Fic, E., P. Bonarek, et al. (2009). "CAMP receptor protein from escherichia coli as a model of signal transduction in proteins - A review." Journal of Molecular Microbiology and Biotechnology **17**(1): 1-11.
Fong, S. S., J. Y. Marciniak, et al. (2003). "Description and Interpretation of Adaptive Evolution of Escherichia coli K-12 MG1655 by Using a Genome-Scale In Silico Metabolic Model." Journal of Bacteriology **185**(21): 6400-6408.
Forst, D., K. Schulein, et al. (1993). "Crystallization and preliminary X-ray diffraction analysis of ScrY, a specific bacterial outer membrane porin." Journal of Molecular Biology **229**(1): 258-262.
Fulton, A. B. (1982). "How crowded is the cytoplasm?" Cell **30**(2): 345-347.
Furusawa, C. and K. Kaneko (2008). "A Generic Mechanism for Adaptive Growth Rate Regulation." PLoS Comput Biol **4**(1): e3.
Galán, A., B. Sot, et al. (2001). "Excluded volume effects on the refolding and assembly of an oligomeric protein. GroEL, a case study." Journal of Biological Chemistry **276**(2): 957-964.
Garrett, D. S., Y.-J. Seok, et al. (1999). "Solution structure of the 40,000 Mr phosphoryl transfer complex between the N-terminal domain of enzyme I and HPr." Nat Struct Mol Biol **6**(2): 166-173.
Goelzer, A. and V. Fromion "Bacterial growth rate reflects a bottleneck in resource allocation." Biochimica et Biophysica Acta (BBA) - General Subjects **In Press, Corrected Proof**.
Gorke, B. and J. Stulke (2008). "Carbon catabolite repression in bacteria: many ways to make the most out of nutrients." Nat Rev Micro **6**(8): 613-624.
Gorke, B. and J. Stulke (2008). "Carbon catabolite repression in bacteria: many ways to make the most out of nutrients." Nat Rev Micro **6**(8): 613.
Gosset, G. (2005). "Improvement of Escherichia coli production strains by modification of the phosphoenolpyruvate:sugar phosphotransferase system." Microbial Cell Factories **4**(1): 14.
Hanamura, A. and H. Aiba (1991). "Molecular mechanism of negative autoregulation of Escherichia coli crp gene." Nucleic Acids Research **19**(16): 4413-4419.
Harman, J. G. (2001). "Allosteric regulation of the cAMP receptor protein." Biochimica et Biophysica Acta - Protein Structure and Molecular Enzymology **1547**(1): 1-17.
Haussinger, D., C. Hallbrucker, et al. (1991). "Cell volume is a major determinant of proteolysis control in liver." FEBS Letters **283**(1): 70-72.
Hernandez-Montalvo, V., F. Valle, et al. (2001). "Characterization of sugar mixtures by an Escherichia coli mutant devoid of the phosphotransferase system." Appl Microbiol Biotechnol **57**: 186 - 191.
Herrgård, M. J., B. S. Lee, et al. (2006). "Integrated analysis of regulatory and metabolic networks reveals novel regulatory mechanisms in Saccharomyces cerevisiae." Genome Research **16**(5): 627-635.
Herzberg, O. (1992). "An atomic model for protein-protein phosphoryl group transfer." Journal of Biological Chemistry **267**(34): 24819-24823.
Herzberg, O., C. C. Chen, et al. (1996). "Swiveling-domain mechanism for enzymatic phosphotransfer between remote reaction sites." Proceedings of the National Academy of Sciences **93**(7): 2652-2657.

Herzberg, O., P. Reddy, et al. (1992). "Structure of the histidine-containing phosphocarrier protein HPr from Bacillus subtilis at 2.0-A resolution." Proceedings of the National Academy of Sciences **89**(6): 2499-2503.

Hoffmann, F., J. Weber, et al. (2002). "Metabolic adaptation of Escherichia coli during temperature-induced recombinant protein production: 1. Readjustment of metabolic enzyme synthesis." Biotechnology and Bioengineering **80**(3): 313-319.

Hofnung, M. (1974). "DIVERGENT OPERONS AND THE GENETIC STRUCTURE OF THE MALTOSE B REGION IN ESCHERICHIA COLI K12." Genetics **76**(2): 169-184.

Hogema, B. M. (1998). "Inducer exclusion in Escherichia coli by non-PTS substrates: the role of the PEP to pyruvate ratio in determining the phosphorylation state of enzyme IIAGlc." Mol. Microbiol. **30**: 487-498.

Hogema, B. M., J. C. Arents, et al. (1999). "Autoregulation of lactose uptake through the LacY permease by enzyme IIAGlc of the PTS in Escherichia coli K-12." Mol. Microbiol. **31**: 1825-1833.

Hogema, B. M., J. C. Arents, et al. (1997). "Catabolite repression by glucose 6-phosphate, gluconate and lactose in Escherichia coli." Molecular Microbiology **24**(4): 857-867.

Holm, A. K., L. M. Blank, et al. (2010). "Metabolic and Transcriptional Response to Cofactor Perturbations in Escherichia coli." Journal of Biological Chemistry **285**(23): 17498-17506.

Hosono, K., H. Kakuda, et al. (1995). "Decreasing accumulation of acetate in a rich medium by Escherichia coli on introduction of genes on a multicopy plasmid." Biosci Biotechnol Biochem **59**: 256 - 261.

Houssin, C., N. Eynard, et al. (1991). "Effect of osmotic pressure on membrane energy-linked functions in Escherichia coli." Biochimica et Biophysica Acta - Bioenergetics **1056**(1): 76-84.

Hu, K.-Y. and M. H. Saier Jr (2002). "Phylogeny of phosphoryl transfer proteins of the phosphoenolpyruvate-dependent sugar-transporting phosphotransferase system." Research in Microbiology **153**(7): 405-415.

Hurley, J., H. Faber, et al. (1993). "Structure of the regulatory complex of Escherichia coli IIIGlc with glycerol kinase." Science **259**(5095): 673-677.

Ihssen, J. and T. Egli (2004). "Specific growth rate and not cell density controls the general stress response in Escherichia coli." Microbiology **150**(6): 1637-1648.

Ihssen, J. and T. Egli (2005). "Global physiological analysis of carbon- and energy-limited growing Escherichia coli confirms a high degree of catabolic flexibility and preparedness for mixed substrate utilization." Environmental Microbiology **7**(10): 1568-1581.

Inada, T., H. Takahashi, et al. (1996). "Down regulation of cAMP production by cAMP receptor protein in Escherichia coli: An assessment of the contributions of transcriptional and posttranscriptional control of adenylate cyclase." Molecular and General Genetics **253**(1-2): 198-204.

Ishii, N., K. Nakahigashi, et al. (2007). "Multiple High-Throughput Analyses Monitor the Response of *E. coli* to Perturbations." Science **316**(5824): 593-597.

Johansson, H. O., Brooks, D. E., Haynes, C. A. (2000). "Macromolecular crowding and its consequences." Int. Rev. Cytol. **192**: 15.

Joly, N., A. Bohm, et al. (2004). "MalK, the ATP-binding Cassette Component of the Escherichia coli Maltodextrin Transporter, Inhibits the Transcriptional Activator MalT by Antagonizing Inducer Binding." J. Biol. Chem. **279**(32): 33123-33130.

Josef, D. (2008). "The mechanisms of carbon catabolite repression in bacteria." Current Opinion in Microbiology **11**(2): 87-93.

Jovanovich, S. B. (1985). "Regulation of a cya-lac fusion by cyclic AMP in Salmonella typhimurium." J. Bacteriol. **161**(2): 641-649.

Jozefczuk, S., S. Klie, et al. (2010). "Metabolomic and transcriptomic stress response of Escherichia coli." Molecular Systems Biology **6**.

K Hayashi, M. N., Y Ishizaki, and A Obayashi "Influence of monovalent cations on the activity of T4 DNA ligase in the presence of polyethylene glycol." Nucleic Acids Res. **13**(9): 10.

K Hayashi, M. N., Y Ishizaki, N Hiraoka, and A Obayashi (1985). "Stimulation of intermolecular ligation with *E. coli* DNA ligase by high concentrations of monovalent cations in polyethylene glycol solutions." Nucleic Acids Res. **13**(22): 7979.

Kaback, H. R. (1997). "A molecular mechanism for energy coupling in a membrane transport protein, the lactose permease of Escherichia coli." Proceedings of the National Academy of Sciences **94**(11): 5539-5543.

Kaback, H. R., M. Sahin-Tóth, et al. (2001). "The kamikaze approach to membrane transport." Nat Rev Mol Cell Biol **2**(8): 610-620.

Kauffman, K. J., P. Prakash, et al. (2003). "Advances in flux balance analysis." Current Opinion in Biotechnology **14**(5): 491-496.

Kawamukai, M., J. Kishimoto, et al. (1985). "Negative regulation of adenylate cyclase gene (cya) expression by cyclic AMP-cyclic AMP receptor protein in Escherichia coli: Studies with cya-lac protein and operon fusion plasmids." Journal of Bacteriology **164**(2): 872-877.

Kholodenko, B. N., J. M. Rohwer, et al. (1998). "Subtleties in control by metabolic channelling and enzyme organization." Molecular and Cellular Biochemistry **184**(1): 311.

Kim, S.-Y., T.-W. Nam, et al. (1999). "Purification of Mlc and Analysis of Its Effects on thepts Expression in Escherichia coli." Journal of Biological Chemistry **274**(36): 25398-25402.

Kimata, K., T. Inada, et al. (1998). "A global repressor (Mlc) is involved in glucose induction of the ptsG gene encoding major glucose transporter in Escherichia coli." Molecular Microbiology **29**(6): 1509-1519.

Kimata, K., H. Takahashi, et al. (1997). "cAMP receptor protein-cAMP plays a crucial role in glucose-lactose diauxie by activating the major glucose transporter gene in Escherichia coli." Proc. Natl Acad. Sci. USA **94**: 12914-12919.

Knorr, A. L., R. Jain, et al. (2007). "Bayesian-based selection of metabolic objective functions." Bioinformatics **23**(3): 351-357.

Koch, A. L. (2002). "Control of the Bacterial Cell Cycle by Cytoplasmic Growth." Critical Reviews in Microbiology **28**(1): 61.

Koebmann, B. J., H. V. Westerhoff, et al. (2002). "The Glycolytic Flux in Escherichia coli Is Controlled by the Demand for ATP." J. Bacteriol. **184**(14): 3909-3916.

Kovárová-Kovar, K. and T. Egli (1998). "Growth kinetics of suspended microbial cells: From single-substrate- controlled growth to mixed-substrate kinetics." Microbiology and Molecular Biology Reviews **62**(3): 646-666.

Lan, G., B. R. Daniels, et al. (2009). "Condensation of FtsZ filaments can drive bacterial cell division." Proceedings of the National Academy of Sciences **106**(1): 121-126.

Lang, F., G. L. Busch, et al. (1998). "Functional significance of cell volume regulatory mechanisms." Physiological Reviews **78**(1): 247-306.

Lavery, P. E. and S. C. Kowalczykowski (1992). "Enhancement of recA protein-promoted DNA strand exchange activity by volume-occupying agents." Journal of Biological Chemistry **267**(13): 9307-9314.

Lee, S.-J., W. Boos, et al. (2000). "Signal transduction between a membrane-bound transporter, PtsG, and a soluble transcription factor, Mlc, of Escherichia coli." EMBO J **19**(20): 5353-5361.

Lengsfeld, C., S. Schonert, et al. (2009). "Glucose- and Glucokinase-Controlled mal Gene Expression in Escherichia coli." J. Bacteriol. **191**(3): 701-712.

Liao DI, K. G., Reddy P, Saier MH Jr, Reizer J, Herzberg O. (1991). "Structure of the IIA domain of the glucose permease of Bacillus subtilis at 2.2-A resolution." Biochemistry **30**(40): 12.

Lindsay, S., R. Bothast, et al. (1995). "Improved strains of recombinant Escherichia coli for ethanol production from sugar mixtures." Appl Microbiol Biotechnol **43**: 70 - 75.
Liu, K. D. and S. Roseman (1983). "Kinetic characterization and regulation of phosphoenolpyruvate-dependent methyl alpha-D-glucopyranoside transport by Salmonella typhimurium membrane vesicles." Proceedings of the National Academy of Sciences **80**(23): 7142-7145.
Liu, M. (2005). "Global transcriptional programs reveal a carbon source foraging strategy by Escherichia coli." J. Biol. Chem. **280**: 15921-15927.
Liu, M., T. Durfee, et al. (2005). "Global Transcriptional Programs Reveal a Carbon Source Foraging Strategy by Escherichia coli." Journal of Biological Chemistry **280**(16): 15921-15927.
Lu, M. and N. Kleckner (1994). "Molecular cloning and characterization of the pgm gene encoding phosphoglucomutase of Escherichia coli." Journal of Bacteriology **176**(18): 5847-5851.
Maertens, J. and P. A. Vanrolleghem (2010). "Modeling with a view to target identification in metabolic engineering: A critical evaluation of the available tools." Biotechnology Progress **26**(2): 313-331.
Mahadevan, R., J. S. Edwards, et al. (2002). "Dynamic Flux Balance Analysis of diauxic growth in Escherichia coli." Biophysical Journal **83**(3): 1331-1340.
Makinoshima, H., A. Nishimura, et al. (2002). "Fractionation of Escherichia coli cell populations at different stages during growth transition to stationary phase." Molecular Microbiology **43**(2): 269-279.
Malan, T. P., A. Kolb, et al. (1984). "Mechanism of CRP-cAMP activation of lac operon transcription initiation activation of the P1 promoter." J. Mol. Biol. **180**: 881-909.
Minton, A. P. (2001). "The Influence of Macromolecular Crowding and Macromolecular Confinement on Biochemical Reactions in Physiological Media." Journal of Biological Chemistry **276**(14): 10577-10580.
Minton, A. P. (2006). "How can biochemical reactions within cells differ from those in test tubes?" Journal of Cell Science **119**(14): 2863-2869.
Minton, A. P., G. C. Colclasure, et al. (1992). "Model for the role of macromolecular crowding in regulation of cellular volume." Proceedings of the National Academy of Sciences of the United States of America **89**(21): 10504-10506.
Molenaar, D., R. Van Berlo, et al. (2009). "Shifts in growth strategies reflect tradeoffs in cellular economics." Molecular Systems Biology **5**.
Møller, T., T. Franch, et al. (2002). "Spot 42 RNA mediates discoordinate expression of the *E. coli* galactose operon." Genes & Development **16**(13): 1696-1706.
Monod, J. (1942). "Recherches sur la croissance des cultures bactériennes." Hermann et Cie, Paris, France.
Motter, A. E., N. Gulbahce, et al. (2008). "Predicting synthetic rescues in metabolic networks." Molecular Systems Biology **4**.
Mukhopadhyay, J., R. Sur, et al. (1999). "Functional roles of the two cyclic AMP-dependent forms of cyclic AMP receptor protein from Escherichia coli." FEBS Letters **453**(1-2): 215-218.
Muller, C., L. Petruschka, et al. (1996). "Carbon catabolite repression of phenol degradation in Pseudomonas putida is mediated by the inhibition of the activator protein PhlR." J. Bacteriol. **178**: 2030-2036.
Nam, T.-W., S.-H. Cho, et al. (2001). "The Escherichia coli glucose transporter enzyme IICBGlc recruits the global repressor Mlc." EMBO J **20**(3): 491-498.
Nelson, S. O., Wright, J. K., Postma, P.W. (1983). "The mechanism of inducer exclusion. Direct interaction between purified IIIGlc of the phosphoenolpyruvate:sugar phosphotransferase system and the lactose carrier of Escherichia coli." The EMBO Journal **2**(5): 715-720.
Nichols, N., B. Dien, et al. (2001). "Use of catabolite repression mutants for fermentation of sugar mixtures to ethanol." Appl Microbiol Biotechnol **56**: 120 - 125.

Okada, Y. (2004). "Ion channels and transporters involved in cell volume regulation and sensor mechanisms." Cell Biochemistry and Biophysics **41**(2): 233-258.
Okamoto, K. and M. Freundlich (1986). "Mechanism for the autogenous control of the crp operon: transcriptional inhibition by a divergent RNA transcript." Proceedings of the National Academy of Sciences **83**(14): 5000-5004.
Orelle, C., T. Ayvaz, et al. (2008). "Both maltose-binding protein and ATP are required for nucleotide-binding domain closure in the intact maltose ABC transporter." Proceedings of the National Academy of Sciences **105**(35): 12837-12842.
Panagiotidis, C. H., W. Boos, et al. (1998). "The ATP-binding cassette subunit of the maltose transporter MalK antagonizes MalT, the activator of the Escherichia coli mal regulon." Molecular Microbiology **30**(3): 535-546.
Panagiotidis, C. H., M. Reyes, et al. (1993). "Characterization of the structural requirements for assembly and nucleotide binding of an ATP-binding cassette transporter. The maltose transport system of Escherichia coli." Journal of Biological Chemistry **268**(31): 23685-23696.
Papenfort, K., V. Pfeiffer, et al. (2008). "Systematic deletion of Salmonella small RNA genes identifies CyaR, a conserved CRP-dependent riboregulator of OmpX synthesis." Molecular Microbiology **68**(4): 890-906.
Papp, B., C. Pál, et al. (2004). "Metabolic network analysis of the causes and evolution of enzyme dispensability in yeast." Nature **429**(6992): 661-664.
Park, Y. H., B. R. Lee, et al. (2006). "In vitro reconstitution of catabolite repression in Escherichia coli." Journal of Biological Chemistry **281**(10): 6448-6454.
Park, Y. H., B. R. Lee, et al. (2006). "In vitro reconstitution of catabolite repression in Escherichia coli." J. Biol. Chem. **281**: 6448-6454.
Pasantes-Morales, H., R. A. Lezama, et al. (2006). "Mechanisms of Cell Volume Regulation in Hypo-osmolality." The American Journal of Medicine **119**(7, Supplement 1): S4.
Patel, H. V., K. A. Vyas, et al. (2006). "Properties of the C-terminal Domain of Enzyme I of the Escherichia coli Phosphotransferase System." Journal of Biological Chemistry **281**(26): 17579-17587.
Patel, H. V., K. A. Vyas, et al. (2006). "The Monomer/Dimer Transition of Enzyme I of the Escherichia coli Phosphotransferase System." Journal of Biological Chemistry **281**(26): 17570-17578.
Peak, M., M. Al-Habori, et al. (1992). "Regulation of glycogen synthesis and glycolysis by insulin, pH and cell volume. Interactions between swelling and alkalinization in mediating the effects of insulin." Biochemical Journal **282**(3): 797-805.
Pederson, T. (2000). "Half a Century of "The Nuclear Matrix"." Molecular Biology of the Cell **11**(3): 799-805.
Plumbridge, J. (1999). "Expression of the phosphotransferase system both mediates and is mediated by Mlc regulation in Escherichia coli." Molecular Microbiology **33**(2): 260-273.
Plumbridge, J. (2002). "Regulation of gene expression in the PTS in Escherichia coli : the role and interactions of Mlc." Curr Opin Microbiol **5**: 187 - 193.
Poelwijk, F., P. Heyning, et al. (2011). "Optimality and evolution of transcriptionally regulated gene expression." BMC Systems Biology **5**(1): 128.
Posfai, G., G. Plunkett, III, et al. (2006). "Emergent Properties of Reduced-Genome Escherichia coli." Science **312**(5776): 1044-1046.
Postma, P. W., J. W. Lengeler, et al. (1993). "Phosphoenolpyruvate:carbohydrate phosphotransferase systems of bacteria." Microbiol. Rev. **57**: 543-594.
Powers DA, R. S. (1984). "The primary structure of Salmonella typhimurium HPr, a phosphocarrier protein of the phosphoenolpyruvate:glycose phosphotransferase system. A correction." J Biol Chem **259**: 3.

Pramanik, J. and J. D. Keasling (1997). "Stoichiometric model of Escherichia coli metabolism: Incorporation of growth-rate dependent biomass composition and mechanistic energy requirements." Biotechnology and Bioengineering **56**(4): 398-421.
R.John, E. (1990). "Molecular chaperones and chloroplast biogenesis." Cell Biology International Reports **14, Supplement 1**(0): 7.
R.John, E. (2001). "Macromolecular crowding: an important but neglected aspect of the intracellular environment." Current Opinion in Structural Biology **11**(1): 114-119.
Raman, K. and N. Chandra (2009). "Flux balance analysis of biological systems: Applications and challenges." Briefings in Bioinformatics **10**(4): 435-449.
Ramos, J. L., M. Martinez-Bueno, et al. (2005). "The TetR Family of Transcriptional Repressors." Microbiol. Mol. Biol. Rev. **69**(2): 326-356.
Ravasz, E., A. L. Somera, et al. (2002). Science **297**(null): 1551.
Reddy, P., J. Hoskins, et al. (1995). "Mapping domains in proteins: Dissection and expression of Escherichia coli adenylyl cyclase." Analytical Biochemistry **231**(2): 282-286.
Reidl, J. and W. Boos (1991). "The malX malY operon of Escherichia coli encodes a novel enzyme II of the phosphotransferase system recognizing glucose and maltose and an enzyme abolishing the endogenous induction of the maltose system." J. Bacteriol. **173**(15): 4862-4876.
Richter, K., M. Nessling, et al. (2007). "Experimental evidence for the influence of molecular crowding on nuclear architecture." Journal of Cell Science **120**(9): 1673-1680.
Richter, K., M. Nessling, et al. (2008). "Macromolecular crowding and its potential impact on nuclear function." Biochimica et Biophysica Acta (BBA) - Molecular Cell Research **1783**(11): 2100.
Rivas, G., J. A. Fernandez, et al. (1999). "Direct Observation of the Self-Association of Dilute Proteins in the Presence of Inert Macromolecules at High Concentration via Tracer Sedimentation Equilibrium: Theory, Experiment, and Biological Significance." Biochemistry **38**(29): 9379-9388.
Rivas, G., J. A. Fernández, et al. (2001). "Direct observation of the enhancement of noncooperative protein self-assembly by macromolecular crowding: Indefinite linear self-association of bacterial cell division protein FtsZ." Proceedings of the National Academy of Sciences **98**(6): 3150-3155.
Rivas, G., F. Ferrone, et al. (2004). "Life in a crowded world." EMBO Rep **5**(1): 23-27.
Robert G, R. (2005). "Transcriptional regulation and the role of diverse coactivators in animal cells." FEBS Letters **579**(4): 909-915.
Robillard, G. T. and J. Broos (1999). "Structure/function studies on the bacterial carbohydrate transporters, enzymes II, of the phosphoenolpyruvate-dependent phosphotransferase system." Biochimica et Biophysica Acta (BBA) - Reviews on Biomembranes **1422**(2): 73-104.
Rohwer, J. M., P. W. Postma, et al. (1998). "Implications of macromolecular crowding for signal transduction and metabolite channeling." Proceedings of the National Academy of Sciences **95**(18): 10547-10552.
Ronald, H. (2004). "A role for macromolecular crowding effects in the assembly and function of compartments in the nucleus." Journal of Structural Biology **146**(3): 281-290.
Ross PD, M. A. (1977). "Analysis of non-ideal behavior in concentrated hemoglobin solutions." Journal of Molecular Biology **112**(3): 15.
Roth, W. G., S. E. Porter, et al. (1985). "Restoration of cell volume and the reversal of carbohydrate transport and growth inhibition of osmotically upshocked Escherichia coli." Biochemical and Biophysical Research Communications **126**(1): 442-449.
Rouzaire-Dubois, B. and J. M. Dubois (1998). "K+ channel block-induced mammalian neuroblastoma cell swelling: A possible mechanism to influence proliferation." Journal of Physiology **510**(1): 93-102.
Rouzaire-Dubois, B., S. O'Regan, et al. (2005). "Cell size-dependent and independent proliferation of rodent neuroblastoma x glioma cells." Journal of Cellular Physiology **203**(1): 243-250.

Saier MH, H. R., Barabote RD. (2005). "Evolution of the bacterial phosphotransferase system: from carriers and enzymes to group translocators." Biochem Soc Trans. **33**(1): 4.
Sasaki, Y., D. Miyoshi, et al. (2007). "Regulation of DNA nucleases by molecular crowding." Nucleic Acids Research **35**(12): 4086-4093.
Sauer, F. G., S. D. Knight, et al. (2000). "PapD-like chaperones and pilus biogenesis." Seminars in Cell and Developmental Biology **11**(1): 27-34.
Schilling, C. H. and B. O. Palsson (1998). "The underlying pathway structure of biochemical reaction networks." Proceedings of the National Academy of Sciences of the United States of America **95**(8): 4193-4198.
Schlegel, A., O. Danot, et al. (2002). "The N Terminus of the Escherichia coli Transcription Activator MalT Is the Domain of Interaction with MalY." J. Bacteriol. **184**(11): 3069-3077.
Schneider, E. (2001). "ABC transporters catalyzing carbohydrate uptake." Research in Microbiology **152**(3-4): 303-310.
Schreiber, V., C. Steegborn, et al. (2000). "A new mechanism for the control of a prokaryotic transcriptional regulator: antagonistic binding of positive and negative effectors." Molecular Microbiology **35**(4): 765-776.
Schuetz, R., L. Kuepfer, et al. (2007). "Systematic evaluation of objective functions for predicting intracellular fluxes in Escherichia coli." Molecular Systems Biology **3**.
Scott, M., C. W. Gunderson, et al. (2010). "Interdependence of Cell Growth and Gene Expression: Origins and Consequences." Science **330**(6007): 1099-1102.
Segrè, D., D. Vitkup, et al. (2002). "Analysis of optimality in natural and perturbed metabolic networks." Proceedings of the National Academy of Sciences of the United States of America **99**(23): 15112-15117.
Seitz, S., S.-J. Lee, et al. (2003). "Analysis of the Interaction between the Global Regulator Mlc and EIIBGlc of the Glucose-specific Phosphotransferase System in Escherichia coli." Journal of Biological Chemistry **278**(12): 10744-10751.
Selvarasu, S., V. V. T. Wong, et al. (2009). "Elucidation of metabolism in hybridoma cells grown in fed-batch culture by genome-scale modeling." Biotechnology and Bioengineering **102**(5): 1494-1504.
Seshasayee, A. S. N., G. M. Fraser, et al. (2009). "Principles of transcriptional regulation and evolution of the metabolic system in *E. coli*." Genome Research **19**(1): 79-91.
Shiomi, D., M. Sakai, et al. (2008). "Determination of bacterial rod shape by a novel cytoskeletal membrane protein." EMBO J **27**(23): 3081.
Silver, R. S. and R. I. Mateles (1969). "Control of Mixed-Substrate Utilization in Continuous Cultures of Escherichia coli." J. Bacteriol. **97**(2): 535-543.
Sondej, M., Y.-J. Seok, et al. (2000). "Topography of the Surface of the Escherichia coli Phosphotransferase System Protein Enzyme IIAglc that Interacts with Lactose Permease." Biochemistry **39**(11): 2931-2939.
Sondej, M., J. L. Vázquez-Ibar, et al. (2003). "Characterization of a Lactose Permease Mutant that Binds IIAGlc in the Absence of Ligand†." Biochemistry **42**(30): 9153-9159.
Sondej, M., A. B. Weinglass, et al. (2002). "Binding of Enzyme IIAGlc, a Component of the Phosphoenolpyruvate:Sugar Phosphotransferase System, to the Escherichia coli Lactose Permease†." Biochemistry **41**(17): 5556-5565.
Stelling, J., S. Klamt, et al. (2002). "Metabolic network structure determines key aspects of functionality and regulation." Nature **420**(6912): 190-193.
Stoll, B., W. Gerok, et al. (1992). "Liver cell volume and protein synthesis." Biochemical Journal **287**(1): 217-222.
Sun, J. (2007). "Toward realistic modeling of dynamic processes in cell signaling: Quantification of macromolecular crowding effects." J. Chem. Phys. **127**(15): 155105.

Swaminathan, R., C. P. Hoang, et al. (1997). "Photobleaching recovery and anisotropy decay of green fluorescent protein GFP-S65T in solution and cells: cytoplasmic viscosity probed by green fluorescent protein translational and rotational diffusion." Biophysical Journal **72**(4): 1900-1907.

Szabolcs, S., K. Sandeep, et al. (2007). "Signal integration in the galactose network of Escherichia coli." Molecular Microbiology **65**(2): 465-476.

Tagami, H. and H. Aiba (1998). "A common role of CRP in transcription activation: CRP acts transiently to stimulate events leading to open complex formation at a diverse set of promoters." EMBO J. **17**: 1759-1767.

Tagkopoulos, I., Y.-C. Liu, et al. (2008). "Predictive Behavior Within Microbial Genetic Networks." Science **320**(5881): 1313-1317.

Takahashi, M., B. Blazy, et al. (1989). "Ligand-modulated binding of a gene regulatory protein to DNA. Quantitative analysis of cyclic-AMP induced binding of CRP from Escherichia coli to non-specific and specific DNA targets." Journal of Molecular Biology **207**(4): 783-796.

Takeuchi, S. (2006). "Analytical assays of human HSP27 and thermal-stress survival of Escherichia coli cells that overexpress it." Biochemical and Biophysical Research Communications **341**(4): 1252.

Tanaka, Y., F. Itoh, et al. (2004). "Membrane localization itself but not binding to IICBGlc is directly responsible for the inactivation of the global repressor Mlc in Escherichia coli." Molecular Microbiology **53**(3): 941-951.

Tseng, C. P., A. K. Hansen, et al. (1994). "Effect of cell growth rate on expression of the anaerobic respiratory pathway operons frdABCD, dmsABC, and narGHJI of Escherichia coli." J. Bacteriol. **176**(21): 6599-6605.

Tsuru, S., J. Ichinose, et al. (2009). "Noisy cell growth rate leads to fluctuating protein concentration in bacteria." Physical Biology **6**(3): 036015.

Tworzydło, M., A. Polit, et al. (2005). "Fluorescence quenching and kinetic studies of conformational changes induced by DNA and cAMP binding to cAMP receptor protein from Escherichia coli." FEBS Journal **272**(5): 1103-1116.

Valgepea, K., K. Adamberg, et al. (2010). "Systems biology approach reveals that overflow metabolism of acetate in Escherichia coli is triggered by carbon catabolite repression of acetyl-CoA synthetase." BMC Systems Biology **4**(1): 166.

van den Ent, F., C. M. Johnson, et al. (2010). "Bacterial actin MreB assembles in complex with cell shape protein RodZ." EMBO J **29**(6): 1081-1090.

van der Vlag J, P. P. (1995). "Regulation of glycerol and maltose uptake by the IIAGlc-like domain of IINag of the phosphotransferase system in Salmonella typhimurium LT2." Mol Gen Genet **248**(2): 6.

Vazquez, A. (2010). "Optimal cytoplasmatic density and flux balance model under macromolecular crowding effects." Journal of Theoretical Biology **264**(2): 356-359.

Vazquez, A., Q. Beg, et al. (2008). "Impact of the solvent capacity constraint on *E. coli* metabolism." BMC Systems Biology **2**(1): 7.

Vazquez, A., Q. K. Beg, et al. (2008). "Impact of the solvent capacity constraint on *E. coli* metabolism." BMC Systems Biology **2**.

Vazquez, A., M. A. de Menezes, et al. (2008). "Impact of Limited Solvent Capacity on Metabolic Rate, Enzyme Activities, and Metabolite Concentrations of <italic>S. cerevisiae</italic> Glycolysis." PLoS Comput Biol **4**(10): e1000195.

Vazquez, A., M. A. De Menezes, et al. (2008). "Impact of limited solvent capacity on metabolic rate, enzyme activities, and metabolite concentrations of S. cerevisiae glycolysis." PLoS Computational Biology **4**(10).

Vazquez, A., J. Liu, et al. (2010). "Catabolic efficiency of aerobic glycolysis: The Warburg effect revisited." BMC Systems Biology **4**(1): 58.

Vazquez, A. and Z. N. Oltvai (2011). "Molecular crowding defines a common origin for the warburg effect in proliferating cells and the lactate threshold in muscle physiology." PLoS ONE **6**(4).
Vidal-Ingigliardi, D. and O. Raibaud (1991). "Three adjacent binding sites for cAMP receptor protein are involved in the activation of the divergent malEp-malKp promoters." Proceedings of the National Academy of Sciences **88**(1): 229-233.
Waldegger, S., J. Matskevitch, et al. (1998). Introduction to cell volume regulatory mechanisms. **123:** 1-7.
Wang, G., J. M. Louis, et al. (2000). "Solution structure of the phosphoryl transfer complex between the signal transducing proteins HPr and IIAGlucose of the Escherichia coli phosphoenolpyruvate:sugar phosphotransferase system." EMBO J **19**(21): 5635-5649.
Weart, R. B., A. H. Lee, et al. (2007). "A Metabolic Sensor Governing Cell Size in Bacteria." **130**(2): 335.
Weber, J., F. Hoffmann, et al. (2002). "Metabolic adaptation of Escherichia coli during temperature-induced recombinant protein production: 2. Redirection of metabolic fluxes." Biotechnology and Bioengineering **80**(3): 320-330.
Weigel, N., M. A. Kukuruzinska, et al. (1982). "Sugar transport by the bacterial phosphotransferase system. Phosphoryl transfer reactions catalyzed by enzyme I of Salmonella typhimurium." Journal of Biological Chemistry **257**(23): 14477-14491.
Weigel, N., D. A. Powers, et al. (1982). "Sugar transport by the bacterial phosphotransferase system. Primary structure and active site of a general phosphocarrier protein (HPr) from Salmonella typhimurium." Journal of Biological Chemistry **257**(23): 14499-14509.
Wood, J. M. (1999). "Osmosensing by bacteria: Signals and membrane-based sensors." Microbiology and Molecular Biology Reviews **63**(1): 230-262.
Wood, J. M. (2006). "Osmosensing by Bacteria." Sci. STKE **2006**(357): pe43-.
Wu, L. F. and M. A. Mandrand-Berthelot (1995). "A family of homologous substrate-binding proteins with a broad range of substrate specificity and dissimilar biological functions." Biochimie **77**(9): 744-750.
Yao, R., Y. Hirose, et al. (2011). "Catabolic regulation analysis of Escherichia coli and its crp, mlc, mgsA, pgi and ptsG mutants." Microbial Cell Factories **10**(1): 67.
Zaslaver, A., A. E. Mayo, et al. (2004). "Just-in-time transcription program in metabolic pathways." Nature Genetics **36**(5): 486-491.
Zimmerman, S. B. (1993). "Macromolecular crowding effects on macromolecular interactions: Some implications for genome structure and function." Biochimica et Biophysica Acta (BBA) - Gene Structure and Expression **1216**(2): 175-185.
Zimmerman, S. B. and A. P. Minton (1993). "Macromolecular Crowding: Biochemical, Biophysical, and Physiological Consequences." Annual Review of Biophysics and Biomolecular Structure **22**(1): 27-65.
Zimmerman, S. B. and S. O. Trach (1991). "Estimation of macromolecule concentrations and excluded volume effects for the cytoplasm of Escherichia coli." Journal of Molecular Biology **222**(3): 599.